NF-kappa B signaling and inflammasome activation in developing fetal lung macrophages

By

Ashley Nicole Stouch

Dissertation

Submitted to the Faculty of the

Graduate School of Vanderbilt University

in partial fulfillment of the requirements

for the degree of

DOCTOR OF PHILOSOPHY

in

Cell and Developmental Biology

May, 2015

Nashville, TN

Approved:

Christopher V. Wright, Ph.D.

Timothy S. Blackwell, M.D.

Alyssa H. Hasty, Ph.D.

Guoqiang Gu, Ph.D.

Lawrence S. Prince, M.D., Ph.D.

To my husband, Ted, my saving grace.

ACKNOWLEDGEMENTS

I would like to thank the Department of Cell and Developmental Biology, for welcoming me into their community and their patience with a long-distance student. I would also like to recognize my thesis committee, Dr. Chris Wright, Dr. Guoqiang Gu, Dr. Alyssa Hasty, and Dr. Timothy Blackwell. Thank you for all of your guidance. A special thank you goes to my mentor, Dr. Lawrence Prince. Thank you for everything; for all of your mantras regarding science and life. You have made me a better scientist, but also a better person. Finally, I would like to acknowledge the National Institute of Health for funding during my graduate training.

I am very grateful for all of the people who been with me on this journey. Our collaboration with the Blackwell lab was very valuable. Thank you for sharing your knowledge of macrophages. To our neighbors, the Hoffman lab, thanks for the fun beach days. I appreciate all of my labmates, Billy, Alyssa, Amanda, Erin, Jin-Hua, and Rachel; who made showing up everyday a pleasure. But I especially want to thank Billy, Alyssa, and Amanda for all of their support, advice, and friendship. It means the world to me. To my family (and my crazy dogs), I couldn't have done it without your encouragement and laughter when I needed it most.

TABLE OF CONTENTS

LIST OF FIGURES

LIST OF ABBREVIATIONS

AbS	Antibodies
ANOVA	Analysis of Variance
ASC	Apoptosis-associated speck-like protein containing a carboxy-terminal CARD
ATP	Adenosine Triphosphate
BCA	Bicinchoninic acid
BMP4	Bone Morphogenetic Protein 4
BMPR1A	Bone Morphogenetic Protein Receptor , type 1A
BPD	Bronchopulmonary Dysplasia
cDNA	complementary DNA
Csf1r	Colony-Stimulating Factor 1 Receptor
DAPI	4',6-diamidino-2-phenylindole
DNA	Deoxyribonucleic acid
DOX	Doxycycline
ELISA	Enzyme-Linked Immunosorbent Assay
FACS	Fluorescence-Activated Cell Sorting
FBS	Fetal Bovine Serum
FGF-10	Fibroblast Growth Factor 10
GFP	Green Fluorescent Protein
GM-CSF	Granulocyte-Macrophage Colony-Stimulating Factor
h	hours
HIV	Human Immunodeficiency Virus
HSC	Hematopoietic Stem Cell
IFNγ	Interferon Gamma
IL-1β	Interleukin-1 beta
IκB	Inhibitor of kappa B
IKKβ	IκB Kinase beta
LPS	Lipopolysaccharide
M-CSF	Macrophage Colony-Stimulating Factor

min	minutes
mm	millimeters
NF-κB	Nuclear Factor kappa-light-chain-enhancer of activated B cells
NGL	NF-κB-GFP-Luciferase reporter mouse
NLRP3	NOD-Like Receptor Family, Pyrin Domain Containing 3
PCR	Polymerase chain reaction
PBS	Phosphate-buffered saline
RPMI	Roswell Park Memorial Institute medium
RNA	Ribonucleic acid
RT-PCR	real-time PCR
TGFβ	Transforming growth factor beta
TLR	Toll-like receptor
TNFα	Tumor necrosis factor alpha
wk	weeks
YFP	Yellow fluorescent protein

Chapter I

Introduction

Overview

Early fetal lung buds progress through multiple stages to become a highly branched organ with an expanded surface area necessary for gas exchange. During the late stages of lung development, pre-alveoli saccules form and expand at the end of airways. Bronchopulmonary dysplasia (BPD) occurs when development of the fetal lung is arrested at the saccular stage in preterm infants (Coalson 2003). Infants with BPD have abnormal lung pathology, with a thickened interstitium and reduced surface area available for gas exchange (Chess et al. 2006). Even if infants survive BPD, there are serious long-term health consequences, including more severe reactions to infections with frequent hospitalizations. Currently, the limited treatment options for BPD are steroids, vitamin A supplementation, and oxygen therapy. In many cases, these treatments do not resolve BPD (Jobe et al. 2001). Additional research is required to define the pathway of fetal lung inflammation and how it leads to BPD.

Changes in developmental cues directing alveolarization can prevent normal septation of saccules into alveoli. Signaling required for airway branching can be disrupted in utero or after birth. In utero exposure to infection or ex utero ventilation, hyperoxia, hypoxia, and infection are risk factors leading to inhibited lung development (Jobe 2003). These risk factors all initiate inflammation in the fetal lung. Proinflammatory cytokines are present in the amniotic fluid and tracheal aspirate fluid isolated from infants with BPD (Cayabyab et al. 2003). Identifying the

components involved with the inflammatory process in the fetal lung will guide the development of new therapies for BPD.

Mouse models have linked inflammation with abnormal fetal lung development, but have not addressed the source of fetal inflammation. In utero, chorioamnionitis led to abnormal lung development in fetal mice. Isolated fetal lung explants exposed to LPS have reduced branching and inhibited expression of growth factors required for lung development (Benjamin et al. 2007). When IL-1β is overexpressed during lung development, there is abnormal postnatal lung morphogenesis (Bry et al. 2007). However, the cells in the fetal lung that detect pathogens and produce an inflammatory response remained unidentifed. Using an NF-κB reporter mouse, we identified macrophages as the first cell type in mouse fetal lung explants to respond to the bacterial endotoxin LPS. Macrophages were also the primary sites of inflammation in the fetal lung. Macrophage activation was required and sufficient to alter fetal lung morphogenesis. We inhibited macrophage activation by depleting macrophages and deleting IKKβ in macrophages. Macrophage depletion and inhibition of NF-κB protected fetal lung explants from the effects of LPS. When we activated NF-κB in macrophages, lung morphogenesis was disrupted, resulting in a BPD-like phenotype. After identifying macrophages as the main cell type driving inflammation, we directed our research to focus on the capabilities of fetal lung macrophages. Fetal lung macrophages isolated in vitro could polarize in response to varying stimuli. However, fetal lung macrophages respond differently in vivo. Isolated macrophages showed that NF-κB activation in vivo does not completely polarize fetal lung macrophages, but induces their maturation. The two fetal macrophage subpopulations, $CD11b^{hi}F4/80^{lo}$ and $CD11b^{lo}F4/80^{hi}$, became skewed during inflammation. With NF-κB activation, there was an increase in the $CD11b^{lo}F4/80^{hi}$ subpopulation of fetal lung macrophages, and these macrophages shared similar

marker expression with mature alveolar macrophages. Fetal lung macrophages have inherent changes after activation. We have shown the importance of macrophages in fetal lung inflammation.

Proinflammatory cytokines are present in the fetal lung of infants with BPD. IL-1β has been suggested as the specific proinflammatory cytokine responsible for abnormal lung development (Bry et al. 2007). To produce IL-1β, the inflammasome is required for processing and release of the active IL-1β peptide. Blocking IL-1β activity, using a neutralizing antibody to IL-1β, protected fetal lung explants from the effects of LPS. Inhibiting the effector component of the inflammasome, caspase1, also protected fetal lung explant branching from LPS. Important inflammasome components are developmentally regulated, with increased expression during the saccular stage. Both IL-1β and the inflammasome contribute to abnormal lung morphogenesis, and both are strong drug targets to quench fetal lung inflammation.

Prior to this research, it was unknown which cells in the fetal lung were responsible for the inflammatory response. We have identified the cell type necessary for fetal lung inflammation, the macrophage. Through NF-κB activation in macrophages, the fetal lung has disrupted airway development. Fetal lung macrophages are capable of polarizing in vitro, but have a unique, complex response to NF-κB in vivo that does not follow the polarization paradigm. By recognizing the large role macrophages have in fetal lung disease, we can begin to understand what factors are involved in fetal inflammation and direct the course of future research in fetal macrophage biology.

Many potential areas of fetal macrophage research can have large impacts for infants with BPD. The jobs of macrophages throughout lung development have not been well characterized. Further, it is unknown how these roles can change during a state of homeostasis to

inflammation. There may be differences in the roles of fetal macrophage subpopulations as well. Due to the large role macrophages have in fetal lung inflammation in mice, there is likely a parallel role for macrophages in the lungs of infants with BPD. Future studies will focus on samples acquired from BPD patients to receive potential therapeutics and determine how macrophages change. Our research provides a new target cell for treatment options for BPD that could potentially be more effective and successful.

Developmental Progression of Lung Morphogenesis

In the mouse, the fetal lung develops from two simple buds into a highly organized and branched network efficient at gas exchange. The endoderm and mesoderm become an interconnected tree-like structure that continuously provides oxygen to the body. Initially, the ventral foregut endoderm is specified as future lung tissue (Cardoso and Lü 2006). After specification, there are five distinct stage of lung development, occurring both pre- and postnatally. The embryonic stage of lung development begins on gestation day 9.5 (E9.5) and is defined by two lung buds protruding from the endoderm into the surrounding mesoderm (Morrisey and Hogan 2010). Further elongation and separation of the lung buds from the endodermal tube form the main bronchi and trachea (Morrisey and Hogan 2010).

After the main branches are formed in the early mouse fetal lung, multiple rounds of regulated branching form the tree-like structure during the pseudoglandular stage. The pseudoglandular stage occurs from E12.5 to E16.5. The fetal lung undergoes highly routine stereotypical branching to form a network of bronchi and bronchioles (Metzger et al. 2008). Following lung bud extension and elongation, lung bud tips swell and bifurcate (Metzger et al. 2008). Tightly controlled signaling and cross-talk between the endoderm and mesoderm are

required for regulated and stereotypical branching to occur. Adjacent endoderm and mesoderm each release combinations of branching activators and inhibitors. Fibroblast growth factor 10 (FGF-10) is produced in the mesoderm adjacent to the tips of distal lung buds and is essential for fetal lung branching (Bellusci et al. 1997). FGF-10 deletion during development prevents fetal lung formation (Min et al. 1998). FGF-10 induces proliferation and elongation in epithelial cells at the tips of branching airways (Park et al. 1998). Sonic hedgehog (Shh) expressed in the distal epithelium and negatively regulates FGF-10 expression to inhibit branching in the wrong location (Bellusci et al. 1997; Chuang et al. 2003; Lebeche et al. 1999). In the mesenchyme, transcription growth factor β (TGFβ) inhibits branching along the stalks and in between airways (Heine et al. 1990; Serra et al. 1994; Zhao et al. 1996). The mesothelial lining of the lung produces FGF-9 to signal the mesenchyme to increase FGF-10 expression (del Moral et al. 2006). By the end of the pseudoglandular stage, these processes have completed branching of the bronchial tree, resulting in terminal end buds that will eventually give rise to the lung respiratory units.

After the large airway network is established in the fetal mouse lung, the formation of the distal airways beings during the canalicular stage. From E16.5-E17.5 the distal buds narrow, becoming respiratory bronchioles and alveolar ducts. In addition to increased branching, vasculature development occurs, increasing fetal lung size (Morrisey and Hogan 2010). The saccular stage occurs from E17.5 until birth. During the saccular stage, the ends of the distal buds form small sacs that become alveoli (Warburton et al. 2010). Additionally, the interstitium begins to thin and both the epithelial and mesenchyme differentiate (Warburton et al. 2010). Epithelial and mesenchymal cell differentiation is important to form the thin structure of alveoli and blood vessel needed for gas exchange. The distal epithelium will differentiate into thin type I

cells, involved in gas exchange, and type II cells, producers of surfactant (Rawlins et al. 2009). The mesoderm differentiates into myofibroblasts, airway smooth muscle cells, pericytes, and vascular smooth muscle cells (Morrisey and Hogan 2010). Blood vessels are arranged adjacent to type I epithelial cells for gas exchange (Morrisey and Hogan 2010). The final stage of lung development, the alveolar stage, begins at birth and is completed at postnatal day 30 (P30) in mice (Warburton et al. 2010). During alveolarization, the saccules undergo further division to increase the overall surface area available for gas exchange. While airway branching ceases postnatally, the lungs continue to grow from the elongation of airways and septation of alveoli (Morrisey and Hogan 2010).

Bronchopulmonary Dysplasia and Disrupted Lung Development

Bronchopulmonary dysplasia (BPD) is a chronic lung disease found in the smallest preterm infants. Up to 50% of very low birth weight (<1000g) preterm infants, or approximately 10,000 infants, develop BPD every year (Christou and Brodsky 2005). Infants are diagnosed with BPD after oxygen dependence for 28 postnatal days (Baraldi and Filippone 2007). Preterm infants born during the late canalicular or early saccular stage, between 24-28 weeks, are the most at risk for developing BPD (Coalson 2003). Lung histology from BPD patients shows dramatic morphological changes. Their lungs have large airways surrounded by a thickened interstitium (Chess et al. 2006). Due to inhibited alveolar septation, there is reduced surface area available for gas exchange (Chess et al. 2006). To stifle inflammation and aid lung function, corticosteroids, surfactant replacement, vitamin A supplementation, and oxygen have been used as therapies (Jobe et al. 2001). Even with current treatment options, 20-40% of infants with BPD do not survive (Christou and Brodsky 2005). Of those that do survive, there are long-term effects

from sustained lung damage (Jacob et al. 1998). After BPD, children have an increased likelihood of developing respiratory infections and an increased frequency of re-hospitalization (Smith et al. 2004).

There are many risk factors that increase the likelihood of developing BPD. Preterm birth is one of the main risk factors for BPD. The largest risk factor for preterm birth is chorioamnionitis, the inflammation of the placenta and extra-embryonic structures due to infection (Romero et al. 2002). Approximately 87% of preterm births delivered before 27 weeks gestation are born to mothers with chorioamnionitis (Chess et al. 2006). Infections causing chorioamnionitis can have multiple different bacteria present, including *Ureaplasma urealyticum*, *Mycoplasma hominis*, *Staphylococcus aureus*, and *Escherichia coli* (Romero et al. 2002). There is a strong association between the presence of IL1β, neutrophils, and macrophages in preterm lungs and maternal chorioamnionitis (Cayabyab et al. 2003). Other risk factors for BPD are postnatal infection, resuscitation, hyperoxia, and mechanical ventilation (Jobe 2003). All of these risk factors can induce the production and release of proinflammatory cytokines (Jobe 2003). Chorioamnionitis may have a role priming the fetal lung for inflammation, as BPD occurs most often in infants with chorioamnionitis and either infection or are on a ventilator (Watterburg et al. 1996). Exposure to multiple risk factors increases the likelihood of BPD (Jobe 2003).

While many risk factors have been identified, the mechanism of BPD development is still being researched. Animal models of chorioamnionitis have been helpful to study lung development during inflammation. Intra-amniotic injections of endotoxin in fetal lambs induced a proinflammatory cytokine response in extraembryonic structures and the fetal lung (Kallapur et al. 2001). While inflammatory cytokines were observed to induce lung maturation, the number of

alveoli was reduced by a third (Willet et al. 2000). IL-1β is one of the proinflammatory cytokines detected in the amniotic fluid of infants born with BPD (Watterburg et al. 1996). A mouse model inducing IL-1β expression in the fetal lung led to an abnormal postnatal lung morphology, resembling BPD (Bry et al. 2007). Saccular stage IL-1β expression impaired alveolarization and angiogenesis (Bry et al. 2007). Using lung samples from BPD patients, mesenchymal cell were disorganized and there was reduced FGF-10 expression (Benjamin et al. 2007). Similarly, a mouse model of chorioamnionitis also shows reduced FGF-10 expression in fetal lung and irregular smooth muscle actin staining (Benjamin et al. 2007). It is clear that inflammation is a major factor in BPD development and it affects the signaling factors needed for lung development. However, research is still needed to define the inflammatory pathway leading to BPD.

Development of Fetal Lung Macrophages

Macrophages were named and described by Mechnikov in the 1890's after he first visualized the uptake of microorganisms by phagocytosis (Ovchinnikov 2008; Lichanska and Hume 2000). Macrophages are part of the innate immune system and classified as leukocytes, or white blood cells (Geissmann et al. 2010). Part of the leukocyte family is the mononuclear phagocytes, which encompass hematopoietic derived cells of the myeloid lineage (Geissmann et al. 2010). Adult hematopoiesis begins with a hematopoietic stem cell that matures into myeloid precursors followed by a promonocyte stage. Promonocytes develop into monocytes, which mature into macrophages (Shepard and Zon 2000).

Before the bone marrow has developed, early embryonic hematopoiesis occurs at different locations. In the early embryo, macrophages are first detected in the yolk sac prior to

the start of hematopoiesis and circulatory development (Lichanska and Hume 2000). The first population of macrophages within the yolk sac is maternally-derived and are thought to be a transient population used for short term support (Bertrand et al. 2005). After maternal macrophages colonize the yolk sac between E7-7.5, fetal-derived myeloid precursors are detected in the yolk sac mesoderm at E8 (Bertrand et al. 2005). These myeloid precursors develop by yolk sac myelopoiesis within blood islands, a process called primitive hematopoiesis. Yolk sac myelopoiesis is unique in that macrophages develop from precursors that bypass an intermediate monocyte stage (Bertrand et al. 2005).

The third population of myeloid cells in the yolk sac develops from hematopoietic stem cell (HSC) precursors. HSC precursors enter circulation and migrate to the aorta-gonad-mesonephros (AGM) region in the E9 embryo (Cumano and Godin 2007; Ovchinnikov 2008). After populating the AGM, HSCs develop from the aorta region of the AGM (de Bruijin et al. 2000). HSCs then colonize the fetal liver at E10.5, which marks the beginning of fetal hematopoiesis (Cumano and Godin 2007; Medvinsky et al. 2011). HSCs in the fetal liver undergo hematopoiesis, also called definitive hematopoiesis, to expand and differentiate (Orkin and Zon 2008; Ovchinnikov 2008). After fetal liver hematopoiesis begins, there is a drastic increase in the number of macrophages throughout the embryo (Ovchinnikov et al. 2008). The spleen and bone marrow, which sustain adult hematopoiesis, are colonized by HSCs at E12.5 and E16.5, respectively (Medvinsky et al. 2011).

Multiple factors are required for a HSC to develop into a macrophage. HSCs are first specified as myeloid progenitor cells, which then become committed monocyte precursors. The transcription factor c-Myb is required for HSCs to develop into myeloid progenitor cells, while PU.1 is required for the differentiation of myeloid progenitors (DeKoter et al 1998; Schulz et al.

2012). c-Myb is expressed by myeloid progenitors, and its expression is reduced as these progenitors differentiate (Mucenski et al. 1991). In the absence of c-Myb, myeloid progenitors are severely reduced in the fetal liver (Mucenski et al. 1991; Sumner et al. 2000). In addition, $CD11b^{+}F4/80^{+}$ macrophages were found in the yolk sacs of $Myb^{-/-}$ embryos, further supporting the role of c-Myb in HSC differentiation (Schulz et al. 2012). PU.1 is a transcription factor expressed in cells derived from hematopoietic precursors, including B cells, macrophages, and granulocytes (McKercher et al. 1996). When PU.1 is absent, these populations are missing in neonates (McKercher et al. 1996; Scott et al. 1994). Differentiated stem cells derived from $PU.1^{-/-}$ embryos express early myeloid markers but are missing late myeloid markers (Olson et al. 1995). $PU.1^{-/-}$ hematopoietic cells did not express Csf1r, leading to an inhibited response to macrophage colony-stimulating factor (M-CSF) (Anderson et al. 1998; DeKoter et al. 1998). This indicates PU.1 is required for myeloid progenitors to differentiate into cell-specific lineages, but is not required for HSCs to become specified as myeloid and lymphoid progenitors (McKercher et al. 1996; Scott et al. 1994; DeKoter et al. 1998). PU.1 regulates transcription of other myeloid-specific genes, including M-CSF, granulocyte-macrophage colony-stimulating factor (GM-CSF), colony-stimulating factor receptor 1 (Csf1r), lysozyme M, CD11b, and IL1β (Hohaus et al. 1995; Lichanska et al. 1999; Pahl et al. 1993; Smith et al. 1996; Zhang et al. 1994). The growth factor M-CSF is necessary for myeloid progenitors to become monocytes and macrophages. M-CSF binds Csf1r and is a factor required for progenitor cell development into macrophages (Stanley et al. 1983). M-CSF induces proliferation and differentiation of myeloid progenitors and macrophages (Stanley et al. 1983). The absence of M-CSF reduces the number of monocytes and macrophages, but does not alter progenitor cell number (Wiktor-Jedrzejczak et al. 1982; Wiktor-Jedrzekczak et al. 1990; Yoshida et al. 1990).

Macrophage Function and Polarization Response

Macrophages have a variety of functions that are niche-specific. Macrophages are required for trophic roles in tissues, such as branching morphogenesis, angiogenesis, and efferocytosis. When macrophages are absent, mammary gland outgrowth and branching is inhibited (Van Nguyen and Pollard 2002). The absence of macrophages prevents normal extracellular remodeling and maintenance of mammary stem cell function (Wynn et al. 2013). When fetal macrophages are absent during pancreas and kidney development, there are abnormalities in tissue formation (Pollard 2009). Macrophages residing in the developing brain as microglia secrete factors for neuron growth and survival (Wynn et al. 2013). Fetal macrophages regulate angiogenesis in ocular development by inducing apoptosis in extraneous endothelial cells (Lobov et al. 2005). A large role for fetal macrophages is efferocytosis, the phagocytosis of apoptotic cells. Early in development, fetal macrophages are located in areas of high apoptosis, such as the interdigital region of the limb buds (Hume 2006, Sasmono et al. 2003). When apoptotic cells cannot be cleared, due to the lack of expression of the phosphatidylserine receptor, fetal lungs have an abnormal morphology, with reduced airspace and a thickened mesenchyme (Li et al. 2003). Fetal macrophages have active roles during embryonic tissue development, leading to altered tissue morphogenesis when macrophage development and function is manipulated.

Macrophage function has been used to help categorize the heterogeneity found among macrophage subsets. Local microenvironment factors and external pathogens contribute to macrophage phenotype polarization. The classical macrophage activation (M1) occurs in response to TLR signaling, INFγ, TNF-α, and tumor cell recognition (Martinez and Gordon

2014; Sharif et al. 2007). M1 macrophages produce antimicrobial products, such as reactive oxygen species, and proinflammatory cytokines as a defense mechanism (Sica and Mantovani 2012). Macrophages that are not following the traditional response are defined as alternatively activated macrophages (M2). In general, M2 macrophages respond to parasitic infection, promote wound healing, and encourage tumor progression (Martinez and Gordon 2014). However, there are multiple types of M2 macrophages, ranging from M2a to M2d, that have different stimuli and responses (Mantovani et al. 2004). IL-4 and IL-13 from injured tissue activate M2a macrophages to produce collagen for new extracellular matrix (Mantovani et al. 2004). When wound healing goes into overdrive and becomes chronic, M2 macrophages contribute to fibrosis (Bellon et al. 2011; Haymann et al. 2009). M2 macrophages also express high levels of scavenger receptors, phosphatidyl serine receptors, and integrins for the clearance of apoptotic cells (Mosser and Edwards 2008).

Interestingly, NF-κB plays a role in both M1 and M2 macrophage activation. TLR signaling activates NF-κB, which increases expression of proinflammatory genes in macrophages (Sica and Mantovani 2012). NF-κB is also present during the resolution of inflammation, which activates M2 macrophages (Sica and Mantovani 2012). There are disease states that have polarized macrophages that contribute to disease progression. M2d macrophages are tumor-associated macrophages that promote tumor growth and metastasis (Pollard 2004). There are cases of macrophages either changing phenotype or being replaced by macrophages of opposing phenotype during disease initiation and progression. M2 macrophages are present in the adipose tissue of lean mice, but shift to M1 macrophages during obesity, contributing to insulin resistance (Lumeng et al. 2007).

IL-1β Production in Macrophages

Proinflammatory signaling in macrophages begins with activation of the NF-κB pathway. Macrophages have pattern recognition receptors (PRRs) to detect pathogen associated molecular patterns (PAMPs), expressed by multiple infectious agents. Specific subsets of PRRs are Toll-like receptors (TLRs). TLRs are expressed by both immune cells, such as macrophages and dendritic cells, but also by non-immnune cells, like fibroblasts and epithelial cells (Kawai and Akira 2007). TLRs form a group of more than thirteen receptors that recognize pathogens ranging from gram negative and positive bacteria, viral proteins, and fungi (Kawai and Akira 2007). After TLR activation, downstream signaling requires a complex of adaptor proteins with MyD88, IRAK, and TRAF that activate the NF-κB pathway (Rothwarf and Karin 1999) (Figure 1.1).

Prior to TLR signaling, NF-κB is sequestered in the cytosol in a non-active form. NF-κB is formed from heterodimers (p65/p50) or homodimers (p50/p50), with p65 and p50 forming canonical NF-κB (Gilmore 2006). To keep NF-κB in the cytosol, inhibitor of NF-κB (IκB) binds and blocks the DNA-binding site of NF-κB (Beg et al. 1992). Upon activation, IκB Kinase (IKKβ) phosphorylates IκB, which is ubiquitinated and degraded (Napetschnig and Wu 2013). NF-κB is free to translocate into the nucleus and bind transcriptional targets. NF-κB

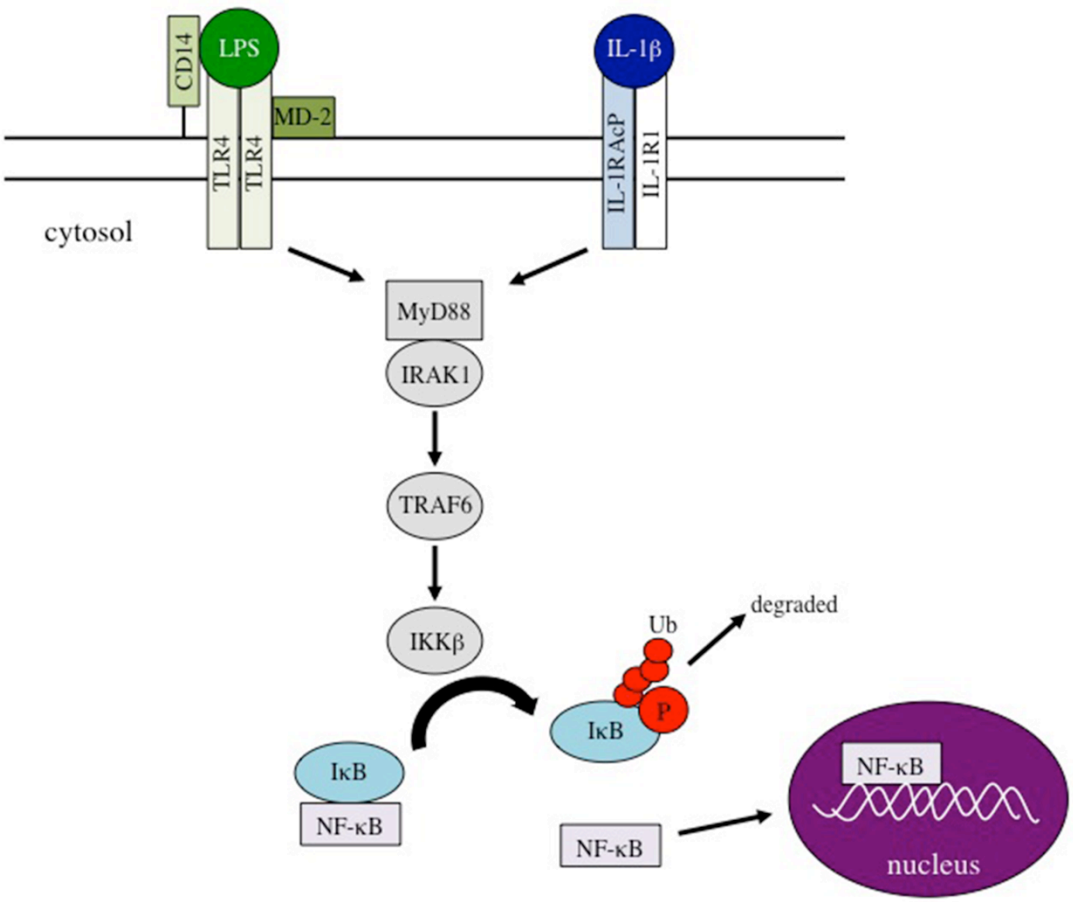

Figure 1.1. TLR4 and IL-1R1 signaling pathway. After TLR4 and IL-1R1 activation, they share intracellular components to activate NF-κB.

increases gene expression of many proinflammatory cytokines and chemokines. NF-κB activation is transient and cyclical as it becomes activated and deactivated from continuous receptor signaling (Gilmore 2006). NF-κB signaling is quenched as IκB is synthesized and binds to nuclear NF-κB, blocking it from future activity (Rothwarf and Karin 1999).

A major target of NF-κB is the proinflammatory cytokine IL-1β. After TLR activation, NF-κB increases transcription of IL-1β. IL-1β is initially formed as a p31 propeptide, which much be cleaved by the inflammasome into a p17 active peptide (Dinarello 1998). While there are different inflammasome models that have varying components, the NLRP3 inflammasome is the most characterized at present. The NLRP3 inflammasome regulates the maturation and secretion of IL-1β and IL-18 (Petrilli et al. 2007). The inflammasome becomes activated by bacteria, fungi, and parasites (Strowig et al. 2012). ATP and the production of reactive oxygen species can also induce inflammasome activation (Schroder and Tschopp 2010). The NLRP3 inflammasome is a multi-protein complex formed with NLRP3, ASC, and cleaved caspase 1 (Strowig et al. 2012). NLRP3 has a nucleotide binding domain and a caspase recruitment domain, which are necessary for its role as scaffolding for the inflammasome (Martinon and Tschopp 2007). ASC acts as an adaptor protein for the complex (Schroder and Tschopp 2012). Caspase-1 exists in an inactive state as a zymogen, but auto-activates upon oligomerization of NLRP3 (Schroder and Tschopp 2012). Interestingly, adult macrophages have ASC and pro-caspase constitutively expressed (Strowig et al. 2012).

Research Plan Description

Inflammation is a big risk factor for developing BPD. Inflammatory cytokines are present in the lungs of infants that develop BPD. In addition, mouse models strongly implicate inflammation in abnormal lung pathology. Bacterial LPS inhibits lung development in chorioamnionitis and lung explant models. However, there are no studies resolving the pathway of events from pathogen detection to abnormal lung morphogenesis. This research focuses on the following questions: Which immune cells are responsible for pathogen recognition in the fetal lung? Are macrophages the critical immune cell required for the fetal lung to respond to pathogens? Can the macrophage response to pathogens be detrimental to lung development? Do fetal lung macrophages become polarized after pathogen detection or NF-κB detection? Does NF-κB activation in macrophages alter the normal macrophage population in the fetal lung? While the role of macrophages in the fetal lung has not been studied in depth, there are examples indicating their potential role. Current research has linked defective efferocyotsis, normally completed by macrophages, to abnormal lung development (Li et al. 2003). The possibility of fetal lung macrophages having many diverse functions supporting lung morphogenesis remains undetermined.

The Prince laboratory first began to investigate these questions. They used multiple mouse models for lung explant culture and in vivo lung studies. Initially, they identified the cells that rapidly respond to pathogens in the fetal lung. The Prince laboratory used lung explants from the NGL reporter mouse to observe the first cells to activate NF-κB in response to LPS. Since macrophages are the initial responders to LPS, they wanted to determine if macrophages controlled the fetal lung inflammatory response. To do so, they used two mouse models that would inhibit NF-κB in macrophages, through IKKβ deletion, or would activate NF-κB in

macrophages, through a constitutively active IKKβ. They measured airway branching and IL-1β protein levels. My initial experiments in the Prince laboratory focused on characterizing the morphology of fetal lungs after IKKβ activation in macrophages. We found that fetal lung development was inhibited by NF-κB activity in macrophages.

From this research, we were able to identify two specific questions that had previously been unanswered: (1) Do fetal lung macrophages have the potential to change phenotype? (2) Do macrophage-released proinflammatory cytokines disrupt fetal lung development? When macrophages were determined to be necessary and sufficient to inhibit lung development upon activation, we used *in vitro* macrophage cultures to understand the phenotype potential of fetal lung macrophages. As a complementary method, we used flow cytometry to identify subpopulations of macrophages in the fetal lung. After measuring increased levels of proinflammatory cytokines released after NF-κB activation in macrophages, we used neutralizing antibodies to proinflammatory cytokines within our in vitro lung explant models. We also used mouse models deleting inflammatory cytokine expression as an *in vivo* model. These projects were the basis for my research on fetal lung macrophages.

Our research, for the first time, linked disrupted fetal lung morphogenesis to a specific cell type, the macrophage. Further, we were able to identify changes within the fetal lung macrophage that did not follow any previously described pattern of activation. We also show that IL-1β is the primary proinflammatory cytokine responsible for the disruption of fetal lung development. Future investigations into BPD can now target a specific cell type, the macrophage, and a specific factor, IL-1β.

References

Anderson, Karen L., K. A. Smith, K. Conners, S. R. McKercher, R. A. Maki, B. E. Torbett (1998) Myeloid development is selectively disrupted in PU.1 null mice. *Blood* **91**: 3702-3710.

Baraldi, Eugenio and M. Filippone (2007) Chronic Lung Disease after Premature Birth. *N. Engl. J. Med.* **357**: 1946-1955.

Beg, Amer A., S. M. Ruben, R. I. Scheinman, S. Haskill, C. A. Rosen, A. S. Baldwin (1992) IκB interacts with the nuclear localization sequences of the subunits of NF-κB: a mechanism for cytoplasmic retention. *Genes Dev* **6**: 1899-1913.

Bellon, Teresa, V. Martinez, B. Lucendo, G. del Peso, M. J. Castro, L. S. Aroeira, A. Rodriguez-Sanz, M. Ossorio, R. Sanchez-Villanueva, R. Selgas, M. A. Bajo (2011) Alternative activation of macrophages in human peritoneum: implications for peritoneal fibrosis. *Nephrol. Dial. Transplant* **26**: 2995-3005.

Bellusci, Savério, J., Grindley, H. Emoto, N. Itoh, B. L.M. Hogan (1997) Fibroblast Growth Factor (FGF10) and branching morophogenesis in the embryonic mouse lung. *Development* **124**: 4867-4878.

Bellusci, Savério, J., Y. Furuta, M. G. Rush, R. Henderson, G. Winnier, B. L. Hogan (1997) Involvement of Sonic hedgehog (Shh) in mouse embryonic lung growth and morphogenesis. *Development* **124**: 53-63.

Benjamin, John T., R. J. Smith, B. A. Halloran, T. J. Day, D. R. Kelly, L. S. Prince (2007) FGF-10 is decreased in bronchopulmonary dysplasia and suppressed by Toll-like receptor activation. *Am. J. Physiol. Lung Cell Mol. Physiol.* **292**: 550-558.

Bertrand, Julien Y., A. Jalil, M. Klaine, S. Jung, A. Cumano, I. Godin (2005) Three pathways to mature macrophages in the early mouse yolk sac. *Blood* **106**: 3004-3011.

Bry, Kristina, J. A. Whitsett, U. Lappalainen (2007) IL-1β Disrupts Postnatal Lung Morphogenesis in the Mouse. *Am. J. Respir. Cell Mol. Biol.* **36**: 32-42.

Cardoso, Wellington V. and J. Lü (2006) Regulation of early lung morphogenesis: questions, facts and controversies. *Development* **133**: 1611-1624.

Cayabyab, Rowena G., C. A. Jones, K. Y. C. Kwong, C. Hendershott, C. Lecart, P. Minoo, R. Ramanathan (2003) Interleukin-1b in the bronchoalveolar lavage fluid of premature neonates: a marker for maternal chorioamnionitis and predictor of adverse neonatal outcome. *J. Matern. Fetal Neonatal Med.* **14**: 205-211.

Chuang, Pao-Tien, T. Kawcak, A. P. McMahon (2003) Feedback control of mammalian Hedgehog signaling by the Hedgehog-binding protein, Hip1, modulates Fgf signaling during branching morphogenesis of the lung. *Genes Dev*. **17**: 342-347.

Chess, Patricia R., C. T. D'Angio, G. S. Pryhuber, W. M. Maniscalco (2006) Pathogenesis of Bronchopulmonary Dysplasia. *Semin. Perinatol*. **30**: 171-178.

Christou, Helen and D. Brodsky (2005) Lung injury and bronchopulmonary dysplasia in newborn infants. *J. Intensive Care Med*. **20**: 76-87.

Coalson, Jacqueline J. (2003) Pathology of new bronchopulmonary dysplasia. *Semin. Neonatol*. **8**: 73-81.

Cumano, Ana and I. Godin (2007) Ontogeny of the Hematopoietuc System. *Annu. Rev. Immunol*. **25**: 745-785.

de Bruijin, Marella F., N. A. Speck, M. C. Peeters, E. Dzierzak (2000) Definitive hematopoietic stem cells first develop within the major arterial regions of the mouse embryo. *EMBO J*. **19**: 2465-2474.

DeKoter, Rodney P., J. C. Walsh, H. Singh (1998) PU.1 regulates both cytokine-dependent proliferation and differentiation of granulocyte/macrophage progenitors. *EMBO J* **17**: 4456-4468.

del Moral, P. M., S. P. De Langhe, F. G. Sala, J. M. Veltmaat, D. Tefft, K. Wang, D. Warburton, S. Bellusci (2006) Differential role of FGF9 on epithelium and mesenchyme in mouse embryonic lung. *Dev. Biol*. **293**: 77-89.

Dinarello, C. A. (1998) Interleukin-1 beta, interleukin-18, and the interleukin-1 beta converting enzyme. *Ann. NY Acad. Sci*. **856**: 1-11.

Geissmann, Frederic, M. G. Manz, S. Jung, M. H. Sieweke, M. Merad, K. Ley (2010) Development of monocytes, macrophages, and dendritic cells. *Science* **327**: 656-661.

Gilmore, T. D. (2006) Introduction to NF-κB: players, pathways, perspectives. *Oncogene* **25**: 6680-6684.

Heine, Ursula I., E. F. Munoz, K. C. Flanders, A. B. Roberts, M. B. Sporn (1990) Colocalization of TGF-beta 1 and collagen I and III, fibronectin and glycosaminoglycans during lung branching morphogenesis. *Development* **109**: 29-36.

Heymann, Felix, C. Trautwein, F. Tacke (2009) Monocytes and macrophages as cellular targets in liver fibrosis. *Inflamm. Allergy Drug Targets* **8**: 307-318.

Hohaus, Stefan, M. S. Petrovick, M. T. Voso, Z. Sun, D. E. Zhang, D. G. Tenen (1995) PU.1

(Spi-1) and C/EBP alpha regulate expression of the granulocyte-macrophage colony-stimulating factor receptor alpha gene. *Mol. Cell. Biol.* **15**: 5830-5845.

Hume, David A. (2006) The mononuclear phagocyte system. *Curr. Opin. Immunol.* **18**: 49-53.

Jobe, Alan H. (2003) Antenatal factors and the development of bronchopulmonary dysplasia. *Semin. Neonatol.* **8**: 9-17.

Jobe, Alan H. and E. Bancalari (2001) Bronchopulmonary Dysplasia. *Am. J. Resp. Crit. Care* **163**: 1721-1729.

Jacob, Sheila, A. Coates, L. Lands, C. MacNeish, S. Riley, L. Hornby (1998) Long-term pulmonary equelae of severe bronchopulmonary dysplasia. *J. Pediatr.* **133**: 193-200.

Kallapur, Suhas G., K. E. Willet, A. H. Jobe, M. Ikegami, C. J. Bachurski (2001) Intra-amniotic endotoxin: chorioamnionitis precedes lung maturation in preterm lambs. *Am. J. Physiol. Lung Cell Mol. Physiol.* **280**: 527-536.

Kawai, Taro and S. Akira (2007) Signaling to NF-κB by Toll-like receptors. *Trends Mol. Med.* **13**: 460-469.

Lebeche, Djamel, S. Malpel, W. V. Cardoso (1999) Fibroblast growth factor interactions in the developing lung. *Mech. Dev.* **86**: 125-136.

Li, Ming O., M. R. Sarkisian, W. Z. Mehal, P. Rakic, R. A. Flavell (2003) Phosphatidylserine receptor is required for clearance of apoptotic cells. *Science* **302**: 1560-1563.

Lichanska, Agnieszka M., C. M. Browne, G. W. Henkel, K. M. Murphy, M. C. Ostrowski, S. R. McKercher, R. A. Maki, D. A. Hume (1999) Differentiation of the mononuclear phagocyte system during mouse embryogenesis: the role of transcription factor PU.1. *Blood* **94**: 127-138.

Lichanska, Agnieszka M., D. A. Hume (2000) Origins and functions of phagocytes in the embryo. *Exp. Hematol.* **28**: 601-611.

Lobov, Ivan B., S. Rao, T. J. Carroll, J. E. Vallance, M. Ito, J. K. Ondr, S. Kurup, D. A. Glass, M. S. Patel, W. Shu, E. E. Morrisey, A. P. McMahon, G. Karsenty, R. A. Lang (2005) WNT7b mediates macrophage-induced programmed cell death in patterning of the vasculature. *Nature* **437**: 417-421.

Lumeng, Carey N., J. L. Bodzin, A. R. Saltiel (2007) Obesity induces a phenotypic switch in adipose tissue macrophage polarization. *J. Clin. Invest.* **117**: 175-184.

Mantovani, Alberto, A. Sica, S. Sozzani, P. Allavena, A. Vacchi, M. Locati (2004) The chemokine system in diverse forms of macrophage activation and polarization. *Trends Immunol.* **25**: 677-686.

Martinez, Fernando O. and S. Gordon (2014) The M1 and M2 paradigm of macrophage activation: time for reassessment. *F1000Prime Reports* **6**: 13.

Martinon, F. and J. Tschopp (2007) Inflammatory caspases and inflammasomes: master switches of inflammation. *Cell. Death Diff.* **14**: 10-22.

McKercher, Scott R., B. E. Torbett, K. L. Anderson, G. W. Henkel, D. J. Vestal, H. Baribault, M. Klemsz, A. J. Feeney, G. E. Wu, C. J. Paige, R. A. Maki (1996) Targeted disruption of the PU.1 gene results in multiple hematopoietic abnormalities. *EMBO J* **15**: 5647-5658.

Medvinsky, Alexander, S. Rybtsov, S. Taoudi (2011) Embryonic origin of the adult hematopoietic system: advances and questions. *Development* **138**: 1017-1031.

Metzger, Ross J., O. D. Klein, G. R. Martin, M. A. Krasnow (2008) The branching programme of mouse lung development. *Nature* **453**: 745-751.

Min, Hosung, D. M. Danilenko, S. A. Scully, B. Bolon, B. D. Ring, J. E. Tarpley, M. DeRose, W. S. Simonet (1998) *Fgf-10* is required for both limb and lung development and exhibits striking functional similarity to *Drosophila branchless*. *Genes Dev*. **12**: 3156-3161.

Morrisey, Edward E. and B. L.M. Hogan (2010) Preparing for the First Breath: Genetic and Cellular Mechanisms in Lung Development. *Dev. Cell* **18**: 8-23.

Mosser, David M., J. P. Edwards (2008) Exploring the full spectrum of macrophage activation. *Nat. Rev. Immunol*. **8**: 958-969.

Mucenski, Michael L., K. McLain, A. B. Kier, S. H. Swerdlow, C. M. Schreiner, T. A. Miller, D. W. Pietryga, W. J. Scott, S. S. Potter (1991) A functional c-myb gene is required for normal murine fetal hepatic hematopoiesis. *Cell* **65**: 677-689.

Napetschnig, Johanna and H. Wu (2013) Molecular Basis of NF-κB Signaling. *Annu. Rev. Biophys*. **42**: 443-468.

Nold, Marcel F., N. E. Mangan, I. Rudloff, S. X. Cho, N. Shariatian, T. D. Samarasinghe, E. M. Skuzka, J. Pederson, A. Veldman, P. J. Berger, C. A. Nold-Petry (2013) Interleukin-1 receptor antagonist prevents murine bronchopulmonary dysplasia induced by perinatal inflammation and hyperoxia. *Proc. Natl. Acad. Sci. U.S.A*. **110**: 14384-14389.

Olson, Marilyn C., E. W. Scott, A. A. Hack, G. H. Su, D. G. Tenen, H. Singh, M. C. Simon (1995) PU.1 is not essential for early myeloid gene expression but is required for terminal myeloid differentiation. *Immunity* **3**: 703-714.

Orkin, Stuart H. and L. I. Zon (2008) Hematopoiesis: an evolving paradigm for stem cell biology. *Cell* **132**: 631-644.

Ovchinnikov, Dmitry A. (2008) Macrophages in the embryo and beyond: much more than just giant phagocytes. *Genesis* **46**: 44-462.

Ovchinnikov, Dmitry A., W. J. M. van Zuylen, C. E. E. DeBats, K. A. Alexander, S. Kellie, D. A. Hume (2008) Expression of Gal4-dependent transgenes in cells of the mononuclear phagocyte system labeled with enhanced cyan fluorescent protein using *Csf1r*-Gal4VP16/UAS-ECFP double-transgenic mice. *J. Leukocyte Biol.* **83**: 430-433.

Pahl, Heike L., Scheibe, Renate J., D. E. Zhang, H. Chen, D. L. Galson, R. A Maki, D. G. Tenen (1993) The proto-oncogene PU.1 regulates expression of the myeloid-specific CD11b promoter. *J. Biol. Chem.* **268**: 5014-5020.

Park, William Y., B. Miranda, D. Lebeche, G. Hasimoto, W. V. Cardoso (1998) FGF-10 is a Chemotactic Factor for Distal Epithelial Buds during Lung Development. *Dev. Biol.* **201**: 125-134.

Petrilli, Virginie, C. Dostert, D. A. Muruve, J. Tschopp (2007) The inflammasome: a danger sensing complex triggering innate immunity. *Curr. Opin. Immunol.* **19**: 615-622.

Pollard, Jeffrey W. (2004) Tumour-educated macrophages promote tumour progression and metastasis. *Nat. Rev. Cancer* **4**: 71-78.

Pollard, Jeffrey W. (2009) Trophic macrophages in development and disease. *Nat. Rev. Immunol.* **9**: 259-270.

Romero, Roberto, J. Espinoza, T. Chaiworapongsa, K. Kalache (2002) Infection and prematurity and the role of preventive strategies. *Semin. Neonatol.* **7**: 259-274.

Rawlins, E. L., C. P. Clark, Y. Xue, B. L. Hogan (2009) The Id2+ distal tip lung epithelium contains individual multipotent embryonic progenitor cells. *Development* **136**: 3741-3745.

Rothwarf, David M. and M. Karin (1999) The NF-kB activation pathway: a paradigm in information transfer from membrane to nucleus. *Science Signaling* **5**: 1-16.

Sasmono, R. Tedjo, D. Oceandy, J. W. Pollard, W. Tong, P. Pavil, B. J. Wainwright, M. C. Ostrowski, S. R. Himes, D. A. Hume (2003) A macrophage colony-stimulating factor receptor-green fluorescent protein transgene is expressed throughout the mononuclear phagocyte system of the mouse. *Blood* **101**: 1155-1163.

Schroder, Kate and J. Tschopp (2010) The inflammasomes. *Cell* **140**: 821-832.

Schulz, Christian, E. G. Perdiguero, L. Chorro, H. Szabo-Rogers, N. Cagnard, K. Kierdoff, M. Prinz, B. Wu, E. R. Jacobsen, J. W. Pollard, J. Frampton, K. J. Liu, F. Geissmann (2012) A lineage of myeloid cells independent of Myb and hematopoietic stem cells. *Science* **336**: 86-90.

Scott, Edward W., M. C. Simon, J. Anastasi, H. Singh (1994) Requirement of transcription factor PU.1 in the development of multiple hematopoietic lineages. *Science* **265**; 1573-1577.

Serra, Rosa R. W. Pelton, H. L. Moses (1994) TGF beta 1 inhibits branching morphogenesis and N-myc expression in lung bud organ cultures. *Development* **120**: 2153-2161.

Sharif, Omar, V. N. Bolshakov, S. Raines, P. Newham, N. D. Perkins (2007) Transcriptional profiling of the LPS induced NF-κB response in macrophages. *BMC Immunology* **8**: 1.

Shepard, Jennifer L. and L. I. Zon (2000) Developmental derivation of embryonic and adult macrophages. *Curr. Opin. Hematol.* **7**: 3-8.

Sica, Antonio, A. Mantovani (2012) Macrophage plasticity and polarization: in vivo veritas. *J. Clin. Invest.* **122**: 787-795.

Smith, Laura T., S. Hohaus, D. A. Gonzalez, S. E. Dziennis, D. G. Tenen (1996) PU.1 (Spi-1) and C/EBP alpha regulate the granulocyte colony stimulating factor receptor promoter in myeloid cells. *Blood* **88**:1234-1247.

Stanley, E. R., L. J. Gullbert, R. J. Tushinski, S. H. Barteimez (1983) CSF-1-A mononuclear phagocyte lineage-specific hematopoietic growth factor. *J. Cell. Biochem.* **21**: 151-159.

Strowig, Till, J. Henao-Mejia, E. Elinav, R. Flavell (2012) Inflammasomes in health and disease. *Nature* **481**: 278-286.

Sumner, Robert, A. Crawford, M. Mucenski, J. Frampton (2000) Initiation of adult myelopoiesis can occur in the absence of c-Myb whereas subsequent development is strictly dependent on the transcription factor. *Oncogene* **19**: 3335-3342.

Van Nguyen, A. and J. W. Pollard (2002) Colony stimulating factor-1 is required to recruit macrophages into the mammary gland to facilitate mammary ductal outgrowth. *Dev. Biol.* **247**: 11-25.

Warburton, David, A. El-Hasah, G. Carraro, C. Tiozzo, F. Sala, O. Rogers, S. De Langhe, P. J. Kemp, D. Riccardi, J. Torgay, S. Bellusci, W. Shi, S. Lubkin, E. Jesudason (2010) Lung Organogenesis. *Curr. Top. Dev. Biol.* **90**: 73-158.

Watterburg, Kristi L., L. M. Demers, S. M. Scott, S. Murphy (1996) Chorioamnionitis and Early Lung Inflammation in Infants in Whom Bronchopulmonary Dysplasia Develops. *Pediatrics* **97**: 210-215.

Wiktor-Jedrzejczak, Wieslaw, A. Ahmed, C. Szczylik, R. Skelly (1982) Hematological characterization of congenital osteopetrosis in op/op mouse. *J. Exp. Med.* **156**: 1516-1527.

Wiktor-Jedrzejczak, Wieslaw, A. Bartocci, A. W. Farrante, A. Ahmed-Ansari, K. W. Sell, J. W. Pollard, E. R. Stanley (1990) Total absence of colony-stimulating factor 1 in the macrophage-deficient osteopetrotic (op/op) mouse. *Proc. Natl. Acad. Sci. U.S.A.* **87**: 4828-4832.

Willet, Karen E., A. H. Jobe, M. Ikegami, J. Newnham, S. Brennan, P. D. Sly (2000) Antenatal Endotoxin and Glucocorticoid Effects on Lung Morphometry in Preterm Lambs. *Pediatr. Res.* **48**: 782-788.

Wynn, Thomas A., A. Chawla, J. W. Pollard (2013) Macrophage biology in development, homeostasis and disease. *Nature* **496**: 445-455.

Yoshida, Hisahiro, S. Hayashi, T. Kunisada, M. Ogawa, S. Nishikawa, H. Okamura, T. Sudo, L. D. Schultz, S. Nishikawa (1990) The murine mutation osteopetrosis is in the coding region of the macrophage colony stimulating factor gene. *Nature* **345**: 442-443.

Zhang, Dong-er, C. J. Hetherington, H. M. Chen, D. G. Tenen (1994) The macrophage transcription factor PU.1 directs tissue-specific expression of the macrophage colony-stimulating factor receptor. *Mol. Cell. Biol.* **14**: 373-381.

Zhao, Jingsong, D. Bu, M. Lee, H. C. Slavkin, F. L. Hall, D. Warburton (1996) Abrogation of transforming growth factor-beta type II receptor stimulates embryonic mouse lung branching morphogenesis in culture. *Dev. Biol.* **180**: 242-257

Chapter II

NF-κB Signaling in Fetal Lung Macrophages Disrupts Airway Morphogenesis

Originally published in *The Journal of Immunology*, vol. 187, pp. 2740-2747, 20 July 2011.

Timothy S. Blackwell, Ashley N. Hipps, Yasutoshi Yamamoto, Wei Han, Whitney J. Barham, Michael C. Ostrowski, Fiona E. Yull and Lawrence S. Prince

Abstract

Bronchopulmonary dysplasia is a common pulmonary complication of extreme prematurity. Arrested lung development leads to bronchopulmonary dysplasia, but the molecular pathways that cause this arrest are unclear. Lung injury and inflammation increase disease risk, but the cellular site of the inflammatory response and the potential role of localized inflammatory signaling in inhibiting lung morphogenesis are not known. In this study, we show that tissue macrophages present in the fetal mouse lung mediate the inflammatory response to LPS and that macrophage activation inhibits airway morphogenesis. Macrophage depletion or targeted inactivation of the NF-κB signaling pathway protected airway branching in cultured lung explants from the effects of LPS. Macrophages also appear to be the primary cellular site of IL-1β production following LPS exposure. Conversely, targeted NF-κB activation in transgenic macrophages was sufficient to inhibit airway morphogenesis. Macrophage activation in vivo inhibited expression of multiple genes critical for normal lung development, leading to thickened

lung interstitium, reduced airway branching, and perinatal death. We propose that fetal lung macrophage activation contributes to bronchopulmonary dysplasia by generating a localized inflammatory response that disrupts developmental signals critical for lung formation.

Introduction

During fetal lung morphogenesis, simple epithelial tubes develop into a complex structure competent for gas exchange (Warburton et al. 2000; Metzger et al. 2008). This process fails to occur normally in preterm infants with bronchopulmonary dysplasia (BPD), a chronic disease that affects ~60% of preterm infants born before 28 wk (Stoll et al. 2010). BPD results from arrested airway morphogenesis during the canalicular and saccular stages of lung development. Normally during these stages, small terminal airways branch, expand, and divide to form alveolar ducts. In patients with BPD, arrested development leads to fewer saccular stage airways, reduced numbers of alveoli, and lower capacity for gas exchange (May et al. 2009). Infants born after the early saccular stage of development rarely develop BPD, suggesting that the canalicular and early saccular stages represent a window of disease susceptibility. Various environmental factors have been implicated in development of BPD, involving either airway epithelial injury or lung inflammation (Bhandari and Bhandari 2009, Baraldi and Filippone 2007). Understanding how these factors lead to arrested airway morphogenesis will be critical for developing new therapeutic approaches.

Several lines of clinical and experimental evidence suggest infection or injury leads to an inflammatory response that causes or exacerbates BPD. First, chorioamnionitis (infection and

inflammation of the amniotic membranes) is detected in up to 70% of preterm deliveries and is associated with increased BPD risk (Lahra et al. 2009). Second, infants that develop BPD often have elevated levels of inflammatory mediators in their airway both at birth and during the later stages of disease progression (Paananen et al. 2009; Benjamin et al. 2010). Third, injecting *Escherichia coli* LPS into the amniotic fluid of pregnant animals inhibits airway branching and prevents subsequent alveolar development (Prince et al. 2005; Willet et al. 2000). In developing an experimental mouse model for studying the mechanisms leading to BPD, we observed that LPS prevents saccular airway branching in both fetal mice and cultured fetal mouse lung explants. These data suggest innate immune activation and inflammatory signaling intersect with developmental pathways, interfering with processes required for branching morphogenesis.

LPS can inhibit airway branching in fetal lung explants in the absence of circulating inflammatory cells (Prince et al. 2005), suggesting that resident lung cells are competent to transduce signals that interrupt normal lung development. We have previously identified multiple gene targets of inflammatory signaling that are critical for normal airway morphogenesis (Benjamin et al. 2010, Benjamin et al. 2009; Benjamin et al. 2007; Miller et al. 2010). However, the cellular site of the initial innate immune response critical for disrupting development is not known. Among the cell types in the fetal lung, airway epithelia and vascular endothelia appear at least somewhat capable of responding to microbial products (Andonegui et al. 2003, Prince et al. 2004). To date, the potential role of macrophages in the fetal lung innate immune response has not been closely examined. Studies involving fetal macrophages have focused primarily on their ability to remove apoptotic cellular debris and remodel extracellular matrix (Henson and Hume

2006; Hopkinson-Woolley et al. 1994; Tomlinson et al. 2008). In this study, we report that macrophages are the primary cellular sites of the fetal lung innate immune response. Macrophage activation is required for the LPS-mediated production of inflammatory mediators that disrupt airway branching. In addition, targeted activation of fetal lung macrophages, both in cultured lung explants and developing mouse lungs in vivo, inhibits airway morphogenesis and produces a lung phenotype that closely resembles human BPD. Our findings indicate that macrophage activation and subsequent lung inflammation may play a key role in BPD pathogenesis.

Methods and Materials

Reagents

Gel-purified *E. coli* LPS (O55:B5) was purchased from Sigma-Aldrich. The following Abs were used for immunolabeling: rat anti-CD68 (Acris), rat anti-F4/80 (Acris), rat anti–E-cadherin (Zymed), rabbit anti-CD14 (Santa Cruz Biotechnology), and rabbit anti-GFP (Abcam). DAPI, TO-PRO-3 iodide, ProLong Gold antifade reagent with DAPI, and Alexa-conjugated secondary Abs were purchased from Invitrogen. Anti-CD11b Microbeads and magnetic separation equipment and reagents were purchased from Miltenyi Biotec. Reagents for preparing liposomal clodronate were obtained from Sigma-Aldrich. All cell culture media were purchased from Invitrogen. FBS was purchased from Thermo Fisher Scientific.

Mouse strains and lung explant culture

All animal experiments were thoroughly reviewed and approved by the Vanderbilt University Institutional Animal Care and Use Committee. BALB/cJ and Rosa26-YFP mice were obtained from The Jackson Laboratory. NGL (Everhart et al. 2006), LysM-Cre:IKK$\beta^{F/F}$ (Greten et al. 2004), and IKFM (L. Connelly, W. Barham, H.M. Onishko, L. Chen, T. Sherrill, T. Zabuawala, M.C. Ostrowski, T.S. Blackwell, and F.E. Yull, submitted for publication) mouse strains were developed and described previously. For timed pregnant matings, embryonal day 0 (E0) was defined as the morning of vaginal plug discovery. To induce transgene expression in IKFM mice, timed pregnant dams were given doxycycline-containing water (2 g/L) ad libitum. E15 fetal mouse lung explants were isolated and cultured as previously described (Prince et al. 2004). For transgenic models, lungs of each mouse embryo were minced and cultured separately. Approximately 20 explants were isolated from each embryo. All explants studied were between 0.8 and 1.2 mm in diameter at initial time of culture. To quantify saccular airway branching in cultured lung explants, brightfield images of explants were acquired every 24 h of culture. Airway branching was expressed as the number of new branches that formed between 24 and 72 h of culture in each explant. For macrophage depletion using clodronate, control or clondronate-containing liposomes were directly added to explants at the initial time of isolation. LPS was then added to the media 24 h later.

Fetal lung macrophage isolation

E15 fetal mouse lungs were dissected free of surrounding tissues and placed in ice-cold PBS. The lungs were homogenized and forced through 100-μm and 40-μm cell strainers. Cells were pelleted by centrifugation and resuspended in the presence of anti-CD11b–conjugated Microbeads (Miltenyi Biotec). The CD11b-labeled cells were collected using a magnetic

separator, washed, and plated in RPMI 1640 with 10% FBS. Following overnight culture at 37°C in 95% air/5% CO_2, macrophages were washed and treated for 4 h with LPS (250 ng/ml). NGL macrophages were similarly isolated, treated with LPS for various time points, and solubilized in Reporter Lysis Buffer (Promega). Luciferase activity was measured using SteadyGlo reagent (Promega) and a Synergy HT microplate reader (Biotek). Luciferase activity was normalized to total protein content as measured by BCA assay (Promega).

RNA isolation, real-time PCR, and IL-1β measurement

Total RNA isolation, cDNA synthesis, and real-time PCR were performed using standard techniques. Gene expression was compared using the $2^{-\Delta\Delta CT}$ method. Independent experiments were performed at least three separate times. Data between groups were compared by ANOVA or Student *t* test to test for significant differences. IL-1β concentrations were measured in homogenized fetal lung using the Quantikine Mouse IL-1β Immunoassay (R&D Systems). IL-1β concentrations were normalized to total protein as measured by BCA assay (Pierce).

Tissue Processing and Immunolabeling

Mouse lung tissue, fetal lung explants, and cultured macrophages were fixed, processed, and immunolabeled using standard techniques. For immunofluorescence, Alexa-conjugated secondary Abs were used for visualization, and nuclei were alternatively labeled with DAPI or TO-PRO-3. Immunohistochemical processing was performed using Vectastain Kits and 3,3′-diaminobenzidine visualization (Vector Laboratories) with Mayer's H&E counterstaining (Sigma-Aldrich).

Imaging and image analysis

Confocal images were acquired using either an Olympus FV1000 (Olympus) or Leica SPE (Leica Microsystems) laser scanning confocal microscope. Widefield fluorescence images and brightfield images of fetal mouse lung explants were obtained using an Olympus IX81 microscope equipped with a Hamamatsu Orca ER CCD monochrome camera and Slidebook software (Olympus). Color images of lung specimens were photographed using a Nikon TE800 and SPOT color CCD camera (Diagnostic Instruments). All microscopy images were saved in the Tagged Image File format and imported into Photoshop (Adobe Systems) for processing. Images for comparison were always identically processed. For live imaging of NF-κB activation, NGL explants were cultured in a stage-top incubator (Okolab) and imaged using an Olympus IX81 inverted microscope (Olympus) with a WeatherStation enclosure. Exact temperature, humidity, and CO_2 concentration were maintained during the imaging experiment. Fluorescence images were acquired every 10 min for the first 2 h and then every 20 min for 2–24 h of culture. Time series images were processed in Slidebook (Olympus). Lung morphometery and cell counting were performed using the Image Processing Tool Kit (Reindeer Graphics) within Photoshop (Adobe Systems). Fractional lung volumes were measured by analyzing images from serial fetal lung sections using a counting grid function. The fractions of airspace, large airway epithelia, small or distal airway epithelia, and mesenchyme were measured on E-cadherin–labeled sections. Septal thickness in newborn lungs was measured using the global intercept function. To account for possible anisotropy, intercepts in each image were measured over multiple iterations with 10° of rotation between each measurement. The mean intercept length for each image was recorded.

Results

LPS activates NF-κB in fetal lung macrophages

Where LPS initially activates the innate immune system in fetal lungs has not been identified. We therefore investigated the localization and kinetics of LPS-induced NF-κB activation in E15 fetal lung explants from NF-κB transgenic reporter mouse (NGL), which expresses GFP and luciferase downstream of a promoter synthesized from the NF-κB–binding repeats within the HIV-1 long terminal repeat (Everhart et al. 2006). Time-lapse imaging of NGL explants demonstrated NF-κB–dependent GFP expression by 90 min after LPS treatment, with continued GFP expression to 12 h (Fig. 2.1A–D). GFP expression localized to cells throughout the lung mesenchyme. To visualize the cellular site of NF-κB–GFP expression at higher resolution, we imaged NGL explants using confocal microscopy. As seen in Fig. 2.1E–M, 2 h of LPS treatment stimulated GFP expression predominantly in cells that colabeled with the macrophage marker CD68. Following 12 h of LPS treatment, GFP reporter expression was detected both in CD68-positive macrophages and in adjacent mesenchymal cells (arrows in Fig. 2.1G, 2.1M). The close proximity of GFP-expressing mesenchymal cells to CD68-postive macrophages suggests release of secondary inflammatory mediators that could then activate NF-κB in nearby cells.

Because macrophages were present in E15 fetal lungs and positioned to regulate inflammatory responses, we examined the timing of macrophage appearance into the fetal mouse

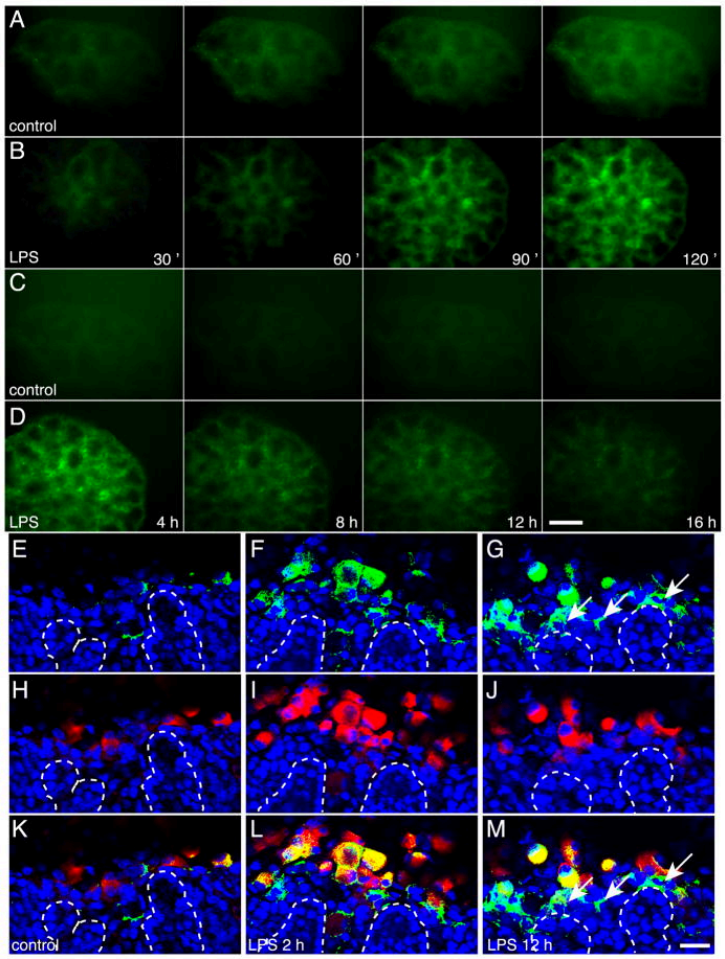

Figure 2.1. LPS stimulates NF-κB–dependent GFP expression in NGL fetal mouse lung explants. E15 fetal lung explants from NGL mice were cultured under control conditions (*A*, *C*) or in the presence of LPS (*B*, *D*) and imaged by time-lapse wide field fluorescence microscopy. Increased GFP expression was detected within 90 min of LPS treatment (*B*) and persisted beyond 12 h (*D*). Scale bar, 100 μm (*A–D*). Confocal images of control and LPS-treated NGL explants were obtained to better identify sites of GFP expression (*E–M*). Explants were fixed and immunostained for CD68 (red, *H–M*) following 2 and 12 h of LPS treatment. Nuclei were labeled with DAPI. In LPS-treated explants, NF-κB–GFP expression colocalized with CD68-postive macrophages following LPS treatment (GFP green, *E–G*; CD68 and GFP merged image in *K–M*). At 12 h, GFP expression was also detected in CD68-negative cells (arrows, *G*, *M*). Saccular airways are indicated by dotted lines. Scale bar, 25 μm (*E–M*).

lung during development. Immunostaining identified CD68-positive cells in the lung mesenchyme as early as E10 during the initial steps of lung formation (Fig. 2.2A). Macrophages

remained present in the mesenchyme throughout fetal development. Fetal lung macrophages also expressed F4/80 (Fig. 2.2B). To measure function, we tested if LPS could directly activate isolated fetal lung macrophages. We obtained macrophages from E15 lungs using anti-CD11b–coated magnetic beads (Fig. 2.2C), exposed them to *E. coli* LPS, and measured gene expression by RT-PCR. LPS stimulated macrophage expression of the inflammatory mediators IL-1β and TNF-α, but did not affect expression of TGF-β or BMP4 (Fig. 2.2D). Using macrophages isolated from E15 NGL mouse lungs, we next showed that LPS directly activates NF-κB–dependent luciferase activity (Fig. 2.2E). These data clearly demonstrate that macrophages within the fetal mouse lung respond to LPS and can produce inflammatory mediators.

Macrophage activation inhibits saccular airway branching

We have previously developed an E15 fetal mouse lung explant model to study the mechanisms regulating canalicular and saccular stage airway branching (Prince et al. 2005; Prince et al. 2004). Following 72 h of culture, the structures along the periphery of these explants resemble early saccular lungs by undergoing type I/type II cell differentiation, thinning of the mesenchyme, and branching of small airways. This model parallels the period of lung development occurring postnatally in extremely preterm infants born between 23 and 28 wk gestation, making it relevant for investigating BPD pathogenesis. Airway branching in E15 explants requires fibronectin, mesenchymal $\alpha_8\beta_1$-integrin expression, and fibroblast growth factor-10 (FGF-10) (Prince et al. 2005; Benjamin et al. 2009; Benjamin et al. 2007). We have also previously shown that TLR agonists, hyperoxia exposure, and

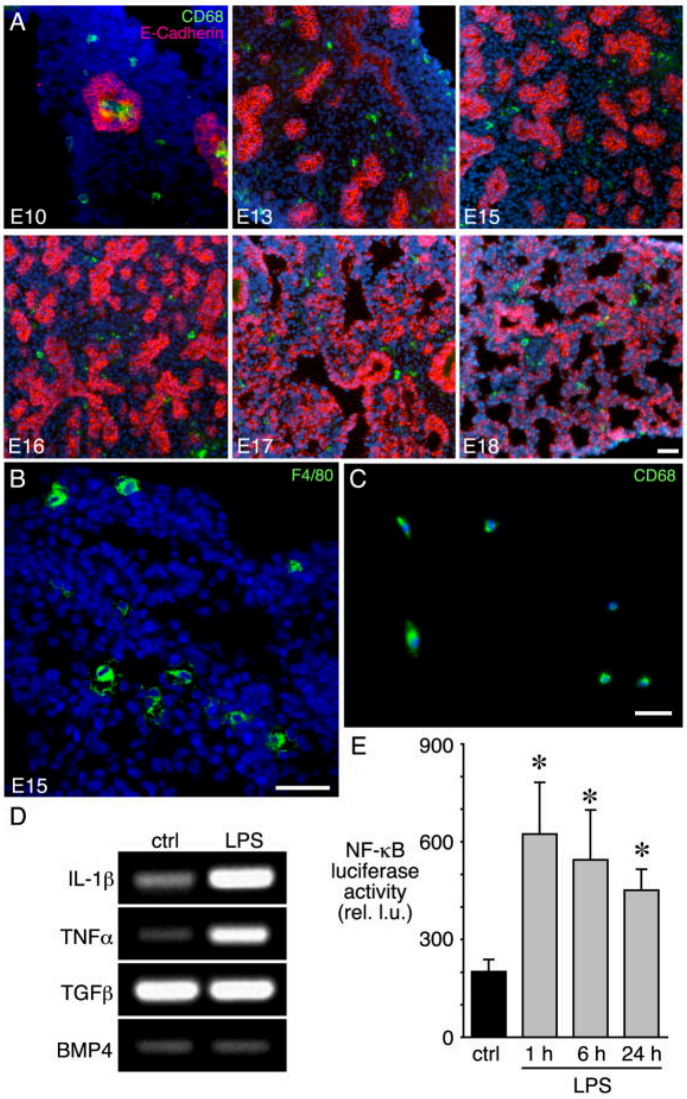

Figure 2.2. Macrophages are present in the fetal mouse lung and respond to LPS. *A*, Frozen sections of E10–E18 fetal mouse lungs were immunostained with Abs against the macrophage marker CD68 (green) and the epithelial marker E-cadherin (red). Nuclei were labeled with DAPI. Scale bar, 50 μm. *B*, Macrophages from E15 lung also express F4/80 (green). Scale bar, 50 μm. *C*, Fetal lung macrophages isolated by anti-CD11b magnetic bead separation from E15 lungs expressed CD68 (green). Scale bar, 50 μm. *D*, Macrophages were treated with *E. coli* LPS for 4 h, and gene expression was measured by RT-PCR. LPS increased IL-1β and TNF-α expression, but had no effect on TGF-β or BMP4. *E*, LPS activates NF-κB in E15 fetal mouse lung macrophages. Macrophages isolated from E15 NGL lungs were treated with LPS for the indicated times. NF-κB–luciferase was measured by luminometry. $*p < 0.05$; $n = 6$.

tracheal aspirate fluid from preterm infants exposed to antenatal inflammation can each inhibit airway branching in cultured explants (Prince et al. 2005; Benjamin et al. 2007; Dieperink et al. 2006). To initially test if the inhibitory effects of LPS on branching required macrophage activation, we depleted macrophages from E15 fetal lung explants using clodronate-containing liposomes (Fig. 2.3). We then measured the number of new airways that formed along the periphery of each explant between 24 h and 72 h. Although LPS inhibited formation of new saccular airways in control and empty liposome-treated explants (Fig. 2.3E, 2.3G), clodronate depletion of macrophages protected saccular airway branching from the effects of LPS (Fig. 2.3F, 2.3G). Macrophage depletion also substantially reduced the amount of LPS-induced IL-1β within lung explants (Fig. 2.3H), suggesting macrophages produce most of the IL-1β within LPS-treated fetal lung explants. Macrophages, therefore, are important for both production of inflammatory mediators within the fetal lung and inhibiting airway branching following exposure to LPS.

As clodronate could have off-target toxic effects, we next used a molecular approach to test if NF-κB activation in macrophages was required for LPS-dependent disruption of saccular airway branching. For these experiments, we used mice with macrophage-specific IκB kinase β (IKKβ) deletion. LysM-Cre:IKKβ$^{f/f}$ mice (IKKβΔ) lack functional IKKβ in myeloid cells, including macrophages and monocytes (Greten et al. 2004). LysM-Cre recombinase activity was confirmed in fetal lung explant macrophages using Rosa26-YFP reporter mice (Fig. 2.4A, 2.4B). We next measured the effects of LPS on explants from IKKβΔ and littermate controls. LPS failed to inhibit saccular airway branching in IKKβΔ explants (Fig. 2.4C, 2.4D), supporting the critical role of macrophages in inflammation-dependent disruption of airway

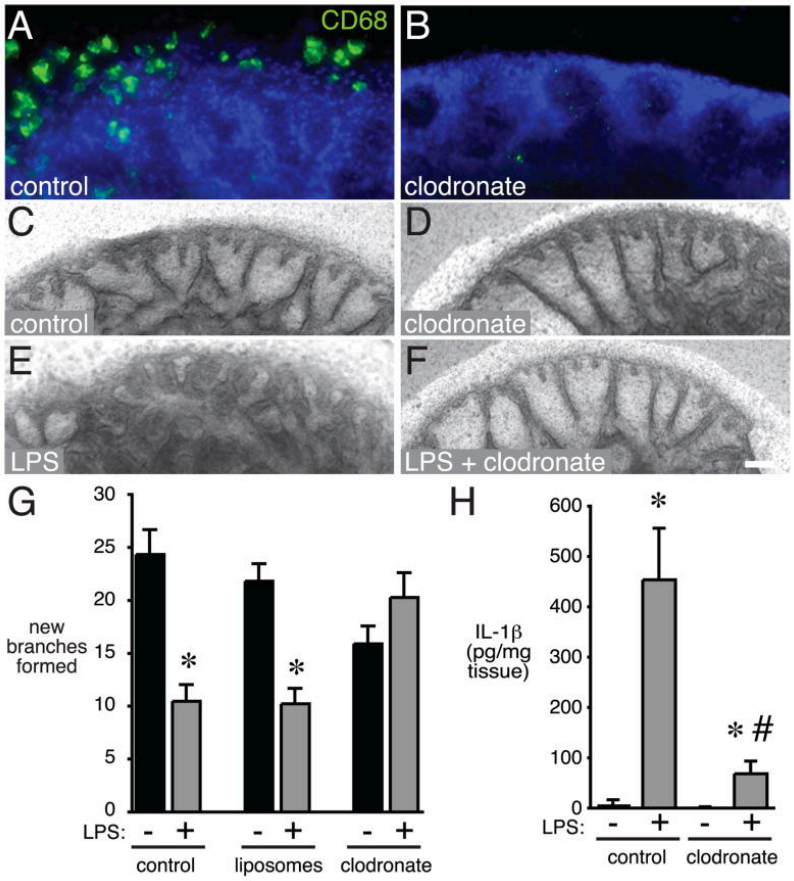

Figure 2.3. Macrophage depletion protects fetal lung explants from the effects of LPS. *A* and*B*, E15 fetal mouse lung explants were cultured in the absence or presence of liposomal clodronate (50 mg/ml). Following 72 h of culture, explants were immunostained with Abs against the macrophage marker CD68 to verify macrophage depletion (*B*). *C–F*, Brightfield images show that LPS inhibits formation of new saccular airway branches (*E*), but this effect is prevented in clodronate-treated explants (*F*). Scale bar, 50 μm (*A–F*). *G*, LPS inhibited formation of new saccular airways in control and empty liposome-treated explants (*$p < 0.001$; $n = 24$). However, LPS did not inhibit branching in clodronate-treated explants. *H*, Clodronate depletion of macrophages reduced the amount of IL-1β released following LPS treatment (*$p < 0.05$ LPS compared with untreated [$n = 4$],$^{\#}p < 0.01$ LPS compared with LPS + clodronate [$n = 4$]).

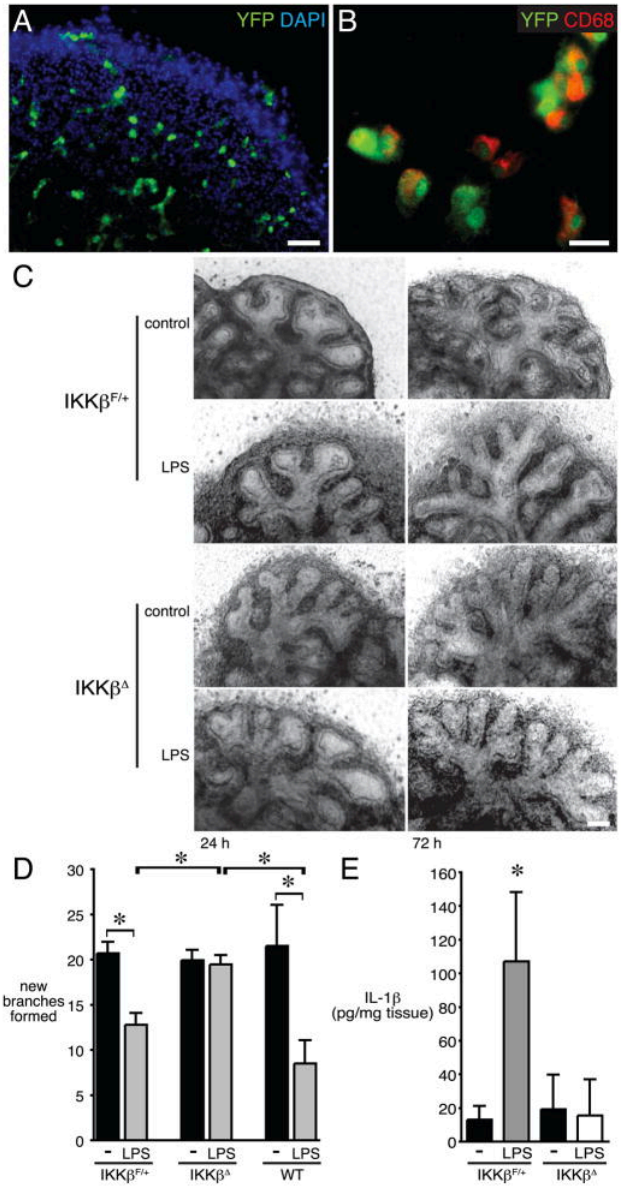

Figure 2.4. Targeted deletion of IKKβ in macrophages protects fetal lung explants from the effects of LPS. *A*, LysM-Cre recombinase activity in E15 fetal mouse lung explants. Fluorescence images of cultured LysM-Cre:Rosa26-YFP reporter explants. YFP expression is seen in macrophages throughout the explant. Cell nuclei visualized with DAPI. Scale bar, 50 μm. *B*, LysM-Cre:Rosa26-YFP macrophages immunostained with Ab against CD68 (red) to show overlapping expression. Scale bar, 10 μm. *C*, LPS does not inhibit saccular airway branching in IKKβΔ explants. Scale bar, 50 μm. *D*, LPS inhibited the number of new saccular airways that formed between 24 and 72 h of culture in $IKK\beta^{F/+}$ and wild-type BALB/cJ (WT) explants, but had no effect on branching in IKKβΔ explants ($*p < 0.05$; $n = 28$). *E*, Macrophage expression of IKKβ is required for normal IL-1β expression following LPS treatment. LPS increased IL-1β production in littermate control $IKK\beta^{F/+}$explants ($*p < 0.05$; $n = 6$), but did not significantly increase IL-1β in IKKβΔ explants ($^{\#}p < 0.05$ compared with LPS in $IKK\beta^{F/+}$ explants; $n = 6$).

morphogenesis and identifying NF-κB as the operative signaling pathway in mediating this effect. The total amount of IL-1β produced in LPS-treated IKKβΔ explants was much lower than in explants from littermate controls, again demonstrating that macrophages are responsible for a majority of the IL-1β produced in the LPS-treated fetal lung (Fig. 2.4E).

Having observed that activation of the NF-κB pathway in macrophages appears to mediate the effects of LPS on saccular airway morphogenesis, we next tested if NF-κB activation in macrophages is sufficient to disrupt airway morphogenesis and whether macrophages can impact airway formation in vivo. For these experiments, we used IKFM transgenic mice that express a macrophage-specific doxycycline-inducible *c-fms* transactivator and a constitutively active IKKβ mutant (cIKKβ) gene downstream of a *tet*-responsive promoter (L. Connelly et al., submitted for publication). We cultured saccular stage fetal lung explants from IKFM mice and control littermates in the absence or presence of doxycycline (Fig. 2.5A, 2.5B). Doxycycline had no effect on branching in control explants, but caused airway dilation and reduced branch formation in IKFM explants (Fig. 2.5B). Excessive IKKβ activity in IKFM macrophages inhibited branching, as did adding LPS (Fig. 2.5C). Inducing cIKKβ expression in macrophages increased IL-1β expression in fetal lung explants, demonstrating activity of the transgene (Fig. 2.5D). These results suggest that NF-κB activation specifically in macrophages is sufficient to disrupt normal fetal lung morphogenesis.

Targeted NF-κB activation in mouse macrophages disrupts lung morphogenesis

We next tested if macrophage-specific overexpression of cIKKβ in IKFM mice could alter lung morphogenesis in intact fetal mice. Pregnant IKFM mice were treated with

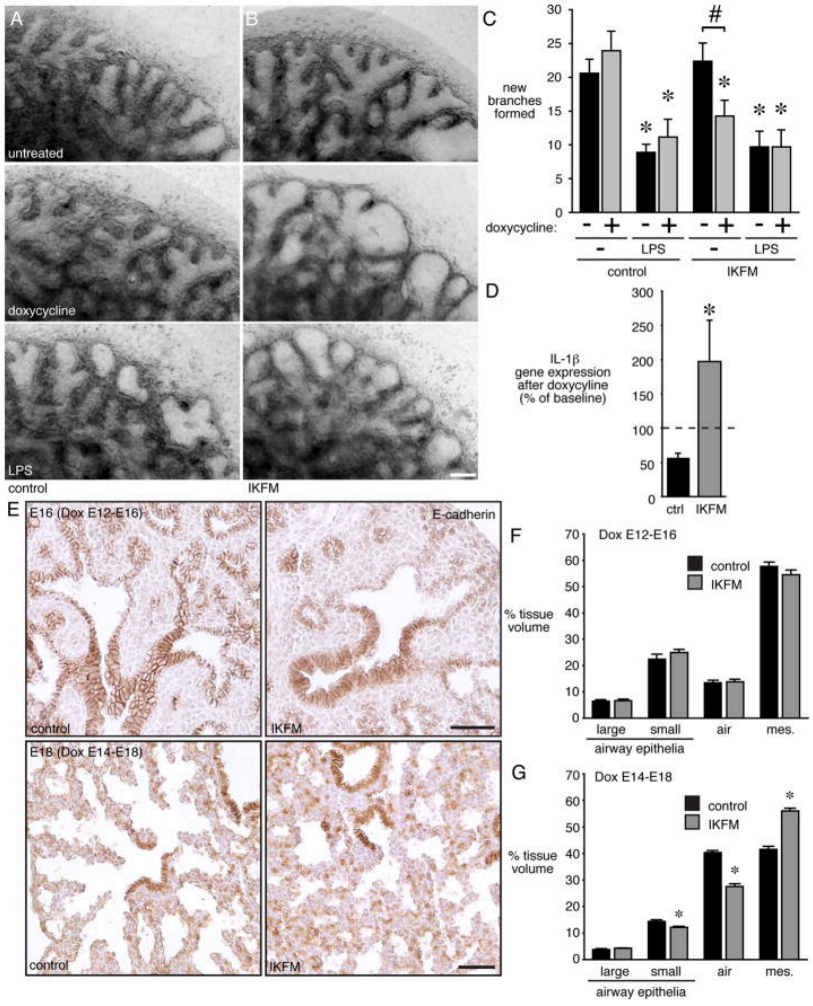

Figure 2.5. IKKβ activity in macrophages is sufficient to inhibit saccular airway branching. Brightfield images of E15 fetal lung explants from IKFM mice (*B*) and littermate controls (*A*) cultured under control conditions (*top panels*), in the presence of doxycycline (*middle panels*), and in the presence of LPS (*bottom panels*). Scale bar, 50 μm (*A*, *B*). *C*, Doxycycline induction if cIKKβ in macrophages inhibited saccular airway branching. Doxycycline had no effect in littermate control explants, whereas LPS inhibited formation of new saccular airway branches in both control and IKFM explants (*$p < 0.05$ compared with branches formed in the absence of doxycycline and without LPS [$n = 9$], #$p < 0.05$ compared with IKFM explants in the absence of doxycycline and without LPS [$n = 9$]). *D*, Doxycycline induction of cIKKβ in macrophages increased IL-1β expression in IKFM explants (*$p < 0.05$; $n = 9$). Dotted line indicates baseline expression level. *E*, Overexpression of cIKKβ in macrophages inhibits saccular stage lung morphogenesis in vivo. IKFM mice were given doxycycline (Dox) from either E12–E16 (*top panels*) or E14–E18 (*bottom panels*). Sections were immunostained using anti–E-cadherin to label epithelia. Scale bars, 100 μm. Lung morphogenesis did not appear altered in mice given Dox from E12–E16, either by histology or morphometric measurement of large and small airway epithelia, airspace (air), and mesenchymal (mes.) volumes (*F*). Dox administration from E14–E18 disrupted normal lung development, with IKFM lungs having smaller airways with reduced branching and expansion (*E*, *G*). Morphometry measurements confirmed decreased airspace and

increased mesenchymal volumes in IKFM mice treated with Dox (G; $*p < 0.001$; $n = 27$).

doxycycline to activate macrophages during either the late pseudoglandular stage (E12–E16) or from the late pseudoglandular stage through the canalicular and early saccular stages (E14-E18, Fig. 2.5E). Doxycycline administration from E12–E16 did not cause apparent changes in airway formation (Fig. 2.5E, 2.5F). However, transgene activation from E14–E18 caused significant changes with less airspace and increased mesenchyme in IKFM lungs compared with littermate controls (Fig. 2.5E, 2.5G). These differences were consistent with defects in saccular airway branching morphogenesis. The lack of effect in mice treated E12–E16 suggests that airway branching in the E14–E18 lung may have a window of vulnerability to macrophage activation. These data support the idea that macrophage activation and subsequent lung inflammation disrupt the later stages of airway formation.

To investigate how the morphological changes observed in IKFM mice affect respiratory function, mice treated with doxycycline from E14–E18 were allowed to deliver at E19 and E20. Disruption of normal lung development in IKFM pups led to reduced survival in the first 24 h. Newborn IKFM mice appeared cyanotic, and many died soon after birth, whereas control littermates appeared healthy (Fig. 2.6A, 2.6B). Histological examination of newborn IKFM lungs again showed a thickened lung interstitium compared with control littermates (Fig. 2.6C, 2.6D). As with mice harvested at E18, the microscopic appearance of newborn IKFM mouse lungs, with thickened interstitium and simplified airways, showed similarities to the lungs of patients with BPD. Macrophages were present both lining the airway lumen and within the interstitium in both control and IKFM newborn lungs (Fig. 2.6E). IKFM mice had increased numbers of F4/80-positive cells, which may represent increased macrophage recruitment, maturation, or

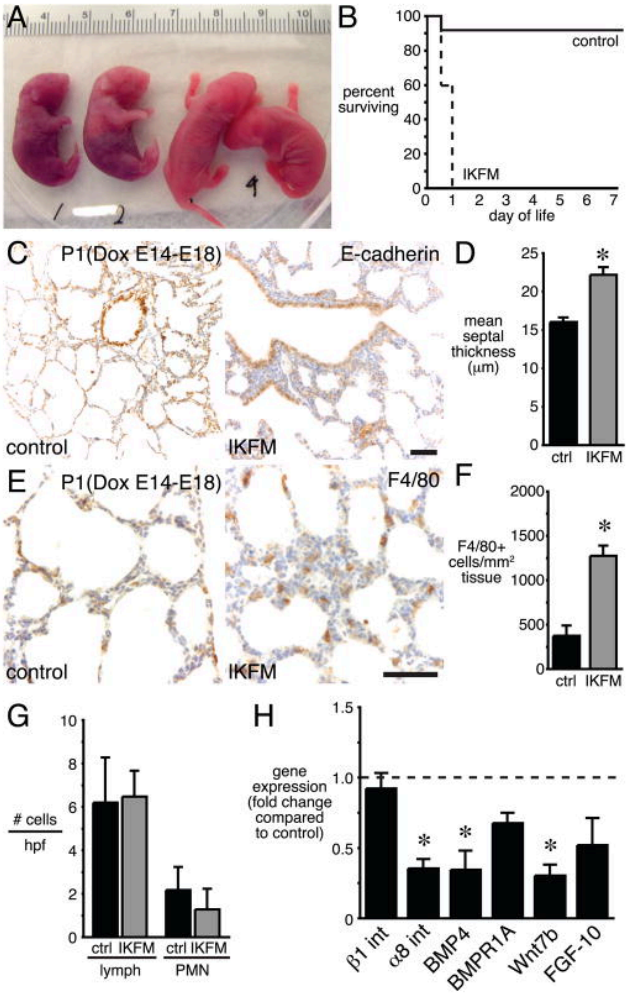

Figure 2.6. Targeted expression of a cIKKβ in fetal macrophages causes arrested lung development and perinatal lethality. *A* and *B*, Pregnant mice were treated with doxycycline from E14–E18 and then allowed to deliver. Newborn IKFM mice were born alive but developed respiratory distress and became cyanotic and lethargic soon after delivery. Littermate controls appeared healthy and vigorous. *C* and *D*, Newborn IKFM lungs have abnormal structure, with wider interstitium between airways and increased mean septal thickness ($*p < 0.01$; $\nu = 15$). Scale bar, 100 μm (*C*, *D*). *E* and *F*, Immunostaining for F4/80 shows increased numbers of macrophages in newborn IKFM lungs compared with control littermates. Scale bar, 100 μm (*E*, *F*). *G*, The numbers of lymphocytes and neutrophils (PMN) in the lungs of newborn IKFM mice and littermate controls were similar. *H*, Reduced expression of genes required for normal branching morphogenesis in newborn IKFM lungs treated from E14–E18 with doxycycline. Expression measured by real-time PCR ($*p < 0.05$; $n = 7$). Dotted line indicates control expression level.

proliferation (Fig. 2.6F). IKFM and control lungs contained similar numbers of lymphocytes and neutrophils (Fig. 2.6G), without signs of consolidated infiltrates or edema. These data further demonstrate that macrophage NF-κB activation, which could occur secondary to infection or other insults, can inhibit saccular airway morphogenesis.

Macrophage activation from E14–E18 in IKFM mice caused a persistent inhibition of expression of multiple genes critical for branching morphogenesis in newborn lungs (Benjamin et al. 2009; Weaver et al. 2000; Rajagopal et al. 2008), including reduced expression of the α_8 integrin subunit, BMP4, and Wnt7b (Fig. 2.6H). Expression of BMPR1A and FGF-10 also trended lower in IKFM lungs. Macrophage activation and release of inflammatory cytokines can therefore inhibit gene expression in the developing lung, leading to altered airway morphogenesis. These findings are consistent with our findings in lung explants, where macrophage activation can inhibit airway branching in the absence of systemic circulation. Activation of NF-κB in fetal lung macrophages could therefore be a common feature of insults that disrupt normal airway morphogenesis. As such, our model of a BPD-like phenotype in IKFM mice may be useful in further defining the pathogenesis and course of BPD.

Discussion

In this study, we demonstrate that NF-κB activation in macrophages is a key initial step in the fetal lung inflammatory response and sufficient to disrupt fetal lung morphogenesis. Macrophages in the canalicular or saccular stage fetal lung reside in the interstitium and respond to endotoxin. The NF-κB–dependent release of inflammatory mediators from these activated

macrophages may then cause a second wave of signaling in neighboring cells, including the mesenchymal cells critical for airway morphogenesis. Even when the entire fetal lung is exposed to LPS, as is the case when explants are treated with LPS, macrophages appear to be the major cellular site of NF-κB activation and cytokine production. Macrophage depletion or targeted IKKβ deletion dramatically reduced the amount of IL-1β produced in response to LPS treatment and protected airway branching from the inhibitory effects of LPS. In addition, targeted activation of fetal lung macrophages was sufficient to disrupt lung morphogenesis, causing perinatal lethality and airway pathology that resembles human BPD.

These findings fill an important gap in our knowledge of how the immature fetal lung responds to inflammatory stimuli. When preterm infants are exposed to chorioamnionitis in utero, inflammatory cytokines accumulate in their airways (Benjamin et al. 2010). The infants with high levels of inflammatory mediators in their lungs at birth are more likely to develop BPD (Choi et al. 2006). Not only are macrophages the major source of inflammatory mediators in the lung, but also their location in the fetal lung interstitium may increase the likelihood that macrophage-derived cytokines can affect immediately adjacent cells. Recent studies have demonstrated increased macrophage recruitment to fetal or newborn lungs following either mechanical or endotoxin-mediated injury (Hillman et al. 2011; Cao et al. 2009). However, our current study is the first to connect macrophage activation and altered lung morphogenesis, to our knowledge. We propose a two-wave mechanism for NF-κB activation leading to arrested lung development in BPD. In this model, microbial products initially activate NF-κB in lung macrophages. The release of inflammatory mediators, particularly IL-1β and/or TNF-α, then causes NF-κB activation in the adjacent mesenchymal cells. NF-κB activation in the

mesenchyme disrupts expression of genes important for the precise, controlled epithelial–mesenchymal interactions that regulate airway branching. This mechanism is supported by our previous findings that NF-κB activation in fetal lung mesenchymal cells interferes with normal expression of important developmental genes, including FGF-10 and integrin $\alpha_8\beta_1$ (Benjamin et al. 2010; Benjamin et al. 2009; Benjamin et al. 2007; Miller et al. 2010). The decreased BMP4 expression in IKFM lungs may be due to the direct effect of inflammatory cytokines on the airway epithelium (Zhu et al. 2007) or secondary to reduced FGF-10 expression in the mesenchyme (Weaver et al. 2000). Although inflammatory mediators that signal via other pathways may also affect lung development, those that can activate NF-κB in target cells appear to be most detrimental.

The IFKM mouse strain may provide an important model for further studying how macrophage activation and inflammation arrests lung development, particularly if the phenotype can be modulated so that affected pups can survive the neonatal period. The inducible cIKKβ transgene allows macrophage activation at distinct stages of lung development, as compared with postnatal rodent models that are restricted to studying the late saccular and alveolar stages of lung development (McGrath-Morrow and Stahl 2001). Human infants born at a comparable stage of lung development to that of newborn mice very rarely develop BPD, making these experimental models less useful for investigating the early mechanisms of BPD pathogenesis (Stoll et al. 2010). IKFM mice may also allow us to test if the effects of macrophage activation are reversible or persistent, how repetitive activations affect lung development, and if macrophage activation alters the susceptibility to other types of injury including hyperoxia, mechanical trauma, and viral infection. These future studies may help us better understand why

some infants develop only mild BPD and others have more severe or progressive disease. The IKFM experimental model will potentially permit studies that target different phases of the inflammatory response in the fetal and newborn lung to better identify potential strategies for treatment.

Although fetal lung macrophages clearly respond to innate immune stimuli, their functional role in normal embryogenesis remains uncertain. In developing tissues, macrophages may remove cellular debris, remodel extracellular matrix, or express growth factors (Ovchinnikov 2008). Removal of apoptotic cells may be critical for lung morphogenesis, as at least one study has demonstrated that mice lacking the phosphoserine receptor are unable to phagocytose apoptotic cells and die following birth with abnormal lung structure (Li et al. 2003). In the developing mammary gland, macrophages localize to collagen fibrils along elongating ductal branches, possibly playing a role in extracellular matrix remodeling (Ingman et al. 2006). Macrophages present in the fetal kidney may contribute to development by expressing specific Wnt ligands (Lin et al. 2010). We do not yet know if fetal lung macrophages play a similar trophic role in normal airway morphogenesis. In addition to the downstream effects of macrophage-derived cytokines on mesenchymal cell gene expression, inflammatory activation could divert macrophages from their yet uncharacterized developmental or trophic roles. This intersection of inflammatory and developmental pathways could therefore be a focal point for disease pathogenesis.

The two-wave model for propagation of inflammatory signals that disrupt branching morphogenesis suggests several potential therapeutic strategies for preventing BPD. Targeting

macrophage activation could prevent the initial wave of fetal lung inflammation. The feasibility of this approach is supported by our experimental data using macrophage depletion and targeted deletion of IKKβ. However, many women clinically present already in preterm labor and with evidence of chorioamnionitis (Romero et al. 2007). In these situations, fetal lung macrophage activation may have occurred prior to delivery. Therefore, alternative strategies could target inflammatory mediators such as IL-1β and TNF-α to prevent the effects of inflammation on mesenchymal gene expression and altered epithelial–mesenchymal interactions. Finally, approaches that restore the mesenchymal cell phenotype to a normal fetal lung gene expression pattern and cell behavior could promote ongoing lung morphogenesis even in preterm infants with previous inflammatory exposures.

References

Andonegui, G., C. S. Bonder, F. Green, S. C. Mullaly, L. Zbytnuik, E. Raharjo, P. Kubes (2003) Endothelium-derived Toll-like receptor-4 is the key molecule in LPS-induced neutrophil sequestration into lungs. *J. Clin. Invest.* **111**: 1011–1020.

Baraldi, E., M. Filippone (2007) Chronic lung disease after premature birth. *N. Engl. J. Med.* **357**: 1946–1955.

Benjamin, J. T., B. J. Carver, E. J. Plosa, Y. Yamamoto, J. D. Miller, J. H. Liu, R. van der Meer, T. S. Blackwell, L. S. Prince (2010) NF-kappaB activation limits airway branching through inhibition of Sp1-mediated fibroblast growth factor-10 expression. *J. Immunol.* **185**: 4896–4903.

Benjamin, J. T., D. C. Gaston, B. A. Halloran, L. M. Schnapp, R. Zent, L. S. Prince (2009) The role of integrin alpha8beta1 in fetal lung morphogenesis and injury. *Dev. Biol.* **335**: 407–417.

Benjamin, J. T., R. J. Smith, B. A. Halloran, T. J. Day, D. R. Kelly, L. S. Prince (2007) FGF-10 is decreased in bronchopulmonary dysplasia and suppressed by Toll-like receptor activation. *Am. J. Physiol. Lung Cell. Mol. Physiol.* **292**: L550–L558.

Bhandari, A., V. Bhandari (2009) Pitfalls, problems, and progress in bronchopulmonary dysplasia. *Pediatrics* **123**: 1562–1573.

Cao, L., J. Wang, I. Tseu, D. Luo, M. Post (2009) Maternal exposure to endotoxin delays alveolarization during postnatal rat lung development. *Am. J. Physiol. Lung Cell. Mol. Physiol.* **296**: L726–L737.

Choi, C. W., B. I. Kim, H. S. Kim, J. D. Park, J. H. Choi, D. W. Son (2006) Increase of interleukin-6 in tracheal aspirate at birth: a predictor of subsequent bronchopulmonary dysplasia in preterm infants. *Acta Paediatr.* **95**: 38–43.

Dieperink, H. I., T. S. Blackwell, L. S. Prince (2006) Hyperoxia and apoptosis in developing mouse lung mesenchyme. *Pediatr. Res.* **59**: 185–190.

Everhart, M. B., W. Han, T. P. Sherrill, M. Arutiunov, V. V. Polosukhin, J. R. Burke, R. T. Sadikot, J. W. Christman, F. E. Yull, T. S. Blackwell (2006) Duration and intensity of NF-kappaB activity determine the severity of endotoxin-induced acute lung injury. *J. Immunol.* **176**: 4995–5005.

Greten, F. R., L. Eckmann, T. F. Greten, J. M. Park, Z. W. Li, L. J. Egan, M. F. Kagnoff, M. Karin (2004) IKKbeta links inflammation and tumorigenesis in a mouse model of colitis-associated cancer. *Cell* **118**: 285–296.

Henson, P. M., D. A. Hume (2006) Apoptotic cell removal in development and tissue homeostasis. *Trends Immunol*. **27**: 244–250.

Hillman, N. H., G. R. Polglase, J. J. Pillow, M. Saito, S. G. Kallapur, A. H. Jobe (2011) Inflammation and lung maturation from stretch injury in preterm fetal sheep. *Am. J. Physiol. Lung Cell. Mol. Physiol*. **300**: L232–L241.

Hopkinson-Woolley, J., D. Hughes, S. Gordon, P. Martin (1994) Macrophage recruitment during limb development and wound healing in the embryonic and foetal mouse. *J. Cell Sci*. **107**: 1159–1167.

Ingman, W. V., J. Wyckoff, V. Gouon-Evans, J. Condeelis, J. W. Pollard (2006) Macrophages promote collagen fibrillogenesis around terminal end buds of the developing mammary gland. *Dev. Dyn*. **235**: 3222–3229.

Lahra, M. M., P. J. Beeby, H. E. Jeffery (2009) Intrauterine inflammation, neonatal sepsis, and chronic lung disease: a 13-year hospital cohort study. *Pediatrics* **123**: 1314–1319.

Li, M. O., M. R. Sarkisian, W. Z. Mehal, P. Rakic, R. A. Flavell (2003) Phosphatidylserine receptor is required for clearance of apoptotic cells. *Science* **302**: 1560–1563.

Lin, S. L., B. Li, S. Rao, E. J. Yeo, T. E. Hudson, B. T. Nowlin, H. Pei, L. Chen, J. J. Zheng, T. J. Carroll, et al (2010) Macrophage Wnt7b is critical for kidney repair and regeneration. *Proc. Natl. Acad. Sci. USA* **107**: 4194–4199.

May, C., M. Prendergast, S. Salman, G. F. Rafferty, A. Greenough (2009) Chest radiograph thoracic areas and lung volumes in infants developing bronchopulmonary dysplasia. *Pediatr. Pulmonol*. **44**: 80–85.

McGrath-Morrow, S. A., J. Stahl (2001) Apoptosis in neonatal murine lung exposed to hyperoxia. *Am. J. Respir. Cell Mol. Biol*. **25**: 150–155.

Metzger, R. J., O. D. Klein, G. R. Martin, M. A. Krasnow (2008) The branching programme of mouse lung development. *Nature* **453**: 745–750.

Miller, J. D., J. T. Benjamin, D. R. Kelly, D. B. Frank, L. S. Prince (2010) Chorioamnionitis stimulates angiogenesis in saccular stage fetal lungs via CC chemokines. *Am. J. Physiol. Lung Cell. Mol. Physiol*. **298**: L637–L645.

Ovchinnikov, D. A (2008) Macrophages in the embryo and beyond: much more than just giant phagocytes. *Genesis* **46**: 447–462.

Paananen, R., A. K. Husa, R. Vuolteenaho, R. Herva, T. Kaukola, M. Hallman (2009) Blood cytokines during the perinatal period in very preterm infants: relationship of inflammatory response and bronchopulmonary dysplasia. *J. Pediatr*. **154**: 39–43.e3.

Prince, L. S., H. I. Dieperink, V. O. Okoh, G. A. Fierro-Perez, R. L. Lallone (2005) Toll-like receptor signaling inhibits structural development of the distal fetal mouse lung. *Dev. Dyn.* **233**: 553–561.

Prince, L. S., V. O. Okoh, T. O. Moninger, S. Matalon (2004) Lipopolysaccharide increases alveolar type II cell number in fetal mouse lungs through Toll-like receptor 4 and NF-kappaB. *Am. J. Physiol. Lung Cell. Mol. Physiol.* **287**: L999–L1006.

Rajagopal, J., T. J. Carroll, J. S. Guseh, S. A. Bores, L. J. Blank, W. J. Anderson, J. Yu, Q. Zhou, A. P. McMahon, D. A. Melton (2008) Wnt7b stimulates embryonic lung growth by coordinately increasing the replication of epithelium and mesenchyme. *Development* **135**: 1625–1634.

Romero, R., J. Espinoza, L. F. Gonçalves, J. P. Kusanovic, L. Friel, S. Hassan (2007) The role of inflammation and infection in preterm birth. *Semin. Reprod. Med.* **25**: 21–39.

Stoll, B. J., N. I. Hansen, E. F. Bell, S. Shankaran, A. R. Laptook, M. C. Walsh, E. C. Hale, N. S. Newman, K. Schibler, W. A. Carlo, et al, Eunice Kennedy Shriver National Institute of Child Health and Human Development Neonatal Research Network (2010) Neonatal outcomes of extremely preterm infants from the NICHD Neonatal Research Network. *Pediatrics* **126**: 443–456.

Tomlinson, M. L., C. Garcia-Morales, M. Abu-Elmagd, G. N. Wheeler (2008) Three matrix metalloproteinases are required in vivo for macrophage migration during embryonic development. *Mech. Dev.* **125**: 1059–1070.

Warburton, D., M. Schwarz, D. Tefft, G. Flores-Delgado, K. D. Anderson, W. V. Cardoso (2000) The molecular basis of lung morphogenesis. *Mech. Dev.* **92**: 55–81.

Weaver, M., N. R. Dunn, B. L. Hogan (2000) Bmp4 and Fgf10 play opposing roles during lung bud morphogenesis. *Development* **127**: 2695–2704.

Willet, K. E., A. H. Jobe, M. Ikegami, J. Newnham, S. Brennan, P. D. Sly (2000) Antenatal endotoxin and glucocorticoid effects on lung morphometry in preterm lambs. *Pediatr. Res.* **48**: 782–788.

Zhu, N. L., C. Li, H. H. Huang, M. Sebald, V. A. Londhe, N. Heisterkamp, D. Warburton, S. Bellusci, P. Minoo (2007) TNF-alpha represses transcription of human Bone Morphogenetic Protein-4 in lung epithelial cells. *Gene* **393**: 70–80.

Chapter III

IκB Kinase Activity Drives Fetal Lung Macrophage Maturation along a Non-M1/M2 Paradigm

Originally published in *The Journal of Immunology*, vol. 193, pp. 1184-1193, 1 August 2014.

Ashley N. Stouch, Rinat Zaynagetdinov, Whitney J. Barham, Amanda M. Stinnett, James C. Slaughter, Timothy S. Blackwell, and Lawrence S. Prince

Abstract

In preterm infants, exposure to inflammation increases the risk of bronchopulmonary dysplasia, a chronic, developmental lung disease. While macrophages are the key cells that initiate lung inflammation, less is known about lung macrophage phenotype and maturation. We hypothesized that fetal lung macrophages mature into distinct subpopulations during mouse development, and that activation could influence macrophage maturation. Expression of the fetal macrophage markers CD68, CD86, CD206, Ym1, fibrinogen-like protein 2 (FGL2), and indolamine-2, 3-dioxygenase (Ido1) were developmentally regulated, with each marker having different temporal patterns. Flow cytometry analysis showed macrophages within the fetal lung were less diverse than the distinctly separate subpopulations in newborn and adult lungs. Similar to adult alveolar macrophages, fetal lung macrophages responded to the TLR4 agonist LPS and the alternative activation cytokines IL-4 and IL-13. Using a macrophage-specific constitutively

active IKKβ transgenic model (IKFM), we demonstrated that macrophage activation increased proinflammatory gene expression and reduced the response of fetal lung macrophages to IL-4 and IL-13. Activation also increased fetal lung macrophage proliferation. Fetal IKFM lungs contained increased percentages of more mature, $CD11b^{lo}F4/80^{hi}$ cells that also expressed higher levels of the alternative activation markers CD204 and CD206. Development of fetal lung macrophages into mature alveolar macrophages may therefore include features of both proinflammatory and alternative activation paradigms.

Introduction

To maintain efficient gas exchange between the airspace and pulmonary circulation, the alveolar environment must remain dry, sterile, and free of particulates. As part of the lung innate immune system, macrophages protect the lung from inhaled pathogens, microbes, and harmful particulates. Within the alveolar environment, macrophages are the primary cells that kill pathogens and remove cellular and foreign debris. Expressing an array of pattern recognition receptors on their cell surface, lung macrophages detect and engulf inhaled microbes (Gordon and Taylor, 2005). Macrophages phagocytose and kill these pathogens by producing antimicrobial reactive oxygen and nitrogen species (Fang, 2004). When unable to completely kill and remove microbial pathogens, macrophages secrete cytokines and chemokines that recruit additional inflammatory cells to the alveolar space (Gutierrez-Ramos et al. 2000). Macrophages then remove both host and microbial cellular debris and promote tissue repair (Mosser and Edwards, 2008).

Like other tissues, the mature lung contains multiple macrophage subpopulations (Laskin et al. 2001). These groups of macrophages appear to differ in their origin, phenotypic marker expression, and functional role in the immune response. During development, macrophages first originate in the yolk sac and later from hematopoietic precursors in the fetal liver (Yona et al. 2013; Geissmann et al. 2010). Cells from both sources populate the lung, with additional bone marrow-derived monocytes migrating to the lung and differentiating into macrophages (Geissmann et al. 2010; Schulz et al. 2012). In addition, proliferation of differentiated cells can sustain macrophage populations within tissues (Yona et al. 2013). In addition to potentially deriving from different macrophage sources, the various macrophage subpopulations may have distinct functional roles.

Proinflammatory macrophages respond robustly to microbial organisms by phagocytosing infectious particles and releasing soluble inflammatory mediators (Sica and Mantovani 2012). In addition to sensing extracellular microbes, infection of proinflammatory macrophages by intracellular pathogens elicits inflammatory cytokine and chemokine release (Ghisletti et al. 2010). Also referred to as M1 or classically activated macrophages, these proinflammatory cells typically express the surface marker CD86 and cytokines IL-1β and TNFα (Ghisletti et al. 2010). TLR agonists, microbial products, and IFN-γ activate proinflammatory macrophages in slightly different ways, giving diversity to the inflammatory response (Sica and Mantovani 2012; Xue et al. 2014). In comparison, macrophages with an alternative phenotype can be classified as M2a, M2b, M2c, or M2d (Mantovani et al. 2004; Duluc et al. 2007). These alternatively activated or M2 macrophages express FGL2, Ym1, and the scavenger receptors CD204 and CD206 (Mantovani et al. 2013; Martinez et al. 2006; Ruffell

et al. 2012). Alternatively activated cells are induced by IL-4 and IL-13 (M2a), TLR or IL1R ligands (M2b), IL-10 (M2c), or the tumor microenvironment (M2d) (Mantovani, Sica et al. 2004; Duluc et al. 2007; Gordon and Martinez 2010). M2 macrophages play roles in parasitic infections (M2a), atopic allergic disorders (M2a), Th2 differentiation (M2b), wound healing (M2c), and tumor progression (M2d) (Mantovani et al. 2004; Duluc et al. 2007). The relative differences and unique properties of M1/M2 macrophages have been investigated in cancer, diabetes, and chronic inflammatory disease (Ruffell et al. 2012; Lumeng et al. 2007; Sindrilaru et al. 2011; Red Eagle and Chawla 2010; Cortez-Retamozo et al. 2013). How this M1/M2 paradigm applies to lung macrophages during both normal lung homeostasis and in disease processes is not completely clear.

Macrophages play important roles in both neonatal and adult lung immunity. However, neonatal lung macrophages, especially those found in preterm infants, may lack fully mature innate immune function. Neonates are particularly susceptible to pneumonia and inhaled pathogens, suggesting either immature killing or inability to control localized lung inflammation (Kollmann, Levy et al. 2012). Previous studies showed that neonatal monocytes responded normally to TLR agonists to produce inflammatory cytokines IL-6 and TNFα, but macrophages from preterm infants have reduced IL-10 release (Blahnik et al. 2001; Angelone et al. 2006; Yerkovich et al. 2007). Recent studies reported an increase in M2 markers in the postnatal mouse lung (Jones et al. 2013). However, detailed characterization of fetal macrophages, how they respond functionally to proinflammatory and alternative activation stimuli, and the developmental signaling pathways regulating maturation are not understood.

Lung inflammation plays a key role in the pathogenesis of bronchopulmonary dysplasia (BPD) in preterm infants (Watterberg et al. 1996). Patients with elevated proinflammatory cytokines in their lungs are more likely to have arrested lung development and develop chronic lung disease (Tullus et al. 1996; Baier et al. 2001; Wang et al. 2002). Macrophages are the primary cellular sources of these soluble inflammatory mediators in the lung. We demonstrated in mice that macrophage activation was required and sufficient for microbial products to cause arrested airway and alveolar morphogenesis (Blackwell et al. 2011). Targeted NF-κB activation in fetal macrophages disrupted normal developmental gene expression in epithelial and mesenchymal cells and led to perinatal lethality (Blackwell et al. 2011). Interestingly, this disruption of lung morphogenesis occurred only during later stages of development, suggesting macrophage maturation might also be playing a role in the connections between lung inflammation and development.

We hypothesized that macrophages undergo significant maturational changes during fetal lung development, with mature macrophages having either a predominantly proinflammatory (M1) or alternative (M2) phenotype. We therefore measured expression of multiple macrophage markers across fetal mouse lung development. Transcriptional responses to LPS and IL-4/IL-13 in fetal and adult lung macrophages tested the effects of macrophage activation on maturation. The changes we observed both with normal development and following activation did not fit neatly within an M1/M2 paradigm, but instead demonstrated unique mixed phenotypes in lung macrophage populations. These data will be essential for future studies examining macrophage differentiation and function in neonatal and pediatric inflammatory lung diseases.

Materials and Methods

Reagents

The following antibodies were used for immunofluorescence: rat anti-CD68 (Acris), rabbit anti-CD86 (Abcam), rat anti-Ym1 (R&D Systems), rabbit anti-CD206 (Abcam), goat anti-macrophage galactose N-acetyl-galactosamine specific lectin (Mgl1/2, R&D Systems), rat anti-Ecadherin (Zymed), mouse anti-alpha-smooth muscle actin-Cy3 (α-SMA, Sigma-Aldrich), rabbit anti-Ki67 (Abcam). ProLong Gold with DAPI mounting media and Alexa-conjugated secondary antibodies were purchased from Invitrogen. DRAQ5 (1,5-bis{[2-(di-methylamino) ethyl]amino}-4, 8-dihydroxyanthracene-9,10-dione) was purchased from Biostatus Limited. Anti-CD11b microbeads and magnetic separation equipment were obtained from Miltenyi Biotec. Gel-purified *Escherichia coli* LPS (O55:B5), deoxyribonuclease I from bovine pancreas Type IV (DNase), and collagenase from clostridium histolyticum, Type XI were obtained from Sigma-Aldrich. Recombinant mouse IL-4 and IL-13 were purchased from R&D Systems. RPMI 1640 media was purchased from Invitrogen, and FBS was purchased from Thermo Fisher Scientific.

Mouse strains

The Institutional Animal Care and Use Committees from Vanderbilt University and the University of California at San Diego approved all animal experiments. C57Bl/6 mice were obtained from Harlan Laboratories. For transgenic expression of enhanced green fluorescent protein (EGFP) in macrophages, we used C57BL/6J-Tg(Csf1r-EGFP-NGFR/FKBP1A/TNFRSF6)2Bck/J mice from the Jackson Laboratory. These mice express EGFP downstream of the *Csf1r* promoter and have no obvious phenotype in the absence of

FKBP dimerization agents (Burnett, Kershen et al. 2004). We have referred to this strain as Csf1r-EGFP in the text. For studies using inducible expression of a constitutively active IKKβ mutant (cIKKβ) in macrophages, female *Csf1r-rtTA* mice were mated with male *Tet-O-caIKKβ* mice to produce IKFM offspring (Connelly, Barham et al. 2011). To induce cIKKβ expression, timed pregnant dams were given doxycycline-containing water (2g/L) ad libitum beginning at E14 until E18. For timed pregnant matings, embryonic day 0 (E0) was defined as the morning of vaginal plug discovery.

Macrophage Isolation

For isolation of fetal macrophages in gene expression and flow cytometry experiments, fetal lungs were dissected free of surrounding tissues and placed in cold PBS. Lung tissue was dissected, minced, and enzymatically digested with DNase (30ug/ml) and collagenase (0.7mg/ml) at 37° C for 30 min. The cell suspension was passed through a 70 μm cell strainer and collected by centrifugation. For gene expression, fetal cells were resuspended in the presence of anti-CD11b-conjugated microbeads and passed through a magnetic separation column (Miltenyi Biotec). CD68 staining confirmed that this isolation technique resulted in >95% macrophages. For IKFM samples, macrophages were isolated from each embryo and cultured separately in the presence of doxycycline.

Adult lung macrophages were isolated by bronchoalveolar lavage. Lung lavage was repeated three times with cold PBS. Cells were cultured and treated the same as fetal macrophages. To isolate peritoneal macrophages, adult mice received an intraperitonal injection of 2 mL 3% thioglycollate medium. After 72h, the peritoneum was lavaged three times with cold PBS to collect macrophages. All macrophages were plated in RPMI 1640 with 10% FBS. After

1h in culture, macrophages were gently washed with PBS and treated with LPS (250 ng/ml), IL-4 (5 ng/ml), or IL-13 (10 ng/ml) for 4h.

RNA isolation and real-time PCR measurement

RNA isolation, cDNA synthesis, and real-time PCR were performed on whole lung or isolated macrophages using standard techniques. Tissue and cells were stored and homogenized (TissueRuptor, Qiagen) in TRIzol (Invitrogen). After total RNA isolation, first strand cDNA was synthesized using an oligo(dT) primer and Superscript III (Invitrogen). Real time PCR was performed using either unlabeled oligonucleotides with SYBR Green or TaqMan probes. PCR was performed using either an iQ5 or CFX96 thermocycler (Bio-Rad). Gene expression comparisons were represented using $2^{-\Delta\Delta Ct}$ method. Experiments were performed at least three independent times. Data between groups were analyzed by comparing ΔC_T values using a multiple regression analysis model or the Mann-Whitney U test.

Tissue processing and immunolabeling

Mouse lung tissue was fixed, processed, and immunolabeled using standard techniques. Dissected lung tissue was fixed in 4% paraformaldehyde (Electron Microscopy Sciences), processed through a sucrose gradient, and frozen in OCT media (Tissue-Tek). Frozen tissue sections (10 μm thick) were postfixed in 2% paraformaldehyde, permeabilized in 0.1% TritonX-100 (Thermo Scientific), and blocked with 5% normal donkey serum for 1h at room temperature. Tissue sections were incubated with antibody overnight at 4° C. Alexa-conjugated secondary antibodies (Invitrogen) were used for visualization. Following antibody labeling, nuclei were labeled with DAPI or DRAQ5.

Imaging and image analysis

Confocal images were acquired using a Leica TCS SPE (Leica Microsystems) laser scanning confocal microscope. Widefield fluorescence images were obtained using an Olympus IX81 microscope equipped with Hamamatsu Orca ER CCD monochrome camera and Slidebook software (Olympus). All microscopy images were saved in Tagged Image Format and imported into Photoshop (Adobe Systems) for processing. Images for comparison were identically processed. Immunofluorescence intensity measurements (relative fluorescent units) of individual macrophages were performed in Slidebook. A reference circle outlined a masked area over each macrophage. Relative fluorescent units for each channel were measured within the masked area and plotted against CD68 intensity values.

Flow cytometry and FACS

The following antibodies were used for flow cytometry and FACS experiments: CD11b-V450, CD86-PE-Cy7, Gr1 PerCP-Cy5.5, and CD45 APC-Cy7 (BD Bioscience); CD204-AF647, CD68-FITC, and CD206-PE (AbD Serotec); F4/80-PE (Invitrogen); CD11c-Pe-Cy5 (BioLegend). Viable cells were identified using the LIVE/DEAD Fixable Red Dead Cell Stain Kit or the LIVE/DEAD Fixable Blue Dead Cell Stain kit (Invitrogen). Fetal and adult macrophages were digested as previously described. Cells were resuspended in ACK Lysing buffer (Invitrogen) to lyse red blood cells. Cells were blocked with 3% FBS for 15min and incubated with primary antibodies against surface markers for 30-60min on ice. For intracellular antibody staining, we used the Intracellular Fixation and Permeabilization kit (eBioscience). Flow cytometry measurements were conducted using a BD Fortessa, and flow sorting was conducted on a BD

FACSAria III. For flow cytometry gating, the initial gate was based on FSC-A against SSC-A. Doublets were excluded with two gates: FSC-A against FSC-H, followed by SSC-A against SSC-H. Viability gating selected cells that were negative for the LIVE/DEAD fixable Red or Blue Dead Cell stain. Out of viable cells, $CD45^+$ cells identified the population of hematopoietic cells. For FACS gating, the initial gate was FSC-A against SSC-A, followed by doublet exclusion with FSC-A against FSH-A and SSC-A against SSH-A. $CD45^+$ cells were separated into $CD11b^{hi}F4/80^{lo}$ and $CD11b^{lo}F4/80^{hi}$. These cell populations were sorted directly into Trizol.

Results

Fetal lung macrophages differentially express phenotype markers during development.

Lung macrophages are clearly important in neonatal lung immunity and disease. However, the differentiation and maturation of lung macrophages during fetal development is just now being characterized. We measured the expression of various macrophage population markers in developing mouse lungs. As shown in Figure 3.1, cells expressing the pan-macrophage marker CD68 were present in the fetal lungs throughout development. The pro-inflammatory macrophage marker CD86, however, was rarely detected at E13 and E15. Cells expressing CD86 were more prevalent later in gestation and in the adult lung. Ym1 and CD206 are markers of alternatively activated macrophages, found commonly associated with tumors or in chronic inflammation models. While we did not detect Ym1 expression in E13 and E15 mouse lungs, staining appeared at E18 and was abundant in adult lungs. In contrast, CD206 was widely present at E13, and appeared to label similar numbers of cells as CD68 throughout mouse lung development. Macrophage galactose N-acetyl-galactosamine–specific lectin 1 (Mgl1/2) was

expressed both by macrophages and airway dendritic cells in the adult lung. Interestingly, Mgl1/2 expression in the fetal lung appeared at E15 and was restricted to cells with a more round macrophage morphology. Macrophage markers were therefore differentially expressed throughout fetal lung development and with distinct temporal patterns.

Gene expression experiments showed similar patterns of macrophage marker expression throughout lung development (Fig. 3.1F-H). CD68 expression increased in postnatal and adult lung, suggesting either a higher CD68 expression or an increase in number of $CD68^{+}$ macrophages. The pro-inflammatory markers CD86 and Ido1 also increased during development, being most highly expressed in adult lung. Similar to the immunofluorescence data in Fig. 3.1D, CD206 gene expression was relatively constant throughout lung development (Fig. 3.1G). In contrast, expression of other alternatively activated macrophage markers was higher in more mature lungs. While Ym1 expression first increased at P7, fibrinogen-like protein 2 (FGL2), another marker of alternatively activated macrophages, increased earlier during development, plateauing around E17. Markers of alternatively activated macrophages and airway dendritic cells (Mgl1/2, CD11c, CD103) were more highly expressed in postnatal and adult lungs (Fig. 3.1H). Both immunofluorescence and gene expression data therefore support developmental regulation of macrophage differentiation and maturation. The temporal changes in expression were distinct for each marker tested and did not clearly follow pro-inflammatory or alternative activation paradigms.

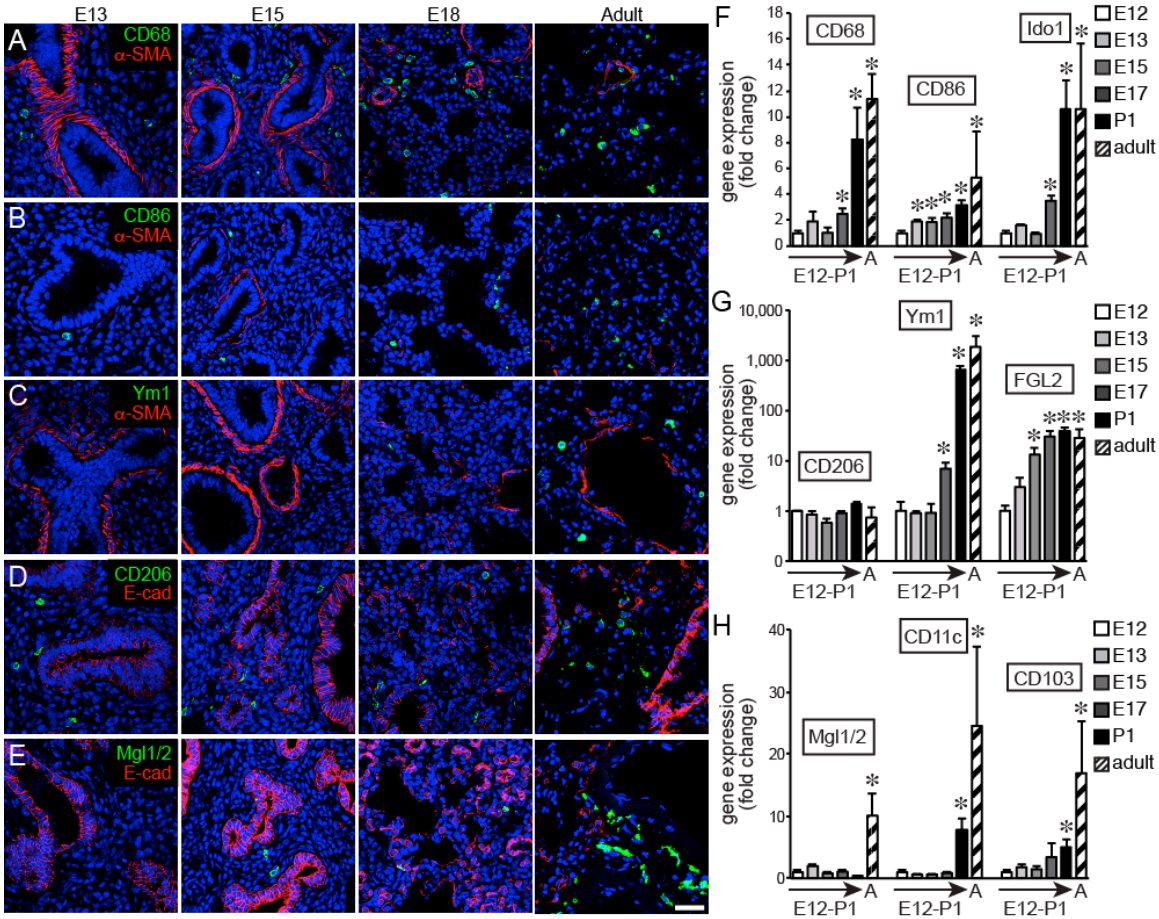

Figure 3.1. Macrophage marker expression during mouse lung development. **(A-E)** Frozen sections of E13, E15, E18 or adult mouse lungs were immunostained with Abs against the pan-macrophage marker CD68 (A) the pro-inflammatory macrophage marker CD86 (B) the alternative activation markers Ym1 (C), CD206 (D) and Mgl1/2 (E). Smooth muscle and myofibroblasts immunolabeled with anti-α-SMA in (A-C; red); epithelial cells immunolabeled with anti-E-cadherin in (D,E; red). Nuclei were labeled with DRAQ5. Images obtained by laser scanning confocal microscopy. (**F-H**) Gene expression of macrophage markers in E12, E13, E15, E17, P1 and adult mouse lungs. (F) Expression of the pan-macrophage marker CD68 and proinflammatory markers CD86 and INDO increased during later stages of development and following delivery. (G) Expression of the alternative activation markers CD206, Ym1, and FGL2 each had distinct temporal expression patterns. (H) The alveolar macrophage/dendritic cell markers Mgl1/2, CD11c, and CD103 were expressed highest in postnatal and adult lung. (n = 4 litters for each embryonic time point, 4 lungs from individuals at P1 and adult; * $p < 0.05$).

Because multiple macrophage markers were expressed in the developing lung, we next tested if these various markers represented distinctly separate macrophage populations. We immunostained multiple sections of developing mouse lungs obtained at E15 with both CD68 and various population-specific markers. Individual cell fluorescence intensity was then measured for all cells expressing either macrophage marker. As shown in Figure 3.2, CD86 expression in $CD68^+$ macrophages was variable in E15 lungs. The separation of CD68 and CD86 expression was more apparent in adult lung, with CD86-expressing cells having lower CD68 staining intensity. Consistent with data in Figure 3.1, only a minority of $CD68^+$ macrophages in E15 lungs expressed Mgl1/2, while a larger population of adult macrophages and airway dendritic cells expressed both CD68 and Mgl1/2 (Fig. 3.2C-D). CD206 was expressed throughout lung development. However, the intensity of CD206 staining in E15 lungs varied (Fig. 3.2E). In contrast, CD206 expression in adult $CD68^+$ cells was relatively low. Using this approach to identify macrophage populations in situ revealed differences in relative marker expression between E15 and adult lung macrophages. However, this immunostaining approach was not able to clearly identify distinct populations of macrophages in the fetal lung with relative differences in expression levels or patterns.

We next tested for the presence of subpopulations of fetal mouse lung macrophages by flow cytometry (Figure 3.3). Lung macrophages were isolated from single cell suspensions obtained from fetal (E15 and E18), postnatal day 7 (P7), and adult *Csf1r*-EGFP lungs. In these mice, GFP-positive cells uniformly expressed CD68 (Fig. 3.3A). Viable, $CD45^+$, *Csf1r*-$EGFP^+$ cells (Fig. 3.3B) were analyzed based on expression of Gr1, CD86, CD11c, CD11b, and F4/80.

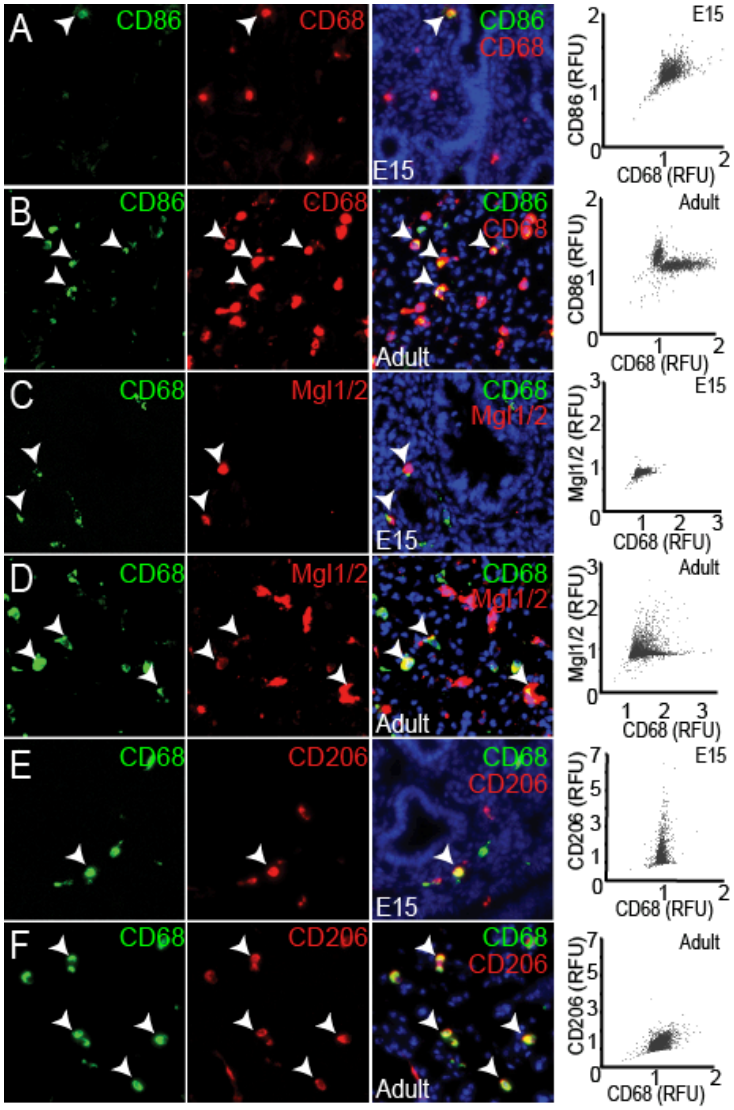

Figure 3.2. Comparison of macrophage populations in fetal and adult mouse lungs. (**A-F**) Frozen sections of E15 and adult mouse lungs were immunostained with Abs against CD68 and CD86 (A-B), Mgl1/2 (C-D), or CD206 (E-F). Nuclei were labeled with DAPI. Macrophages labeled in were identified by widefield fluorescence microscopy. Multi-channel fluorescence of each cell was measured and plotted to demonstrate potential populations of cells with differing expression levels. Macrophages in E15 mouse lungs expressed relatively similar marker levels, with the exception of CD206 (E), which had a larger expression range. Adult lungs contained more clearly identified populations of macrophages based on CD86 (B) and Mgl1/2 (D) expression. (n = 4 different lung samples from each stage, 20 images were measured per lung).

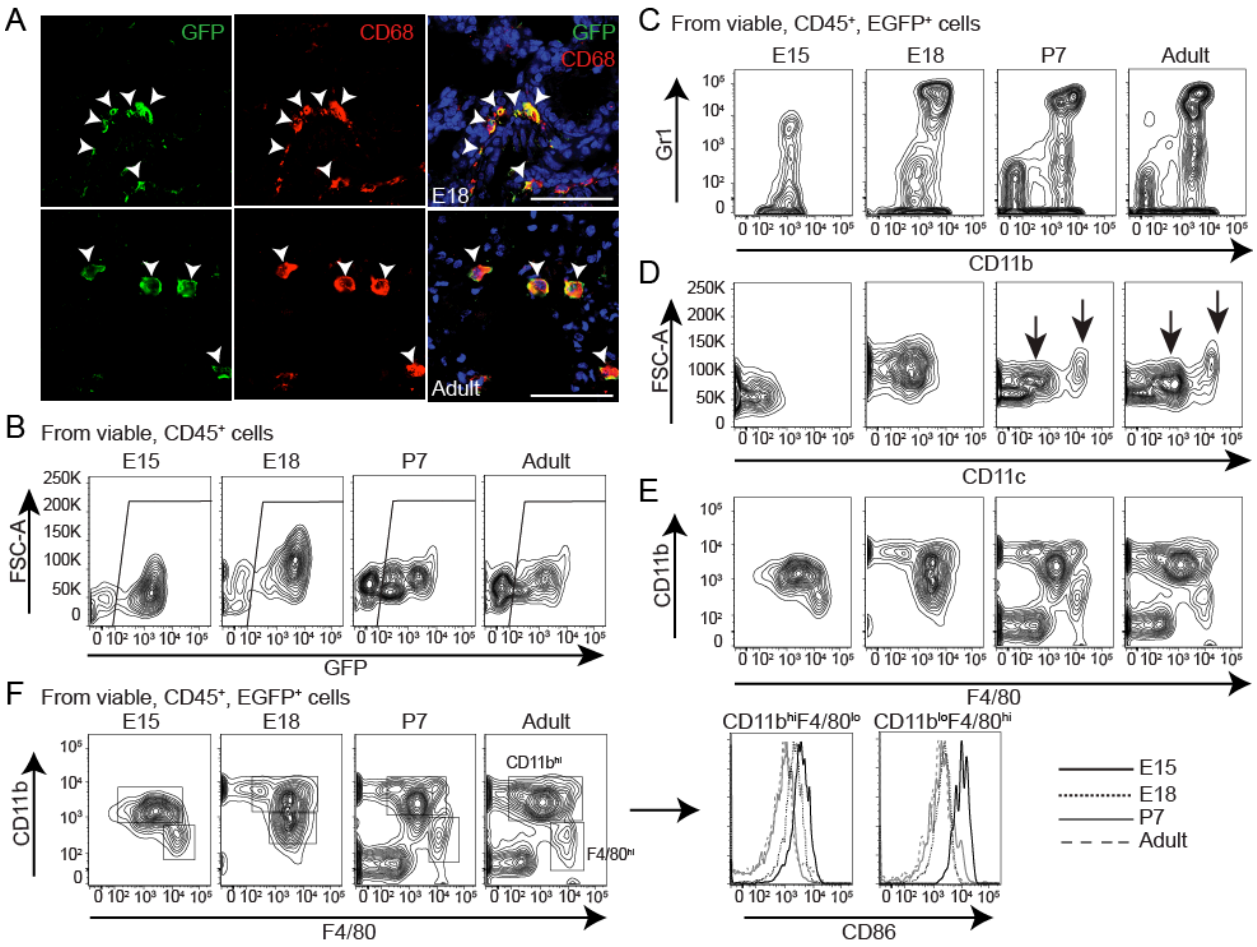

Figure 3.3. Developmental maturation of lung macrophages occurs after birth. *Csf1r*-EGFP^{+} cells were positive for CD68 (A). CD45^{+} cells were gated for GFP expression (B). (**C-F**) Flow cytometric analysis of *Csf1r*-EGFP^{+}, CD45^{+} macrophages from E15, E18, P7, and adult mouse lungs. CD11b and Gr1 expression show potential neutrophil populations in E18, P7, and adult lungs (C). Broad expression of CD11c^{+} (D), and CD11b^{+}/F4/80^{+} (E) cells were detected in P7 and adult lungs, consistent with mature alveolar macrophage differentiation. CD11b^{hi}F4/80^{lo} and CD11b^{lo}F4/80^{hi} populations were gated and analyzed for CD86 expression (F). (n = 3 adult mice, 3 E15 litters, 3 E18 litters, 3 P7 pups).

Cells from E15 lungs expressed Gr1, CD11b, and F4/80, but the patterns of expression suggest less diversity when compared to macrophages from more mature lungs. Expression of CD11c was low in E15 lungs, increased at E18, and was clearly present by P7 (Fig. 3.3D). Distinct populations of $CD11c^{+}$ cells were observed in P7 and adult lungs, consistent with previous data showing CD11c expression in mature alveolar macrophages (Zaynagetdinov, Sherrill et al. 2013; Guilliams, Dr Kleer et al. 2013). This flow cytometry expression pattern followed the real time PCR data, where CD11c expression was low in fetal lung but increased at birth (Fig. 3.1H).

The most consistent separation of E15 macrophages into distinct subpopulations was observed with gating $CD11b^{+}F4/80^{+}$ cells (Fig. 3.3E). The distribution of $CD11b^{hi}F4/80^{lo}$ and $CD11b^{lo}F4/80^{hi}$ cells in E15 lungs was consistent with recently reported data suggesting these two subpopulations may arise from distinct cellular precursors (Schulz, Gomez et al. 2012). Interestingly, macrophage subpopulations based on CD11b and F4/80 expression appeared to be more diverse in P7 and adult lungs. These data confirmed that the fetal lung does contain subpopulations of macrophages, but with less diversity than more mature lungs. To test if the $CD11b^{hi}F4/80^{lo}$ and $CD11b^{lo}F4/80^{hi}$ subpopulations had uniquely different proinflammatory markers, we compared CD86 expression in both populations. As seen in Figure 3.3F, both $CD11b^{hi}F4/80^{lo}$ and $CD11b^{lo}F4/80^{hi}$ macrophages expressed CD86 in E15 lungs.

We next tested if fetal lung macrophages responded to the proinflammatory stimulus LPS and the alternative activation cytokines IL-4 and IL-13 (Figure 3.4). LPS treatment of E15 fetal lung macrophages increased expression of CXCL-10, CCL-3, IL-1β, and TNFα, consistent with a robust proinflammatory response. IL-4 and IL-13 each inhibited expression of CXCL-10 and

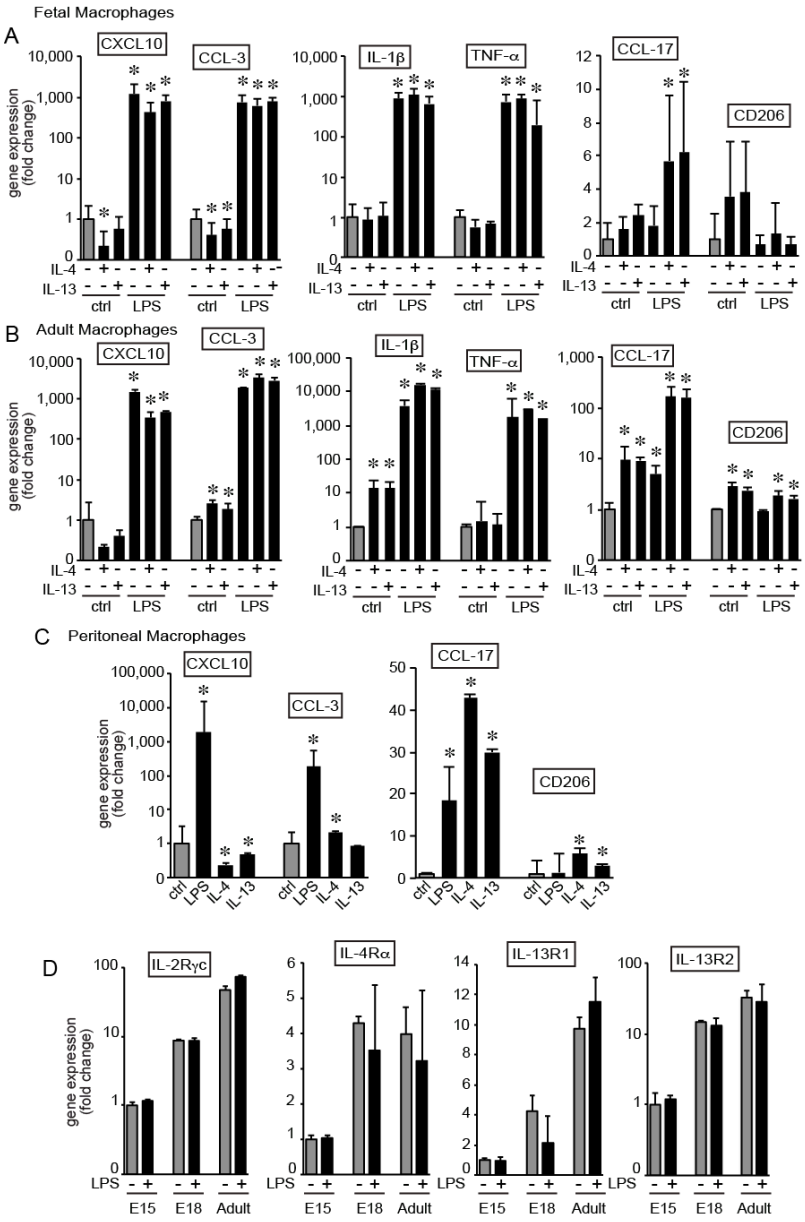

Figure 3.4. Transcriptional response of fetal mouse lung macrophages in response to LPS, IL-4, and IL-13. **(A)** Macrophages were isolated from E15 fetal C57/BL6 mouse lungs and treated with LPS (250 ng/ml), IL-4 (5 ng/ml), and IL-13 (10 ng/ml) for 4 h as indicated. Following RNA isolation, real time PCR measured expression of proinflammatory markers (CXCL10, CCL-3, IL-1β, TNFα) and alternative activation markers (CCL-17, CD206). For each marker, expression was compared to control, untreated samples (* $p < 0.05$; n = 6 litters). (**B**) Adult mouse alveolar macrophages were isolated by bronchoalveolar lavage and cultured with LPS, IL-4, and IL-13 as in (A) (* $p < 0.05$; n = 3). (**C**) To demonstrate control macrophage response to both LPS and IL-4 and IL-13, peritoneal macrophages were isolated from thioglycollate-injected C57/BL6 adult mice. Isolated cells were cultured in the presence of LPS, IL-4, or IL-13 for 4 h and gene expression measured by real time PCR (* $p < 0.05$; n = 3 mice for adult and peritoneal samples, 6 litters used for E15 samples). (**D**) IL-4R components were measured in macrophages from different stage lungs by real-time PCR. (* $p < 0.05$; n = 3).

CCL-3, but did not dampen the response to LPS. Treating E15 macrophages with IL-4 or IL-13 caused only a modest and statistically insignificant increase in the alternative activation markers CCL-17 and CD206. However, adding both LPS and IL-4/IL-13 did increase CCL-17 expression above levels seen with any agonist alone. In adult lung macrophages, IL-4 and IL-13 both increased CCL-17 and CD206 expression (Fig. 3.4B). Interestingly, IL-4 and IL-13 also upregulated expression of CCL-3 and IL-1β, although much less than LPS (Fig. 3.4B). As an additional comparison, IL-4 and IL-13 decreased CXCL-10 and increased CCL-17 and CD206 in adult peritoneal macrophages (Fig. 3.4C). Therefore E15 fetal lung macrophages responded similarly to LPS as adult macrophages, but appeared to have reduced sensitivity to the alternative activation cytokines IL-4 and IL-13. This reduced sensitivity to IL-4 and IL-13 could be due to low receptor expression in E15 cells compared to adult cells, as suggested by gene expression data for IL4Rα, IL13R1, etc. (Fig. 3.4D). LPS did not significantly change receptor gene expression in E15, E18, or adult lung macrophages (Fig. 3.4D).

We used a transgenic approach to further test if inflammatory signals and specifically NF-κB activation could regulate fetal lung macrophage development and maturation. IKFM double transgenic mice express a constitutively active IKKβ mutant in macrophages upon doxycycline exposure (Blackwell et al. 2011; Connelly et al. 2011). Pregnant dams were given doxycycline from E14-E18; lung macrophages were isolated from E18 IKFM and littermate controls. We then measured expression of the pro-inflammatory mediators CXCL-10, CCL-3, IL-1β, and TNFα in addition to the alternative activation markers CCL-17 and CD206 (Figure 3.5). IKFM macrophages expressed higher levels of CXCL-10, CCL-3, IL-1β, and TNFα, consistent with NF-κB activation (Fig. 3.5A-B). While E18 control macrophages

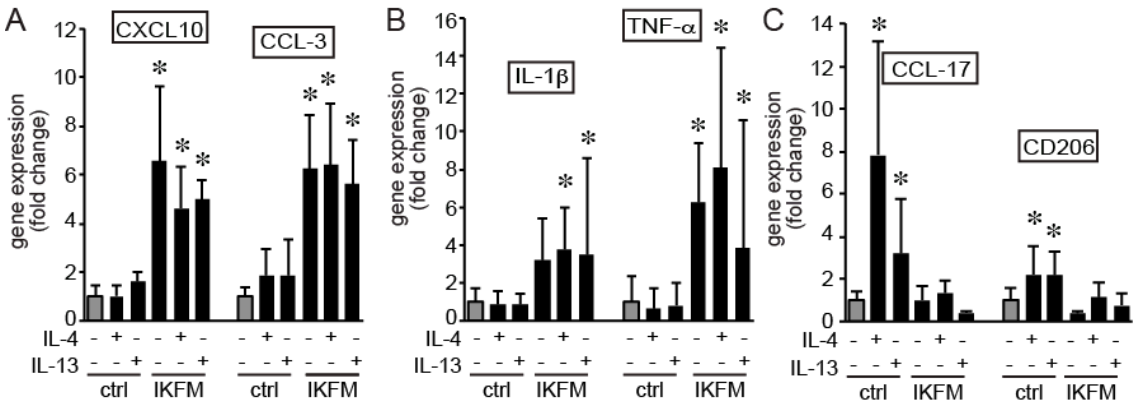

Figure 3.5. NF-κB activation in fetal mouse lung macrophages stimulated a proinflammatory response and reduced the response to IL-4 and IL-13. IKFM mice expressing a tetracycline-inducible constitutively active IKKb mutant were given doxycycline from E14-E18. Fetal lung macrophages from E18 IKFM fetal mouse lungs and littermate controls were cultured with IL-4 or IL-13. (**A-C**) RNA was isolated and expression of proinflammatory markers (CXCL10, CCL-3, IL-1β, TNFα) and alternative activation markers (CCL-17, CD206) were measured by real time PCR (* $p < 0.05$; n = 5 litters).

expressed increased CCL-17 and CD206 following IL-4 and IL-13 treatment, IL-4 and IL-13 had less effect on IKFM macrophages (Fig. 3.5C). These data suggested that fetal lung macrophage NF-κB activation could promote functional resistance to IL-4 and IL-13.

Immunostaining of IKFM and control lung sections did not reveal dramatic differences in the relative populations of cells expressing CD86, Mgl1/2, or CD206 in situ (Figure 3.6). However, flow cytometry showed shifts in relative CD11b and F4/80 expression. The increased relative percentage of $CD11b^{lo}F4/80^{hi}$ macrophages in IKFM lungs was consistent between litters (Fig. 3.7A-C). These $CD11b^{lo}F4/80^{hi}$ cells also expressed higher levels of IL-1β (Fig. 3.7D). Differences in gene expression were not due to selective transgene expression, as the cIKKβ transgene was expressed in both $CD11b^{hi}F4/80^{lo}$ and $CD11b^{lo}F4/80^{hi}$ cell populations (Fig. 3.7E). We previously measured increased macrophage cell number in IKFM lungs (Blackwell, Hipps et al. 2011). This increase could be due to proliferation of resident lung macrophages. Immunostaining showed that IKFM lungs contained a higher percentage of macrophages expressing phospho-HistoneH3 (Fig. 3.7F) and Ki67 (Fig. 3.7G). The increase in proliferation was associated with the relative increase in cyclinD1 expression in $CD11b^{lo}F4/80^{hi}$ macrophages (Fig. 3.7H). Therefore, in addition to stimulating expression of inflammatory mediators, NF-κB activation increased macrophage proliferation within fetal lung tissue.

The increase in $CD11b^{lo}F4/80^{hi}$ macrophages in IKFM lungs is consistent with increased differentiation, as mature alveolar macrophages are also $CD11b^{lo}F4/80^{hi}$ (Zaynagetdinov, Sherrill et al. 2013). Similarly, we measured increased CD204 and CD206 expression in IKFM lungs, both of which are expressed on the surface of mature alveolar macrophages (Fig. 3.7I). IKFM

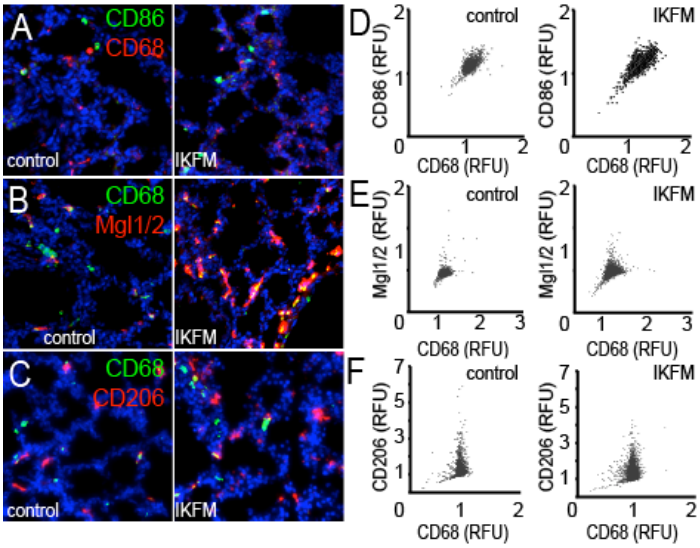

Figure 3.6. NF-κB activation in fetal mouse lung macrophages did not cause major shifts in macrophage populations. IKFM female mice were given doxycycline from E14-E18. Lungs from IKFM and control littermates were isolated at E18. (**A-C**) Frozen sections of littermate control and IKFM fetal lungs were co-immunostained with Abs against the pan-macrophage marker CD68 (green) and proinflammatory marker CD86 (A) or the alternative activation markers Mgl1/2 (B) and CD206 (C). Nuclei were labeled with DAPI. (**D-F**) Macrophages labeled in (A-C) were identified by widefield fluorescence microscopy. Multi-channel fluorescence of each cell was measured and plotted to demonstrate potential populations of cells with differing expression levels. Sum fluorescent intensity of individual macrophages was measured using Slidebook software. The patterns of macrophage marker intensity were similar between IKFM and control littermates. (n = 3 control littermate and 3 IKFM lungs, 20 images were counted from each lung).

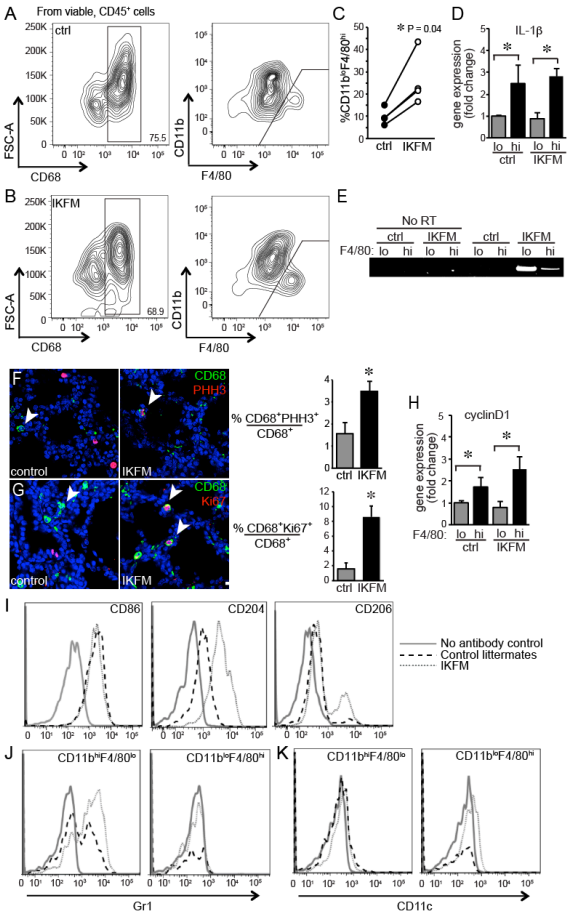

Figure 3.7. NF-κB activation increased alveolar macrophage phenotype markers in fetal mouse lung. Single cell suspensions were isolated from E18 IKFM and control-littermate fetal lungs. (**A,B**) Viable, $CD45^{+}CD68^{+}$ cells were gated on F4/80 and CD11b expression. IKFM lungs contained a more identifiable subpopulation of $CD11b^{lo}F4/80^{hi}$ macrophages (B). (**C**) Percentage of $CD11b^{lo}F4/80^{hi}$ macrophages within the $CD68^{+}$ population was increased in IKFM lungs compared to control littermates. Four independent litters are shown (* $p = 0.04$). **(D)** $CD11b^{lo}F4/80^{hi}$ macrophages produced higher mRNA levels in both IKFM and littermate-controls. **(E)** Both $CD11b^{hi}F4/80^{lo}$ and $CD11b^{lo}F4/80^{hi}$ macrophages from IKFM fetal lungs expressed the cIKKβ transgene when exposed in utero to doxycycline. **(F-G)** Frozen sections of E18 control littermate and IKFM lungs were immunostained stained with the macrophage marker CD68 and phosphohistone H3 (PHH3) or Ki67. IKFM lungs had increased number of $PHH3^{+}$ and $Ki67^{+}$ macrophages that were not due to overall increased cell proliferation throughout the lung. **(H)** $CD11b^{lo}F4/80^{hi}$ macrophages expressed increased cyclinD1 mRNA in both IKFM and control littermate fetal lungs (* $p < 0.05$; n = 3 control and 3 IKFM). **(I)** IKFM macrophages expressed increased CD204 and CD206. **(J-K)** Increased Gr1 expression in IKFM macrophages was only detected in the $CD11b^{hi}F4/80^{lo}$ subpopulation (J), while $CD11b^{lo}F4/80^{hi}$ macrophages from IKFM lungs expressed slightly elevated levels of CD11c (K). (n = 4 litters for A-C, I-J; 3 control and IKFM samples for D, E, H; 4 individual control and IKFM lungs were used in F-G, with approximately 10 images per lung).

lungs also contained higher numbers of $Gr1^{+}$ macrophages (Fig. 3.7J), suggesting possible recruitment of fetal monocytes. Importantly, Gr1 expression was only detected in $CD11b^{hi}F4/80^{lo}$ populations. Increased macrophage differentiation in IKFM lungs did not lead to large increases in CD11c, which remained very low in both $CD11b^{hi}F4/80^{lo}$ and $CD11b^{lo}F4/80^{hi}$ cells (Fig. 3.7K). Therefore, NF-κB stimulated changes in macrophage marker expression were most consistent with lung macrophage maturation and did not follow a clear proinflammatory/alternative activation or M1/M2 paradigm.

Discussion

Fetal lung macrophages undergo significant differentiation and maturational changes during development. While fetal lung macrophages expressed relatively consistent levels of CD68 and CD206 at each stage tested, other macrophage lineage markers increased significantly. Both proinflammatory and alternative activation markers increased during development without following a consistent M1/M2, proinflammatory/alternative activation paradigm. Developing lung macrophages were functional, as immature macrophages from E15 mouse lungs responded to the proinflammatory stimulus LPS. The partial response to IL-4 and IL-13 suggest that E15 lung macrophages may indicate a relative functional polarization toward a proinflammatory phenotype.

The notion of M1/M2 macrophage polarization derives largely from studies using tumor-associated macrophages and chronic inflammation models (Mitsuhashi et al. 2013; Starossom et al. 2012; Mantovani and Locati 2009). So while activation of M1 macrophages and M2

polarization may contribute to disease, this classification paradigm may not directly apply to the developmental phenotypes of lung macrophages. Adult alveolar macrophages express both M1 and M2 markers (Zaynagetdinov et al. 2013). We speculate that the constant exposure to inhaled pathogens and particulates requires that lung macrophages possess both robust killing activity (typically thought of as M1) and the ability to resolve or suppress inflammation and injury (an M2 process). Recent work demonstrated that macrophages in the postnatal lung express the alternative activation or M2 genes, Arg1, CCL-17, and Mrc1 (Jones, Williams et al. 2013). These studies also showed a downward trend of expression for some proinflammatory genes in later postnatal stages (Jones et al. 2013). However, mature alveolar macrophages also possess the ability to mount a strong proinflammatory immune response. Recent publications have in fact expanded M1/M2 classification into a spectrum model for classifying macrophage phenotype (Xue et al. 2014). Additionally, tissue macrophages in various developing organs appear to acquire unique phenotypic features (Laskin et al. 2001; Guillemin and Brew 2004). How these unique expression patterns might regulate differential or tissue-specific macrophage function remains unclear.

During lung development, the relative abundance of $CD11b^{hi}F4/80^{lo}$ and $CD11b^{lo}F4/80^{hi}$ macrophages undergo dynamic shifts. Distinct subpopulations are seen early in lung development and again around the time of birth as fetal monocytes/macrophages develop into postnatal and adult lung macrophages. Consistent with Guilliams et al. (Guilliams et al. 2013), we also observed increasing CD11c expression when fetal macrophage subpopulations differentiated into alveolar macrophages. Maturational changes in macrophage marker expression correlated with postnatal migration of macrophages into the alveolar air space. Our

data showing differences in CD11b and F4/80 expression with maturation and activation suggest that NF-κB signaling accelerates macrophage differentiation. IKKβ activity in fetal macrophages increased the percentage of $CD11b^{lo}F4/80^{hi}$ cells within the developing lung. The $CD11b^{lo}F4/80^{hi}$ subpopulation expressed higher levels of IL-1β mRNA, suggesting macrophage activation leads to the developmental maturation or recruitment of a proinflammatory subpopulation. However, the overall increase in the M2-like scavenger receptors CD204 and CD206 again emphasizes that lung macrophage differentiation is more complex than a simple M1/M2 classification. Previous studies show NF-κB activation also influences dendritic cell maturation. Deleting both RelA and p50 subunits of NF-κB prevented normal $CD11c^{+}$ dendritic cell development in the livers of mice in adoptive transfer studies (Ouaaz, Zheng et al. 2002). In studies using GM-CSF and IL-4 to induce dendritic cell differentiation and maturation in human monocytes, NF-κB inhibition reduced expression of CD1a and DC-SIGN and reduced dendritic progenitor cell number (van de Laar, van de Bosch et al. 2010). How NF-κB signaling might interact with other factors regulating macrophage development (i.e. PU.1, CEBP, Myb, Maf) also remains unclear (Sharif et al. 2007).

Recent findings demonstrating proliferation and self-renewal of resident tissue macrophages have challenged the notion that macrophage populations are solely comprised of recruited monocytic cells (Yona et al. 2013). Local production of the macrophage mitogens CSF-1 and CCL-2 stimulate macrophage proliferation within tissues via JAK/STAT signaling pathways (Pierce et al. 1990; Pixley and Stanley 2004; Lin et al. 2002; Qian et al. 2011). Here we showed that transgenic expression of a constitutively active IKKβ transgene in macrophages also stimulated proliferation within fetal mouse lungs. NF-κB activation could increase

production of intermediate factors that drive cell proliferation via autocrine loops or via neighboring cells residing within a multicellular niche. Alternatively, increased IKKβ activity could facilitate signaling through additional intracellular pathways connected with cell proliferation. In cancer cell models, NF-κB promotes cyclinD1 expression and is required for cell growth and proliferation (Montano-Almendras et al. 2012; Tang et al. 2013). While both $CD11b^{hi}F4/80^{lo}$ and $CD11b^{lo}F4/80^{hi}$ macrophage populations in IFKM fetal mouse lungs expressed the cIKKβ transgene, macrophages with the highest F4/80 and IL-1β expression also contained the highest expression of cyclinD1. These data suggested that more mature $CD11b^{lo}F4/80^{hi}$ cells in the fetal lung may have increased capacity for both cytokine expression and proliferation.

Our data demonstrate that immature fetal lung macrophages respond robustly to LPS exposure. The relative pro-inflammatory and anti-inflammatory functions of developing lung macrophages remain unclear. How IL-4 and IL-13 regulate these functions may be important in disease, as IL-13 induces Th2 inflammation in asthmatic lungs (Zhu et al. 2002; Cho et al. 2006). Previous studies comparing adult and neonatal monocytes from different sources measured variable cytokine responses following exposure to TLR agonists (Kollmann et al. 2009; Berner et al. 2002; Taniguchi et al. 1993). Consistent differences were reported primarily in interferon production in response to co-cultures and macrophage activators (Wilson et al. 1986; Taylor and Bryson 1985; Scott et al. 1997). However, relative differences in production of cytokines such as IL-1β or TNFα and changes to the kinetics of transcriptional activation and subsequent silencing could still lead to important physiological differences in the innate immune response within immature lungs.

The ability of macrophage activation to increase maturation as well as release inflammatory mediators could have significant implications in disease. Preterm infants are often exposed to multiple agents capable of activating immature but functional lung macrophages (Newton 1993; Martius and Eschenbach 1990; Speer 2009). Early macrophage activation in IKFM mice disrupts structural lung morphogenesis, possibly modeling BPD pathogenesis in human patients. In addition, inflammation-induced macrophage maturation might sensitize the lung innate immune response to repeated infectious challenges. This two-hit hypothesis has been frequently suggested as important in the pathogenesis of neonatal chronic lung disease and BPD (Jobe 1999; Wright and Kirpalani 2011). Increased macrophage maturation in the immature lung and reduced responsiveness to IL-4 and IL-13 could limit the ability to resolve lung inflammation and promote wound healing. Investigating these new paradigms in macrophage biology and development will lead to new therapeutic strategies for pediatric lung disease.

References

Angelone, D. F., M. R. Wessels, M. Coughlin, E. E. Suter, P. Valentini, L. A. Kalish, and O. Levy (2006) Innate immunity of the human newborn is polarized toward a high ratio of IL-6/TNF-alpha production in vitro and in vivo. *Pediatr. Res.* **60**: 205-209.

Baier, R. J., J. Loggins, and T. E. Kruger (2001) Monocyte chemoattractant protein-1 and interleukin-8 are increased in bronchopulmonary dysplasia: relation to isolation of *Ureaplasma urealyticum*. *J. Investig. Med* **49**: 362-369.

Berner, R., P. Welter, and M. Brandis (2002) Cytokine expression of cord and adult blood mononuclear cells in response to *Streptococcus agalactiae*. *Pediatr. Res.* **51**: 304-309.

Blackwell, T. S., A. N. Hipps, Y. Yamamoto, W. Han, W. J. Barham, M. C. Ostrowski, F. E. Yull, and L. S. Prince (2011) NF-kappaB signaling in fetal lung macrophages disrupts airway morphogenesis. *J. Immunol.* **187**: 2740-2747.

Blahnik, M. J., R. Ramanathan, C. R. Riley, and P. Minoo (2001) Lipopolysaccharide-induced tumor necrosis factor-alpha and IL-10 production by lung macrophages from preterm and term neonates. *Pediatr. Res.* **50**: 726-731.

Burnett, S. H., E. J. Kershen, J. Zhang, L. Zeng, S. C. Straley, A. M. Kaplan, and D. A. Cohen (2004) Conditional macrophage ablation in transgenic mice expressing a Fas-based suicide gene. *J. Leukoc. Biol.* **75**: 612-623.

Cho, S. J., M. J. Kang, R. J. Homer, H. R. Kang, X. Zhang, P. J. Lee, J. A. Elias, and C. G. Lee (2006) Role of early growth response-1 (Egr-1) in interleukin-13-induced inflammation and remodeling. *J. Biol. Chem.* **281**: 8161-8168.

Connelly, L., W. Barham, H. M. Onishko, L. Chen, T. P. Sherrill, T. Zabuawala, M. C. Ostrowski, T. S. Blackwell, and F. E. Yull (2011) NF-kappaB activation within macrophages leads to an anti-tumor phenotype in a mammary tumor lung metastasis model. *Breast Cancer Res.* **13**: R83.

Cortez-Retamozo, V., M. Etzrodt, A. Newton, R. Ryan, F. Pucci, S. W. Sio, W. Kuswanto, P. J. Rauch, A. Chudnovskiy, Y. Iwamoto, R. Kohler, B. Marinelli, R. Gorbatov, G. Wojtkiewicz, P. Panizzi, M. Mino-Kenudson, R. Forghani, J. L. Figueiredo, J. W. Chen, R. Xavier, F. K. Swirski, M. Nahrendorf, R. Weissleder, and M. J. Pittet (2013) Angiotensin II drives the production of tumor-promoting macrophages. *Immunity* **38**: 296-308.

Duluc, D., Y. Delneste, F. Tan, M. P. Moles, L. Grimaud, J. Lenoir, L. Preisser, I. Anegon, L. Catala, N. Ifrah, P. Descamps, E. Gamelin, H. Gascan, M. Hebbar, and P. Jeannin (2007)

Tumor-associated leukemia inhibitory factor and IL-6 skew monocyte differentiation into tumor-associated macrophage-like cells. *Blood* **110**: 4319-4330.

Fang, F. C (2004) Antimicrobial reactive oxygen and nitrogen species: concepts and controversies. *Nat. Rev. Microbiol.* **2**: 820-832.

Geissmann, F., M. G. Manz, S. Jung, M. H. Sieweke, M. Merad, and K. Ley (2010) Development of monocytes, macrophages, and dendritic cells. *Science* **327**: 656-661.

Ghisletti, S., I. Barozzi, F. Mietton, S. Polletti, F. De Santa, E. Venturini, L. Gregory, L. Lonie, A. Chew, C. L. Wei, J. Ragoussis, and G. Natoli (2010) Identification and characterization of enhancers controlling the inflammatory gene expression program in macrophages. *Immunity* **32**: 317-328.

Gordon, S., and F. O. Martinez (2010) Alternative activation of macrophages: mechanism and functions. *Immunity* **32**: 593-604.

Gordon, S., and P. R. Taylor (2005) Monocyte and macrophage heterogeneity. *Nat. Rev. Immunol.* **5**: 953-964.

Guillemin, G. J., and B. J. Brew (2004) Microglia, macrophages, perivascular macrophages, and pericytes: a review of function and identification. *J. Leukoc. Biol.* **75**: 388-397.

Guilliams, M., I. De Kleer, S. Henri, S. Post, L. Vanhoutte, S. De Prijck, K. Deswarte, B. Malissen, H. Hammad, and B. N. Lambrecht (2013) Alveolar macrophages develop from fetal monocytes that differentiate into long-lived cells in the first week of life via GM-CSF. *J. Exp. Med.* **210**: 1977-1992.

Gutierrez-Ramos, J. C., C. Lloyd, M. L. Kapsenberg, J. A. Gonzalo, and A. J. Coyle (2000) Non-redundant functional groups of chemokines operate in a coordinate manner during the inflammatory response in the lung. *Immunol. Rev.* **177**: 31-42.

Jobe, A. J. (1999) The new BPD: an arrest of lung development. *Pediatr. Res.* **46**: 641-643.

Jones, C. V., T. M. Williams, K. A. Walker, H. Dickinson, S. Sakkal, B. A. Rumballe, M. H. Little, G. Jenkin, and S. D. Ricardo (2013) M2 macrophage polarisation is associated with alveolar formation during postnatal lung development. *Respir. Res.* **14**: 41.

Kollmann, T. R., J. Crabtree, A. Rein-Weston, D. Blimkie, F. Thommai, X. Y. Wang, P. M. Lavoie, J. Furlong, E. S. Fortuno, 3rd, A. M. Hajjar, N. R. Hawkins, S. G. Self, and C. B. Wilson (2009) Neonatal innate TLR-mediated responses are distinct from those of adults. *J. Immunol.* **183**: 7150-7160.

Kollmann, T. R., O. Levy, R. R. Montgomery, and S. Goriely (2012) Innate immune function by Toll-like receptors: distinct responses in newborns and the elderly. *Immunity* **37**: 771-783.

Laskin, D. L., B. Weinberger, and J. D. Laskin (2001) Functional heterogeneity in liver and lung macrophages. *J. Leukoc. Biol.* **70**: 163-170.

Lin, E. Y., V. Gouon-Evans, A. V. Nguyen, and J. W. Pollard (2002) The macrophage growth factor CSF-1 in mammary gland development and tumor progression. *J. Mammary Gland Biol. Neoplasia* **7**: 147-162.

Lumeng, C. N., J. L. Bodzin, and A. R. Saltiel (2007) Obesity induces a phenotypic switch in adipose tissue macrophage polarization. *J. Clin. Invest.* **117**: 175-184.

Mantovani, A., S. K. Biswas, M. R. Galdiero, A. Sica, and M. Locati (2013) Macrophage plasticity and polarization in tissue repair and remodelling. *J. Pathol.* **229**: 176-185.

Mantovani, A., and M. Locati (2009) Orchestration of macrophage polarization. *Blood* **114**: 3135-3136.

Mantovani, A., A. Sica, S. Sozzani, P. Allavena, A. Vecchi, and M. Locati (2004) The chemokine system in diverse forms of macrophage activation and polarization. *Trends Immunol.* **25**: 677-686.

Martinez, F. O., S. Gordon, M. Locati, and A. Mantovani (2006) Transcriptional profiling of the human monocyte-to-macrophage differentiation and polarization: new molecules and patterns of gene expression. *J. Immunol.* **177**: 7303-7311.

Martius, J., and D. A. Eschenbach (1990) The role of bacterial vaginosis as a cause of amniotic fluid infection, chorioamnionitis and prematurity--a review. *Arch. Gynecol. Obstet* **247**: 1-13.

Mitsuhashi, A., H. Goto, T. Kuramoto, S. Tabata, S. Yukishige, S. Abe, M. Hanibuchi, S. Kakiuchi, A. Saijo, Y. Aono, H. Uehara, S. Yano, J. G. Ledford, S. Sone, and Y. Nishioka (2013) Surfactant protein A suppresses lung cancer progression by regulating the polarization of tumor-associated macrophages. *Am. J. Pathol.* **182**: 1843-1853.

Montano-Almendras, C. P., A. Essaghir, H. Schoemans, I. Varis, L. A. Noel, A. I. Velghe, D. Latinne, L. Knoops, and J. B. Demoulin (2012) ETV6-PDGFRB and FIP1L1-PDGFRA stimulate human hematopoietic progenitor cell proliferation and differentiation into eosinophils: the role of nuclear factor-kappaB. *Haematologica* **97**: 1064-1072.

Mosser, D. M., and J. P. Edwards (2008) Exploring the full spectrum of macrophage activation. *Nat. Rev. Immunol.* **8**: 958-969.

Newton, E. R. (1993) Chorioamnionitis and intraamniotic infection. *Clin. Obstet. Gynecol.* **36**: 795-808.

Ouaaz, F., J. Arron, Y. Zheng, Y. Choi, and A. A. Beg (2002) Dendritic cell development and survival require distinct NF-kappaB subunits. *Immunity* **16**: 257-270.

Pierce, J. H., E. Di Marco, G. W. Cox, D. Lombardi, M. Ruggiero, L. Varesio, L. M. Wang, G. G. Choudhury, A. Y. Sakaguchi, P. P. Di Fiore, and et al (1990) Macrophage-colony-stimulating factor (CSF-1) induces proliferation, chemotaxis, and reversible monocytic differentiation in myeloid progenitor cells transfected with the human c-fms/CSF-1 receptor cDNA. *Proc. Natl. Acad. Sci. USA* **87**: 5613-5617.

Pixley, F. J., and E. R. Stanley (2004) CSF-1 regulation of the wandering macrophage: complexity in action. *Trends Cell Biol.* **14**: 628-638.

Qian, B. Z., J. Li, H. Zhang, T. Kitamura, J. Zhang, L. R. Campion, E. A. Kaiser, L. A. Snyder, and J. W. Pollard (2011) CCL2 recruits inflammatory monocytes to facilitate breast-tumour metastasis. *Nature* **475**: 222-225.

Red Eagle, A., and A. Chawla (2010) In obesity and weight loss, all roads lead to the mighty macrophage. *J. Clinical Invest.* **120**: 3437-3440.

Ruffell, B., N. I. Affara, and L. M. Coussens (2012). Differential macrophage programming in the tumor microenvironment. *Trends Immunol.* **33**: 119-126.

Schulz, C., E. Gomez Perdiguero, L. Chorro, H. Szabo-Rogers, N. Cagnard, K. Kierdorf, M. Prinz, B. Wu, S. E. Jacobsen, J. W. Pollard, J. Frampton, K. J. Liu, and F. Geissmann (2012) A lineage of myeloid cells independent of Myb and hematopoietic stem cells. *Science* **336**: 86-90.

Scott, M. E., M. Kubin, and S. Kohl (1997) High level interleukin-12 production, but diminished interferon-gamma production, by cord blood mononuclear cells. *Pediatr. Res.* **41**: 547-553.

Sharif, O., V. N. Bolshakov, S. Raines, P. Newham, and N. D. Perkins (2007) Transcriptional profiling of the LPS induced NF-kappaB response in macrophages. *BMC Immunol.* **8**: 1.

Sica, A., and A. Mantovani (2012) Macrophage plasticity and polarization: in vivo veritas. *J. Clin. Invest.* **122**: 787-795.

Sindrilaru, A., T. Peters, S. Wieschalka, C. Baican, A. Baican, H. Peter, A. Hainzl, S. Schatz, Y. Qi, A. Schlecht, J. M. Weiss, M. Wlaschek, C. Sunderkotter, and K. Scharffetter-Kochanek (2011) An unrestrained proinflammatory M1 macrophage population induced by iron impairs wound healing in humans and mice. *J. Clin. Invest.* **121**: 985-997.

Speer, C. P. (2009) Chorioamnionitis, postnatal factors and proinflammatory response in the pathogenetic sequence of bronchopulmonary dysplasia. *Neonatology* **95**: 353-361.

Starossom, S. C., I. D. Mascanfroni, J. Imitola, L. Cao, K. Raddassi, S. F. Hernandez, R. Bassil, D. O. Croci, J. P. Cerliani, D. Delacour, Y. Wang, W. Elyaman, S. J. Khoury, and G. A. Rabinovich (2012) Galectin-1 deactivates classically activated microglia and protects from inflammation-induced neurodegeneration. *Immunity* **37**: 249-263.

Tang, H., Y. Sun, Z. Shi, H. Huang, Z. Fang, J. Chen, Q. Xiu, and B. Li (2013) YKL-40 induces IL-8 expression from bronchial epithelium via MAPK (JNK and ERK) and NF-kappaB pathways, causing bronchial smooth muscle proliferation and migration. *J. Immunol.* **190**: 438-446.

Taniguchi, T., N. Matsuzaki, K. Shimoya, R. Neki, T. Okada, H. Kitajima, F. Saji, and O. Tanizawa (1993) Fetal mononuclear cells show a comparable capacity with maternal mononuclear cells to produce IL-8 in response to lipopolysaccharide in chorioamnionitis. *J. Reprod. Immunol.* **23**: 1-12.

Taylor, S., and Y. J. Bryson (1985) Impaired production of gamma-interferon by newborn cells in vitro is due to a functionally immature macrophage. *J. Immunol.* **134**: 1493-1497.

Tullus, K., G. W. Noack, L. G. Burman, R. Nilsson, B. Wretlind, and A. Brauner (1996) Elevated cytokine levels in tracheobronchial aspirate fluids from ventilator treated neonates with bronchopulmonary dysplasia. *Euro. J. Pediatr.* **155**: 112-116.

van de Laar, L., A. van den Bosch, S. W. van der Kooij, H. L. Janssen, P. J. Coffer, C. van Kooten, and A. M. Woltman (2010) A nonredundant role for canonical NF-kappaB in human myeloid dendritic cell development and function. *J. Immunol.* **185**: 7252-7261.

Watterberg, K. L., L. M. Demers, S. M. Scott, and S. Murphy (1996) Chorioamnionitis and early lung inflammation in infants in whom bronchopulmonary dysplasia develops. *Pediatrics* **97**: 210-215.

Wang, H., J. Oei, K. Lui, and R. Henry (2002) Interleukin-16 in tracheal aspirate fluids of newborn infants. *Early Hum.* **67**: 79-86.

Wilson, C. B., J. Westall, L. Johnston, D. B. Lewis, S. K. Dower, and A. R. Alpert (1986) Decreased production of interferon-gamma by human neonatal cells. Intrinsic and regulatory deficiencies. *J. Clin. Invest.* **77**: 860-867.

Wright, C. J., and H. Kirpalani (2011) Targeting inflammation to prevent bronchopulmonary dysplasia: can new insights be translated into therapies? *Pediatrics* **128**: 111-126.

Xue, J., S. V. Schmidt, J. Sander, A. Draffehn, W. Krebs, I. Quester, D. De Nardo, T. D. Gohel, M. Emde, L. Schmidleithner, H. Ganesan, A. Nino-Castro, M. R. Mallmann, L. Labzin, H. Theis, M. Kraut, M. Beyer, E. Latz, T. C. Freeman, T. Ulas, and J. L. Schultze (2014) Transcriptome-based network analysis reveals a spectrum model of human macrophage activation. *Immunity* **40**: 274-288.

Yerkovich, S. T., M. E. Wikstrom, D. Suriyaarachchi, S. L. Prescott, J. W. Upham, and P. G. Holt (2007) Postnatal development of monocyte cytokine responses to bacterial lipopolysaccharide. *Pediatr. Res.* **62**: 547-552.

Yona, S., K. W. Kim, Y. Wolf, A. Mildner, D. Varol, M. Breker, D. Strauss-Ayali, S. Viukov, M. Guilliams, A. Misharin, D. A. Hume, H. Perlman, B. Malissen, E. Zelzer, and S. Jung (2013) Fate mapping reveals origins and dynamics of monocytes and tissue macrophages under homeostasis. *Immunity* **38**: 79-91.

Zaynagetdinov, R., T. P. Sherrill, P. L. Kendall, B. H. Segal, K. P. Weller, R. M. Tighe, and T. S. Blackwell (2013) Identification of Myeloid Cell Subsets in Murine Lungs Using Flow Cytometry. *Am. J. Respir. Cell Mol. Biol*. **49**: 180-189.

Zhu, Z., B. Ma, T. Zheng, R. J. Homer, C. G. Lee, I. F. Charo, P. Noble, and J. A. Elias (2002) IL-13-induced chemokine responses in the lung: role of CCR2 in the pathogenesis of IL-13-induced inflammation and remodeling. *J. Immunol.* **168**: 2953-2962.

CHAPTER IV

IL-1beta and Inflammasome Activity Link Macrophage Activation with Abnormal Lung Airway Morphogenesis

Introduction

Lung infection and inflammation cause significant illness and death in newborn infants. Both adult and neonatal lungs contact the atmosphere and inhale various pathogens and injurious agents. However, the particular susceptibility of neonatal lungs to disease suggests developmental immaturity of the lung innate immune system. In preterm infants, infection and inflammation injures the developing lung, preventing normal airway morphogenesis and causing bronchopulmonary dysplasia (BPD) (Romero et al 2002; Jobe 2003). Developing specific therapies to prevent BPD have been restricted by our lack of complete understanding of how the lung innate immune system matures and how activation of immunity disrupts normal developmental pathways.

Inhaled microbes and particles interact with multiple cell populations in the lung. Among the various lung cells, macrophages are the primary sites of inflammatory activation (Blackwell et al. 2011). Even in the fetal lung where immature macrophages reside largely in the interstitium, macrophages are the major cells that respond to microbial products and release inflammatory mediators. Other cell populations including airway epithelia, vascular endothelia, and mesenchymal cells play supporting roles in the innate immune response and are targets of macrophage-derived soluble inflammatory mediators. Even though macrophages appear to be required for initiating lung inflammation, the effects of microbial products on lung development

and airway morphogenesis require innate immune signaling and NF-κB activation in target mesenchymal and epithelial cells (Benjamin et al. 2010). Therefore connecting macrophage activation and abnormal lung development requires production and release of paracrine inflammatory mediators.

Among the soluble inflammatory mediators released by lung macrophages, IL-1β appears to play a key role in neonatal lung injury. Recent studies have linked IL-1β signaling to hyperoxia-induced defects in alveolar development in neonatal mice (Nold et al. 2013). Transgenic IL-1β overexpression can inhibit normal fetal lung development (Bry et al. 2007). Interestingly, these effects appear developmentally regulated, with more pronounced effects during the late canalicular and saccular stages of fetal lung development. Similarly, we previously observed that macrophage activation early in lung development did not have the same inhibitory effects on morphogenesis as during the later stages (Blackwell et al. 2011). These data suggested that the effects of IL-1β on lung morphogenesis were developmentally regulated, either at the level of IL-1β release or the responsiveness to IL-1β by target cells.

Here we use complementary mouse models to demonstrate that IL-1β is the key cytokine connecting activation of the initial inflammatory response in fetal lung macrophages and abnormal saccular airway branching morphogenesis. Consistent with this mechanism, functional inflammasome activity was required and sufficient for abnormal late stage fetal lung development. While target mesenchymal cells in the developing lung were responsive to inflammatory mediators at each stage tested, the expression of multiple inflammasome components were expressed at much higher levels in newborn and adult lung macrophages. In addition, inflammatory activation accelerated the normal developmental expression of the inflammasome. Development of a functional inflammasome and release of IL-1β following

inflammatory activation are therefore required for the defects in lung development similar to that seen in human disease.

Methods and Materials

Reagents

The following antibodies were used in explant cultures and were obtained from R&D Systems: anti-IL1β, anti-TNFα, goat IgG, and rat IgG. Gel-purified *Escherichia coli* LPS (O55:B5) was purchased from Sigma-Aldrich, and Caspase-1 Inhibitor I (YVAD-CHO) was purchased from Calbiochem. The following antibodies were used for immunofluorescence: rat anti-CD68 (Acris), rabbit anti-caspase 1 p10 (Santa Cruz Biotechnology), rabbit anti-NALP1 (NLRP1, Santa Cruz Biotechnology), rabbit anti-ASC (Abcam), and rabbit anti-Cryopyrin (NLRP3, Santa Cruz Biotechnology). ProLong Gold with DAPI mounting media and Alexa-conjugated secondary antibodies (AF488, AF555) were obtained from Invitrogen. The nuclear stain DRAQ5 was purchased from Thermo Scientific. Fetal lung mesenchymal cells were treated with recombinant IL-1β (rIL1β, R&D Systems), recombinant TNFα (rTNFα, R&D Systems), recombinant IL18 (rIL18, MBL International Corporation), and Pam_3Cys-Ser-$(Lys)_4$ (Millipore). Luciferase activity was measured with the luciferase assay system from Promega. Cells were cultured in media from Corning's Cellgro and 10% FBS (Thermo Scientific). DNase I from bovine pancreas type IV (DNase) and collagenase from clostridium histolyticum type XI were purchased from Sigma-Aldrich.

Mouse strains and lung explant culture

Animal experiments were approved by the Institutional Animal Care and Use Committee from the University of California at San Diego. C57Bl/6 mice were used as wild-type controls and were obtained from Harlan Laboratories. IL-1β$^{-/-}$, NLRP3^{L351P}CreL, and IKFM mouse strains were developed and described previously. To generate NLRP3^{L351P}CreL mutants, homozygous LysM-Cre mice were crossed with heterozygous NLRP3^{L351P} mice. NLRP3^{L351P}CreL offspring have macrophages with constitutively active NLRP3 inflammasome. IKFM mice are a doxycycline inducible model obtained from Csf1r-rtTA mice crossed to a Tet-O-cIKKβ. IKFM mice have macrophages with constitutively active IKKβ. Doxycycline-containing water (2g/L) was given to pregnant dams to induce transgene expression in IKFM embryos. The morning of plug identification was embryonic day 0 (E0). Fetal lung explant isolation and culture has previously been described. Briefly, E15 fetal lungs were isolated, minced into approximately 1mm size, and cultured on a transwell with an air-liquid interface. Brightfield images of explants were taken at 24h and 72h. Saccular airway branching was quantified as the number of branches newly formed between 24h and 72h. For luciferase activity in NGL explants, explants were isolated and ground in reporter lysis buffer (Promega) and measured with a luciferase assay system (Promega).

Fetal lung macrophage isolation

Isolation of fetal lung macrophages has previously been described. Briefly, fetal lungs are dissected and enzymatically digested with DNase (30 ug/ml) and collagenase (0.7 mg/ml). Cells were passed through a 70 um cell strainer to obtain a single cell suspension. Adult alveolar macrophages were isolated by bronchoalveolar lavage as previously described.

Tissue processing, immunolabeling, and imaging

Fetal mouse lung tissue was dissected and fixed in 4% paraformaldehyde (Electron Microscopy Sciences), washed, and processed through a sucrose gradient for embedding into OCT media (Tissue-Tek) or a dehydrating series for embedding into paraffin. For immunofluorescence on frozen sections, Alexa-conjugated secondary antibodies aided antibody visualization and DRAQ5 labeled nuclei. Confocal images were acquired using a Leica TCS SPE (Leica microsystems) laser-scanning confocal microscope. Eosin (Ricca Chemical) and Mayer's hematoxylin (Dako) were used on paraffin sections for H&E staining. Serial lung H&E sections were measured for fractional lung volumes of tissue and airspace. Intersection points of a grid overlay on H&E images were defined as tissue or airspace within ImageJ (NIH). Images from explants were obtained from an Olympus IX8I microscope with a Hamamatsu Orca ER CCD camera and Slidebook software or from a Touptek Toupcam with Toupview software. NGL explant GFP images were taken on a EVOS Cell Imaging System (Invirtrogen).

Flow Cytometry

The following antibodies were used for flow cytometry: CD11b-V450, CD86-Pe-Cy7, Gr1 PerCP-Cy5.5, and CD45 allophycocyanin-Cy7 (BD Biosciences); CD204-AF647, CD68-FITC, and CD206-PE (AbD Serotec); F4/80-PE (Invitrogen); and CD11c-Pe-Cy5 (BioLegend). Viable cells were selected using the LIVE/DEAD Fixable Blue Dead Cell Stain Kit (Invitrogen). Fetal and adult lungs were digested to a single cell suspension with DNase and collagense. Red blood cells were lysed with ACK lysing buffer (Invitrogen). On ice, 3% FBS was used to block cells for 15 min, and was followed by incubation with cell surface antibodies for 30-60 min.

Intracelluar antibodies were incubated with cells for 30min on ice after using the Intracellular Fixation and Permeabilization Kit (eBioscience). Flow cytometry measurements were conducted on a BD LSR II. The gating strategy: Doublets were excluded based on FSC-A against FSC-H followed by SSC-A against SSC-H. Cells negative for LIVE/DEAD Fixable Blue Stain defined viable cells. Further gating was for $CD45^{+}$ and $CD68^{+}$ cells, which were separated into $CD11b^{hi}F4/80^{lo}$ and $CD11b^{lo}F4/80^{hi}$ cells.

Results

IL-1β inhibits fetal airway morphogenesis

Macrophage activation inhibits normal lung morphogenesis. Soluble inflammatory mediators released by macrophages disrupt expression of key developmental genes in lung epithelia and adjacent mesenchyme. Since IL-1β and TNFα activated NF-κB in target mesenchymal cells, we tested if these mediators were required to link macrophage activation and abnormal airway morphogenesis. We initially used neutralizing antibodies against IL-1β and TNFα in a saccular stage fetal mouse lung explant model (Figure 4.1). As we previously demonstrated, adding *E. coli* LPS prevented the normal formation of new airways along the periphery of cultured explants. Including anti-IL1β in the culture media prevented this decrease, allowing normal airway branching (Figure 4.1B). However, anti-TNFα antibodies had no effect (Figure 4.1C). Including both anti-IL1β and anti-TNFα antibodies gave similar protection as anti-IL1β alone (Figure 4.1D). These initial experiments suggested that IL-1β signaling was required for LPS to prevent normal airway morphogenesis. The protective effects of anti-IL-1β did not appear to be due to overall inhibition of inflammation, as LPS induced similar CCL2

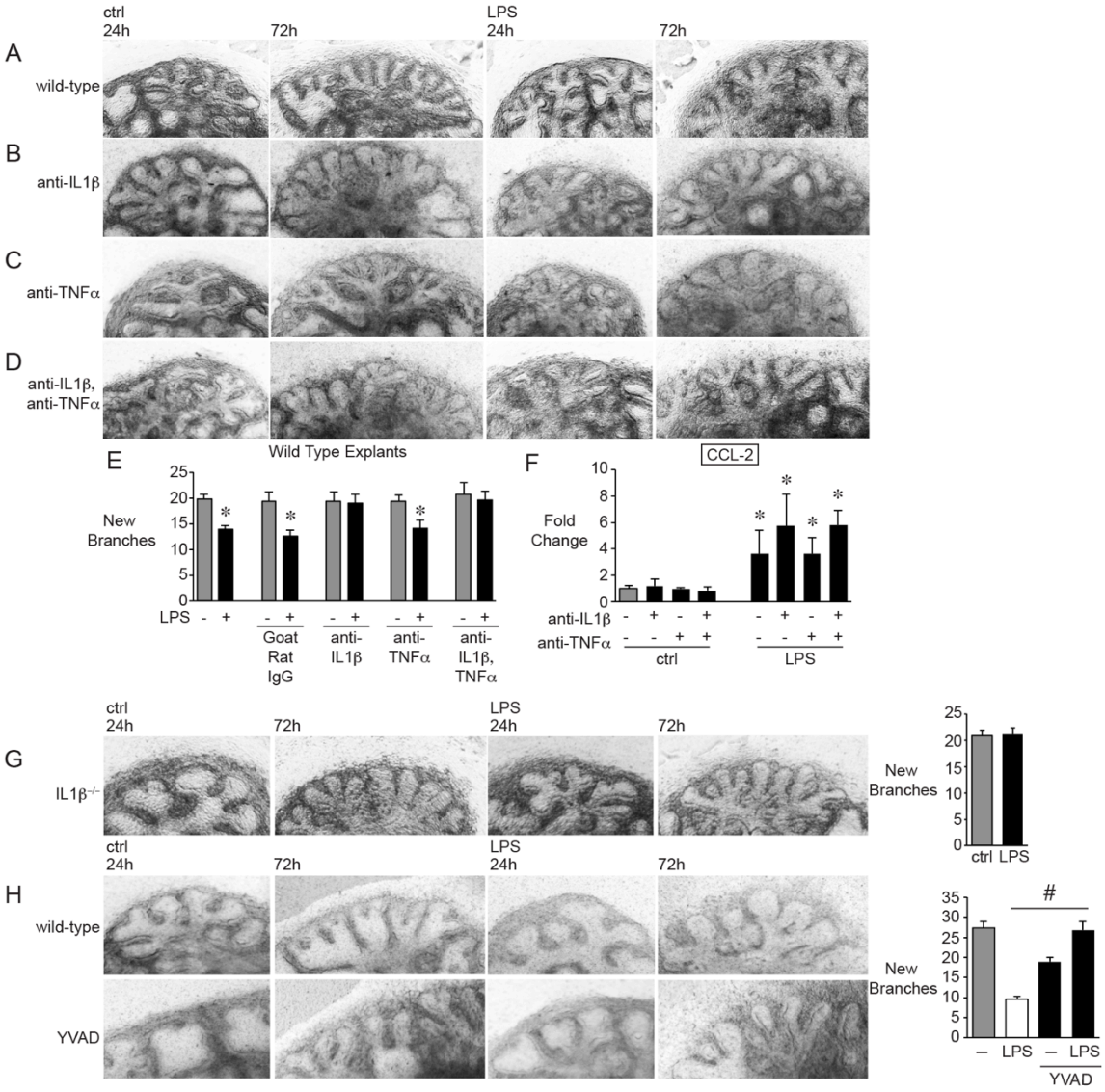
ctrl
24h
72h
LPS
24h
72h
A
wild-type
B
anti-IL1β
C
anti-TNFα
D
anti-IL1β,
anti-TNFα
E
Wild Type Explants
New
Branches
LPS
Goat
Rat
IgG
anti-
IL1β
anti-
TNFα
anti-
IL1β,
TNFα
F
CCL-2
Fold
Change
anti-IL1β
anti-TNFα
ctrl
LPS
G
IL1β−/−
H
wild-type
YVAD
New
Branches
ctrl
LPS
#
YVAD

Figure 4.1. Inhibiting IL-1β activity protects fetal mouse lung explants from the effects of LPS. E15 fetal lung explants from C57Bl/6 mice were cultured under control conditions and in the presence of LPS (250 ng/ml), a neutralizing antibody to IL-1β (10ng/ml), or a neutralizing antibody to TNFα (10ng/ml). Explant images show LPS inhibits new airway branching, but anti-IL-1β prevents this effect. Anti-TNFα does not rescue lung branching in explants cultured with LPS. Explants treated with a combination of LPS, anti-IL1β, and anti-TNFα have normal airway branching. Brightfield images were obtained using a 4X objective. LPS inhibited the number of new branches explants formed between 24h and 72h. Control IgG was negligible on the effect of LPS. LPS had no effect on branching in explants cultured with anti-IL1β and anti-IL1β/anti-TNFα. LPS increases gene expression of inflammatory cytokine, CCL-2, even in the presence of anti-IL1β and anti-TNFα. IL-1$\beta^{-/-}$ E15 fetal lung explants were cultured under control conditions and with LPS. LPS did not inhibit airway branching in IL-1$\beta^{-/-}$ explants, and the number of new branches was consistent between control and LPS treated explants. E15 fetal lung explants from C57Bl/6 mice were cultured in the presence of the caspase-1 inhibitor I (YVAD, 1 μM). YVAD protected fetal lung explants from the effects of LPS. n = at least 16 explants from 3 different litters, *$p < 0.05$, #$p < 0.01$.

expression in anti-IL1β-treated explants (Figure 4.1F). To further test the requirement of IL-1β, we measured the effects of LPS on airway morphogenesis using fetal lung explants from IL-1β$^{-/-}$ mice (Figure 4.1G). LPS did not affect airway branching in these mutant lungs, further demonstrating that IL-1β release and signaling linked LPS-stimulated inflammation and abnormal airway formation.

Inflammatory activation in macrophages produces IL-1β precursor peptide that is cleaved by inflammasome-associated caspase-1 and secreted to the extracellular space (Dinarello 1998). Inhibiting inflammasome-associated caspase-1 activity prevents IL-1β release. To test the requirement of inflammasome-mediated cytokine release, we treated fetal lung explants with the peptide-based caspase-1 inhibitor Ac-Tyr-Val-Ala-Asp-CHO (Figure 4.1H). As seen in Figure 1, adding Ac-Tyr-Val-Ala-Asp-CHO to the explant media both prevented IL-1β release following LPS treatment and also preserved formation of new airways around the explant periphery.

We previously observed that macrophage activation did not alter airway morphogenesis during early embryonal stages of development (< E16) (Stouch et al. 2014). Because inflammasome-mediated IL-1β release appeared to be required for abnormal lung morphogenesis, we hypothesized that developmental regulation of the inflammasome might determine when lung morphogenesis becomes sensitive to inflammatory stimuli. To further define the points during development when macrophage activation can influence lung morphogenesis, we used an inducible, constitutively active IKKβ mouse model (IKFM). In these mice, doxycycline induces expression of constitutively active IKKβ in *Csf1r*-expressing macrophages. Giving pregnant dams doxycycline from E14-E16 had no effect on fetal lung

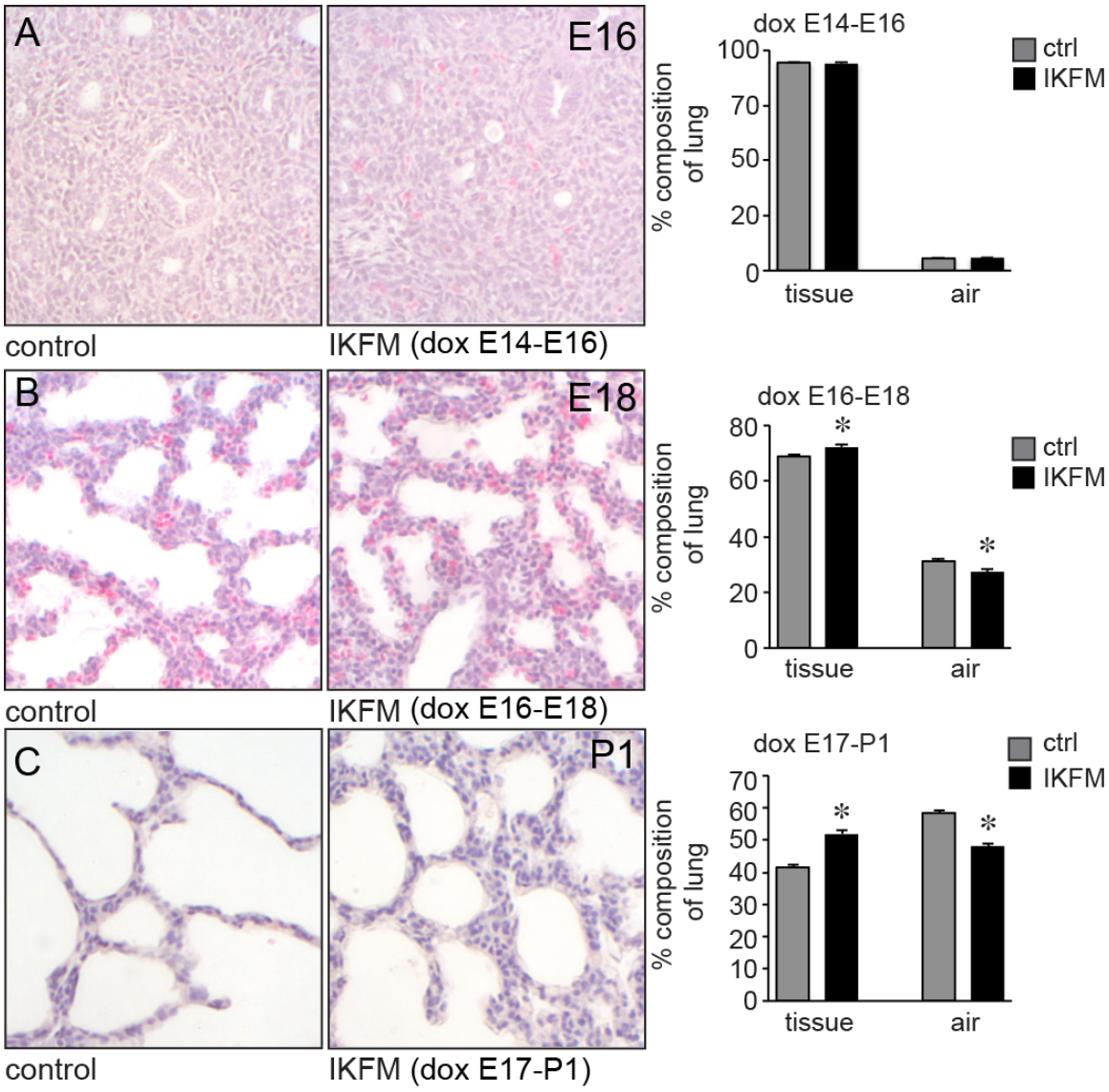

Figure 4.2. Macrophage activation during the saccular stage of lung development is sufficient to inhibit airway morphogenesis during a window of susceptibility to inflammation. Pregnant mice were treated with doxycycline (2g/L) for 48h, from E14-E16, E16-E18, and E17-P1. E16 control and IKFM lungs did not have notable differences. Lung morphometry measurements show increased mesenchyme tissue and decreased airspace in E18 and P1 IKFM lungs. n = at least 5 control and 5 IKFM lungs from 2 different litters, 20 images per lung, *p < 0.01. Images were obtained with a 20X objective.

airway morphology, but doxycycline from E16-E18 caused reduced airway branching and expansion in IKFM embryos compared to littermate controls (Figure 2A-B). Even more dramatic changes were seen in newborn IKFM pups following doxycycline treatment from E17-P1 (Figure 4.2C). These data suggest NF-κB activation in macrophages is not capable of disrupting lung morphogenesis until E17-E18, when the developing lung transitions from the canalicular to saccular stage of development.

Because IL-1β appears to be required to inhibit normal development, we hypothesized that the ability to release bioactive IL-1β via the inflammasome was developmentally regulated and did not occur until late in fetal development. To initially test this hypothesis, we measured expression of inflammasome components in fetal mouse lung tissue by immunostaining. Caspase-1 expression was detected in $CD68^{+}$ macrophages throughout development, with increased immunostaining intensity in adult lung macrophages (Figure 4.3A). However, NLRP3, NLRP1a, and ASC were present in adult lung macrophages but not detected in fetal lung (Figure 4.3B-D). Gene expression measurements confirmed developmental regulation of inflammasome components. ASC, Casp1, and Casp4, steadily increased during lung development (Figure 4.3E). Expression of the various Nod-Like Receptors and intracellular sensors detected was highest in postnatal day 1 and adult cells (Figure 4.3G). In addition to the inflammasome machinery, expression of the inflammasome substrates IL-1β, and IL-18 also increased during development with highest expression in postnatal and adult lung (Figure 4.3H). The additional findings that IL1R and TNFR expression increased with lung maturation suggested a comprehensive developmental regulation of the pulmonary innate immune system (Figure 4.3F).

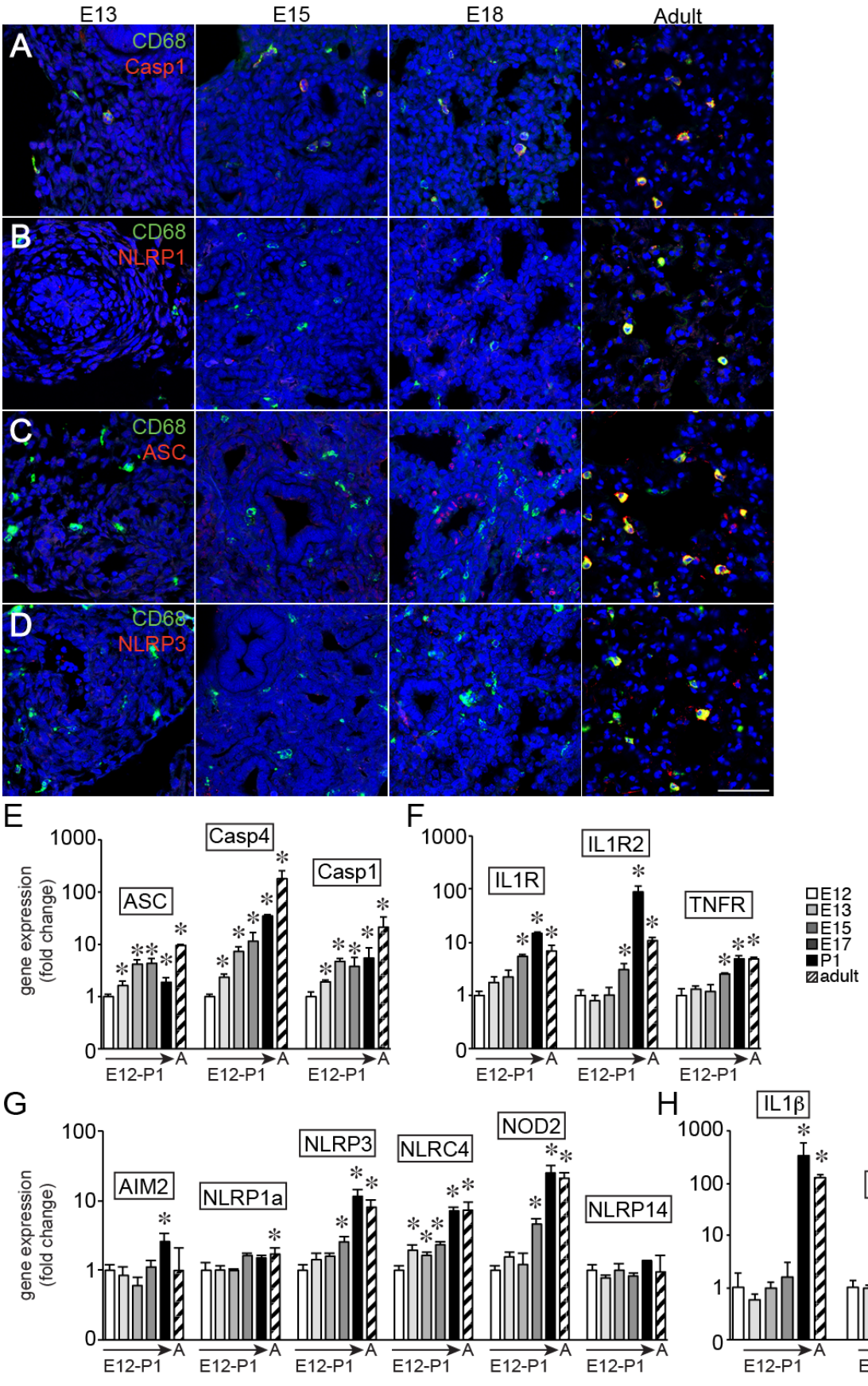
E13
E15
E18
Adult
A
CD68
Casp1
B
CD68
NLRP1
C
CD68
ASC
D
CD68
NLRP3
E
F
G
H
gene expression (fold change)
ASC
Casp4
Casp1
IL1R
IL1R2
TNFR
AIM2
NLRP1a
NLRP3
NLRC4
NOD2
NLRP14
IL1β
IL18
E12-P1
A
E12
E13
E15
E17
P1
adult

Figure 4.3. Expression of the inflammasome is developmentally regulated. Frozen sections of fixed E13, E15, E18, and adult mouse lung were immunostained with antibodies against Casp1, NLRP1, ASC, and NLRP3. Macrophages were immunolabeled with CD68. Nuclei were labeled with DRAQ5. Images were obtained by laser scanning confocal microscopy. Scale bar, 50 μm. Gene expression of inflammasome components in E12, E13, E15, E17, P1, and adult lung. Expression of ASC, Casp4, and Casp1 increased incrementally throughout development. Expression of IL1R, IL1R2, and TNFR increased in saccular stage lung, beginning at E17 to adult. AIM2, NLRP1a, and NLRP14 had mostly consistent expression levels throughout development. NLRP3 and NOD2 had increased expression in saccular stage lung, beginning at E17 to adult. IL-1β, and IL18 increased after birth. n = 4 litters, pooled, from each embryonic time point or 4 individual lungs from P1 and adult, *$p < 0.05$.

But could the response to microbial products and TLR agonists also be developmentally regulated? To test this possibility, we added LPS to fetal lung explants from E13 and E15 NF-κB-GFP-Luciferase (NGL) reporter mouse. Within 6 h, LPS induced GFP reporter expression throughout both E13 and E15 lungs (Figure 4.4A-B). Quantitative measurement of NF-κB-dependent luciferase activity confirmed the response in E13 and E15 lungs, with higher relative levels in E13 lungs (Figure 4.4C). Therefore, the TLR-NF-κB axis was clearly functional as early as E13 and not likely responsible for the developmental window of susceptibility. Similarly, fetal lung mesenchymal cells targeted by inflammation were sensitive to soluble inflammatory mediators early in development. Primary cultures of E13, E15, and E18 NGL lung mesenchyme each responded to LPS, the TLR2 agonist Pam3CSK4, TNFα, and IL-1β (Figure 4.4D). Interestingly, IL-18 had no effect. These data suggested that the early stage fetal lung has the capacity to respond to extracellular inflammatory signals. However, inflammatory macrophage activation can inhibit lung morphogenesis only later in development around the time of inflammasome expression and activity.

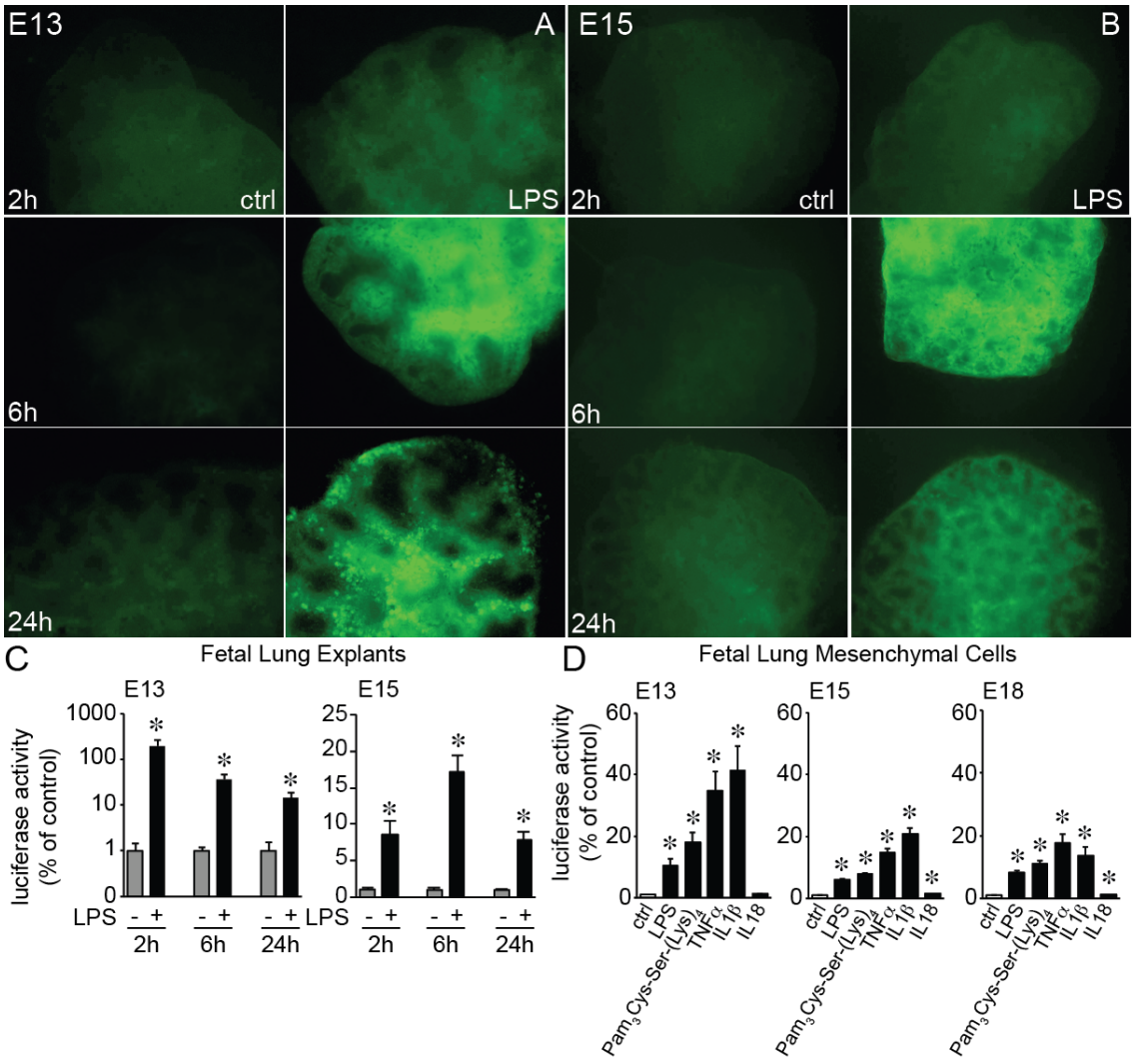

Figure 4.4. Early fetal mouse lung explants respond to LPS. Fetal NGL lungs, with NF-κB-dependent GFP, were isolated and made into explants at E13 and E15. Explants were cultured with LPS. Increased GFP fluorescence was detected within 2h of LPS, but peaked at 6h, in both E13 and E15 fetal lung explants. GFP images were obtained on an EVOS Cell Imaging System using a 10X objective. NF-κB activation, measured by luminometry, is induced by LPS in E13 and E15 explants. n = 6 explants from 3 separate litters. LPS (250ng/ml), $Pam_3Cys\text{-}Ser\text{-}(Lys)_4$ (1ug/ml), TNFα (10ng/ml), and IL-1β (10ng/ml) activate NF-κB in fetal lung mesenchymal cells isolated from E13, E15, and E18 NGL lungs. IL18 (10ng/ml) stimulates NF-κB activation in E15 and E18 mesenchymal cells. n = 4 separate litters, *$p < 0.05$.

We next tested if inflammatory signals and NF-κB activation could increase expression of the inflammasome and therefore accelerate the developmental process. To evaluate this potential priming mechanisms, we immunostained LPS-treated E15 fetal lung explants using antibodies against NLRP3. LPS did increase NLRP3 immunostaining but interestingly the expression remained restricted to $CD68^{+}$ macrophages (Figure 4.5A). We obtained similar results in IKFM fetal lungs, with increased Casp1 expression in transgenic $CD68^{+}$ macrophages (Figure 4.5B). To test if activation could increase inflammasome expression in a cell autonomous manner, we isolated and cultured primary fetal lung macrophages. LPS increased expression of Casp1 in E18 and adult macrophages and increased Casp4 expression in E15, E18, and adult cells (Figure 4.5C). The effect of LPS on other components was variable. While LPS increased NLRP3 expression, activation had little effect on NLRC4 and actually decreased expression of ASC. Transgenic macrophage activation also had variable effects on inflammasome components, with increased Casp1 and Casp4 expression in IKFM macrophages but only increased Casp4 expression in $NLRP3^{L351P}$CreL cells (Figure 4.5D). Similarly, NLRC4 expression was increased in IKFM but not in $NLRP3^{L351P}$CreL macrophages. Therefore while expression of some inflammasome components could clearly be induced by inflammatory activation, the effects were variable and gene specific.

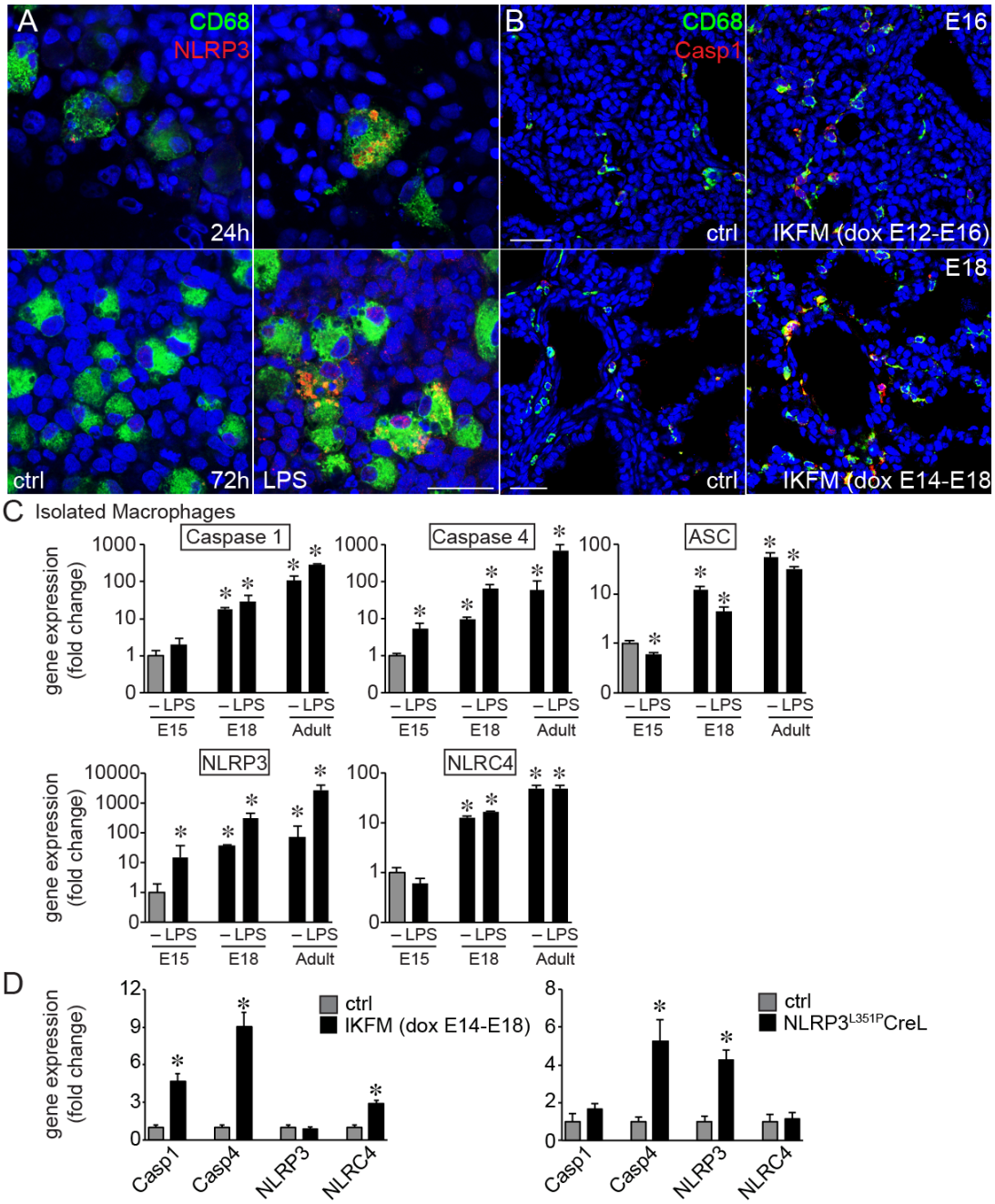
A
CD68
NLRP3
24h
ctrl
72h
LPS
B
CD68
Casp1
E16
ctrl
IKFM (dox E12-E16)
E18
ctrl
IKFM (dox E14-E18)
C
Isolated Macrophages
Caspase 1
Caspase 4
ASC
NLRP3
NLRC4
gene expression (fold change)
– LPS
E15
E18
Adult
D
ctrl
IKFM (dox E14-E18)
NLRP3L351PCreL
Casp1
Casp4
NLRP3
NLRC4

Figure 4.5. Macrophage activation induces inflammasome expression in fetal mouse lungs. Fetal lung explants cultured with LPS for 24h and 72h were immunostained with NLRP3. LPS exposure induced NLRP3 speck formation in macrophages. Pregnant dams were give doxycycline from E12-E16 or E14-E18. IKFM fetal lungs isolated at E16 and E18 were immunostained for caspase 1. IKFM macrophages had increased caspase 1 expression. Images were obtained by laser scanning microscopy. Scale bar, 30 μm and 100 μm. Isolated macrophages from E15, E18, and adult lung exposed to LPS increased expression of the inflammasome components Casp1, Casp4, NLRP3, and NLRC4. Macrophages reduced expression in ASC in the presence of LPS. n = 3 litters or adult lungs. E18 IKFM macrophages have increased Casp1, Casp4, and NLRC4 expression. n = 4 control and 4 IKFM samples. E18 $NLRP3^{L351P}$CreL lungs have increased Casp4 and NLRP3 expression. n = 7 control and 7 $NLRP3^{L351P}$CreL lungs, $*p < 0.05$.

As fetal lung macrophages mature, cells gain F4/80 expression with similar to slightly lower CD11b expression. We previously demonstrated that NF-κB activation increased the percentage of $CD11b^{lo}F4/80^{hi}$ macrophages in the fetal lung, consistent with accelerated alveolar macrophage maturation (Stouch et al. 2014). To test if inflammasome activation could similarly increase fetal lung macrophage maturation, we used flow cytometry to identify different macrophage subtypes $NLRP3^{L351P}$CreL lungs. Among live, $CD45^{+}$, $CD68^{+}$ macrophages, fetal $NLRP3^{L351P}$CreL mice had higher percentages of $CD11b^{lo}F4/80^{hi}$ macrophages compared to littermate controls (Figure 4.6A). In addition, these $CD11b^{lo}F4/80^{hi}$ macrophages expressed CD204 and CD206, consistent with alveolar macrophage maturation (Figure 4.6B). These data show that macrophages not only acquire inflammasome expression as they develop, but also that activation can influence development.

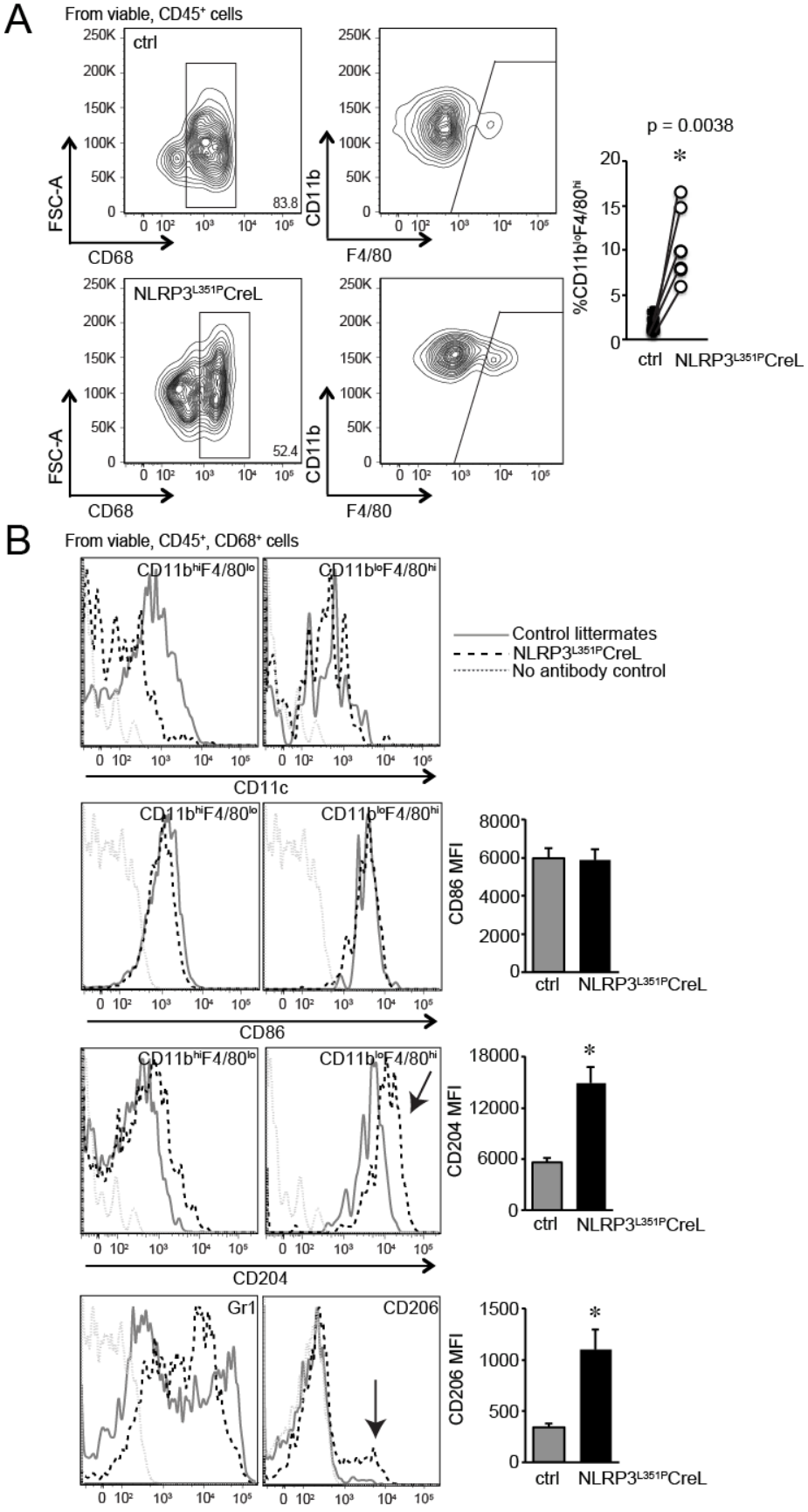
A
From viable, CD45+ cells
ctrl
NLRP3L351PCreL
FSC-A
CD68
CD11b
F4/80
83.8
52.4
p = 0.0038
%CD11bloF4/80hi
ctrl
NLRP3L351PCreL
B
From viable, CD45+, CD68+ cells
CD11bhiF4/80lo
CD11bloF4/80hi
Control littermates
NLRP3L351PCreL
No antibody control
CD11c
CD86
CD86 MFI
CD204
CD204 MFI
Gr1
CD206
CD206 MFI

Figure 4.6. Inflammasome activation induces maturation of fetal lung macrophages. E18 NLRP3^{L351P}CreL and control littermate fetal lungs were digested into single cell suspensions in preparation for flow cytometry. After doublet exclusion and selection for viable, CD45^{+}, CD68^{+} cells, macrophages were gated for CD11b and F4/80 expression. NLRP3 activation in macrophages increased the proportion of CD11b^{lo}F4/80^{hi} macrophages in fetal lung. CD204 expression increased in NLRP3^{L351P}CreL CD11b^{lo}F4/80^{hi} macrophages. NLRP3^{L351P}CreL and control littermate CD11b^{lo}F4/80^{hi} macrophages had similar CD86 and CD11c expression. NLRP3^{L351P}CreL CD68^{+} macrophages had increased CD206 expression. n = 7 control and 7 NLRP3^{L351P}CreL lungs from 2 litters, *$p < 0.01$.

Discussion

Our data show the important role of IL-1β in connecting the initial inflammatory response in lung macrophages to the developmental defects in airway morphogenesis seen when the fetal lung is exposed to inflammation and injury. While LPS can induce expression of multiple of inflammatory mediators, blocking IL-1 signaling, inhibiting inflammasome-mediated IL-1β cleavage, and genetic deletion of IL-1β each protected fetal mouse lung airway branching from inhibition by LPS. While other released inflammatory mediators can affect various developmental processes, the effects of LPS on formation and expansion of new saccular airways appears directly tied to IL-1β. Whether the importance of IL-1β over other inflammatory mediators is due to relative abundance, proximity to receptors on target cells, or other unique aspects of IL-1β biochemistry is not clear. The requirement of proteolytic IL-1β cleavage by the inflammasome identifies another intriguing mechanism regulating the lung innate immune response and a potential therapeutic strategy.

We showed that multiple gene components of the inflammasome are developmentally regulated. While immature fetal lung macrophages are capable of responding to LPS by activating NF-κB, the lack of a functional inflammasome prevents the release of bioactive IL-1β. The lack of inflammasome expression and/or function in immature macrophages may explain why NF-κB activation early in lung development fails to produce changes in lung morphogenesis. We show here that even E11 lung mesenchymal cells are very responsive to NF-κB dependent inflammatory mediators, but the lack of an inflammasome appears to protect these cells from IL-1β exposure following macrophage activation. The transcriptional mechanisms regulating inflammasome component gene expression during development are not yet clear.

Interestingly, several genes were much higher in newborn and adult macrophages while other components were more consistently expressed throughout development. How inflammasome gene expression parallels the normal development of macrophages and other myeloid lineages also warrants further investigation.

Previously we demonstrated that increased IKKβ activity and NF-κB activation in developing lung macrophages increased expression of more mature alveolar macrophage markers (Stouch et al. 2014). Here we observed similar results with gain of function inflammasome mutant mice, with increased percentages of $CD11b^{lo}F4/80^{hi}$ macrophages. Fetal lung $NLRP3^{L351P}$CreL macrophages also expressed higher levels of CD204 and CD206, both expressed on more mature alveolar macrophages. We speculate that IL-1β may function in a cell autonomous manner in fetal lung macrophages to accelerate the maturation process. How IL-1β affects macrophage function and biology in response to a second activating stimulus or in their role healing wounds and injury remains unknown. We have also not yet completely characterized the contribution of recruited fetal monocytes to this maturation of the lung macrophage populations.

Identifying inflammasome expression, function, and IL-1β release as important mechanisms linking inflammation and abnormal development opens new therapeutic possibilities. Perhaps blocking IL-1β signaling or inflammasome function in specific cell populations could prevent the negative effects of inflammation on lung development seen in patients with BPD. Subsequent studies will need to test if targeting macrophages or lung mesenchyme and epithelia will be feasible strategies. In addition, we do not yet know if accelerated macrophage maturation following inflammation is beneficial or detrimental to the developing lung innate immune system. Also, strategies to prevent the inflammation-induced

expression of inflammasome components in immature macrophages could be protective for the developing lung or could prevent the preterm lung from properly killing inhaled pathogens and removing aerosolized particles.

References

Benjamin, John T., B. J. Carver, E. J. Plosa, Y, Yamamoto, J. D. Miller, J. Liu, R. van der Meer, T. S. Blackwell, L. S. Prince (2010) NF-kappaB activation limits airway branching through inhibition of Sp1-mediated Fibroblast Growth Factor-10 expression. *J. Immunol.* **185**: 4896-4903.

Blackwell, Timothy S., A. N. Hipps, Y. Yamamoto, W. Han, W. J. Barham, M. C. Ostrowski, F. E. Yull, L. S. Prince (2011) NF-κB signaling in fetal lung macrophages disrupts airway morphogenesis. *J. Immunol.* **187**: 2740-2747.

Bry, Kristina, J. A. Whitsett, U. Lappalainen (2007) IL-1β disrupts postnatal ling morphogenesis in the mouse. *Am. J. Respir. Cell Mol. Biol.* **36**: 32-42.

Dinarello, C. A. (1998) Interleukin-1 beta, interleukin-18, and the interleukin-1 beta converting enzyme. *Ann. NY Acad. Sci.* **856**: 1-11.

Nold, Marcel F., N. E. Mangan, I. Rudloff, S. X. Cho, N. Shariatian, T. D. Samarasinghe, E. M. Skuza, J. Pederson, A. Veldman, P. J. Berger, C. A. Nold-Petry (2013) Interleukin-1 receptor antagonist prevents murine bronchopulmonary dysplasia induced by perinatal inflammation and hyperoxia. *Proc. Natl. Acad. Sci. USA* **110**: 14384-14389.

Romero, Roberto, J. Espinoza, T. Chaiworapongsa, K. Kalache (2002) Infection and prematurity and the role of preventative strategies. *Semin. Neonatal.* **7**: 259-274.

Stouch, Ashley N., R. Zaynagetdinov, W. J. Barham, A. M. Stinnett, J. C. Slaughter, F. E. Yull, H. M. Hoffman, T. S. Blackwell, L. S. Prince (2014) IκB Kinase activity drives fetal lung macrophage maturation along a non-M1/M2 paradigm. *J. Imunnol.* **193**: 1184-1193.

CHAPTER V

Conclusions and Future Directions

Our goal of this research was to advance the understanding of fetal lung inflammation. Before our research, different cell types had been suggested as initiating and propagating inflammation in the fetal lung. It was also unclear, although our evidence suggested, as to which inflammation pathway was responsible. We began by asking: How does the inflammatory response begin in the fetal lung? Are macrophages present and responsible for inflammatory signaling? Is it the NF-κB pathway that is the primary signaling pathway involved? Are fetal lung macrophages responsive to polarization stimuli? Do fetal lung macrophages change their phenotype during inflammation? In order to answer these questions, we would: identify the cells responsive to LPS in the fetal lung; determine if macrophage activation, through inducing NF-κB, was required for the inflammatory response and its effects on lung development; and determine if macrophage activation changed fetal lung macrophage phenotype.

What cell type initially responds to LPS in the fetal lung and is that cell type responsible for abnormal lung branching after exposure to LPS?

To identify which cells in the fetal lung first responded to LPS, we used the NF-κB reporter mouse (NGL) to detect GFP expression after NF-κB activation. We isolated fetal lung explants from NGL mice and treated them with LPS. This allowed us to identify the cells that first activate NF-κB through the colocalization of GFP with cell-specific markers, such as CD68. Since macrophages were the first cell type to respond to LPS, we then wanted to test if

macrophages had a role inhibiting airway branching. Using clodronate to deplete macrophages in fetal lung explants, there was normal airway branching after LPS exposure. These results suggest macrophages are the cell type in the fetal lung that begin inflammatory signaling in response to LPS and are required to induce abnormal airway branching.

Do macrophages require NF-κB activation to disrupt lung development?

To determine if the NF-κB pathway in macrophages drives fetal lung inflammation, we isolated fetal lung explants from mouse models that would either inhibit or activate NF-κB solely in macrophages. LysM-Cre:IKKβ$^{f/f}$ fetal lung explants were protected from the effects of LPS, while Cfms-rtTA:Tet-O-Cre-cIKKβ (IKFM) fetal lung explants had inhibited airway branching. Using whole sections of saccular-stage IKFM fetal lungs, we observed reduced airspace and a thickened mesenchyme. These results confirm that macrophages are sufficient to inhibit lung development, and NF-κB is the inflammatory pathway utilized by fetal lung macrophages.

Can fetal lung macrophages change phenotype?

We first identified and measured a panel of recognized M1 and M2 phenotype markers during normal lung development. RT-PCR and immunofluorescence imaging showed increased expression of macrophage phenotype markers during later stages of embryonic development, immediately after birth, and in adult macrophages. In vitro exposure to LPS, IL-4, or IL-13 increased expression in M1 or M2 markers in fetal lung macrophages. However, flow cytometry of E18 IKFM lungs showed macrophages did not exclusively increase M1 markers. Instead, IKFM lung macrophages had an increased population of CD11b^{lo}F4/80^{hi} cells, in addition to increased CD204 and CD206 expression. Mature, alveolar macrophages express higher levels of

CD204 and CD206 (Zaynagetdinov et al. 2013). While we expected fetal lung macrophages to follow typical polarization expression patterns, our results showed that fetal lung macrophages begin a maturation process after NF-κB activation.

Is IL-1β the primary proinflammatory cytokine that disrupts fetal lung development?

To determine if IL-1β was a necessary factor to disrupt lung development, we treated fetal lung explants with an IL-1β neutralizing antibody in the presence of LPS. Inhibiting IL-1β activity protected fetal lung explants from LPS. Using an $IL1\beta^{-/-}$ mouse model, airway branching in fetal lung explants was protected from LPS. This data supports the idea that IL-1β is the primary factor causing abnormal fetal lung development during inflammation.

Overall, this research has shown multiple ways that fetal lung macrophages respond to inflammation. NF-κB activation, whether through LPS signaling or cIKKβ, increases fetal lung macrophage recruitment, proliferation, and maturation (Figure 5.1). Activated fetal lung macrophages increase expression of chemokines. These chemokines recruit additional immune cells to the fetal lung. IKFM lungs have an influx of monocytes. IKFM lungs also have increased numbers of $PHH3^{+}$ and $Ki67^{+}$ macrophages.

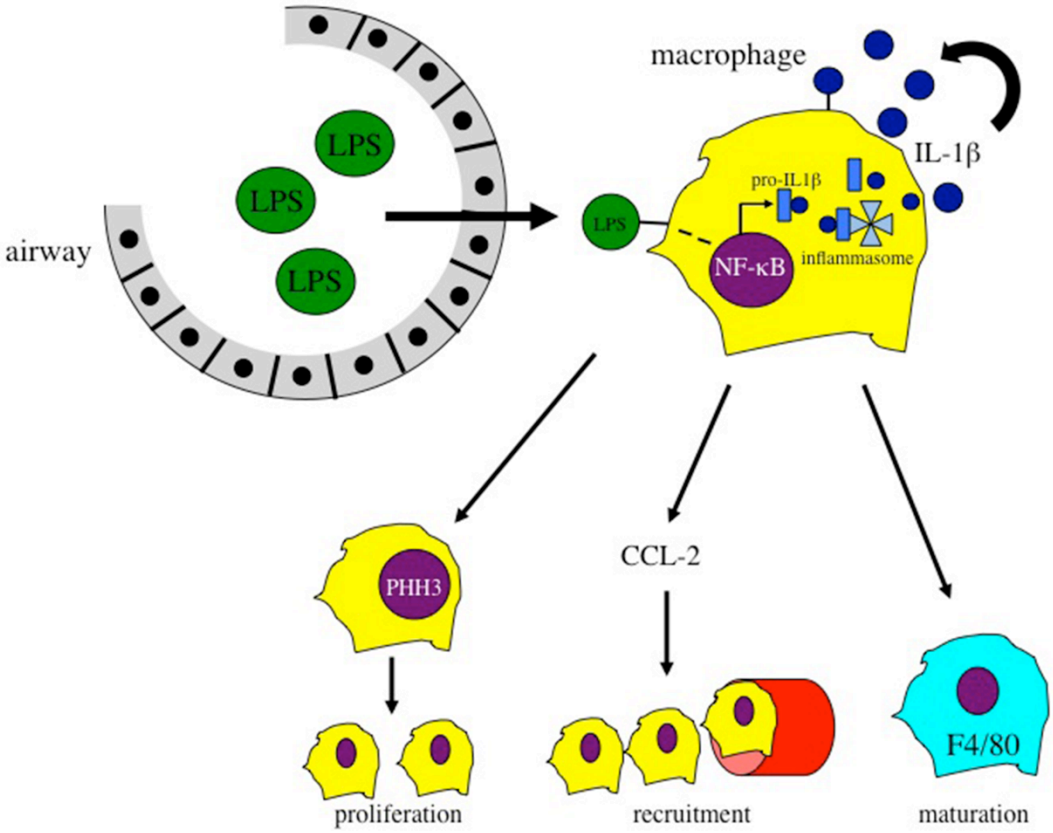

Figure 5.1. Fetal lung macrophage response to inflammation. Fetal lung macrophages can become activated through LPS signaling, NF-κB activation, and inflammasome activation/IL-1β signaling. Macrophage activation leads to increased proliferation, increased recruitment through chemokine expression, and maturation.

Inflammasome activation or cIKKβ in fetal lung macrophages increases the proportion of $CD11b^{lo}F4/80^{hi}$ macrophages, and, along with increased expression of CD204 and CD206, indicates a maturation of fetal lung macrophages.

Our research on fetal lung macrophages can contribute to the search for more effective prevention and treatment options for infants with BPD. We have shown a clear relationship between fetal lung macrophages, altered lung development, and IL-1β signaling. New therapies could target fetal lung macrophages by intervening during their activation. Our research can be used as supporting data to begin studies on macrophages isolated from infants with BPD. Fetal macrophages from BPD patients could be treated with new therapies targeting macrophages and their released factors. The responsiveness of macrophages directly isolated from BPD patients would be an indicator of potentially viable treatment options.

Our interest in fetal macrophage biology and the role of macrophages in the fetal lung has only increased. There are many directions to follow in our future research. Some of the guiding questions are: Do fetal lung macrophages need to undergo maturation prior to releasing proinflammatory cytokines? What factors control fetal macrophage maturation? Can macrophage maturation be prevented, which in turn could prevent the release of proinflammatory cytokines?

Future Directions

Determine if NF-κB regulates transcription factors that induce fetal macrophage maturation.

PU.1 and M-CSF are required factors for normal macrophage development. PU.1 is necessary for myeloid progenitor cell differentiation and is a regulator of Csf1r transcription, the corresponding receptor for M-CSF (DeKoter et al. 1998; DeKoter et al. 2000; Zhang et al. 1994). M-CSF is required throughout macrophage development from their early monocyte precursors (Becker et al. 1987). Another role for PU.1 is acting in macrophages as an initiator of macrophage specific genes (Ross et al. 1998). The network of genes that PU.1 regulates includes Myb, Egr2, Ly96, Foxp1, and KLF4 (Weigelt et al. 2009; Shi et al. 2008; Feinberg et al. 2007). In alveolar macrophages, GM-CSF regulates PU.1 expression (Shibata et al. 2001). GM-CSF is required for normal levels of PU.1 and normal functioning of alveolar macrophages (Shibata et al. 2001). Currently, it is unclear how inflammation influences any of the factors involved in fetal macrophage maturation.

NF-κB activation in macrophages during fetal lung development increased the $CD11b^{lo}F4/80^{hi}$ subpopulation. This indicates NF-κB may have a role in regulating the transcription factors that control macrophage maturation. In preliminary searches, we have identified NF-κB binding sites in the promoters of macrophage differentiation genes PU.1 and Csf1r and in the macrophage matrix metalloproteinase MMP12. Early data of isolated macrophages from IKFM and control littermate lungs show increases in PU.1 expression, along with increases in the PU.1 targets MMP12 and Csf1r (Figure 5.2). Further experiments should use ChiP assays to confirm the presence of NF-κB within these genes' promoters.

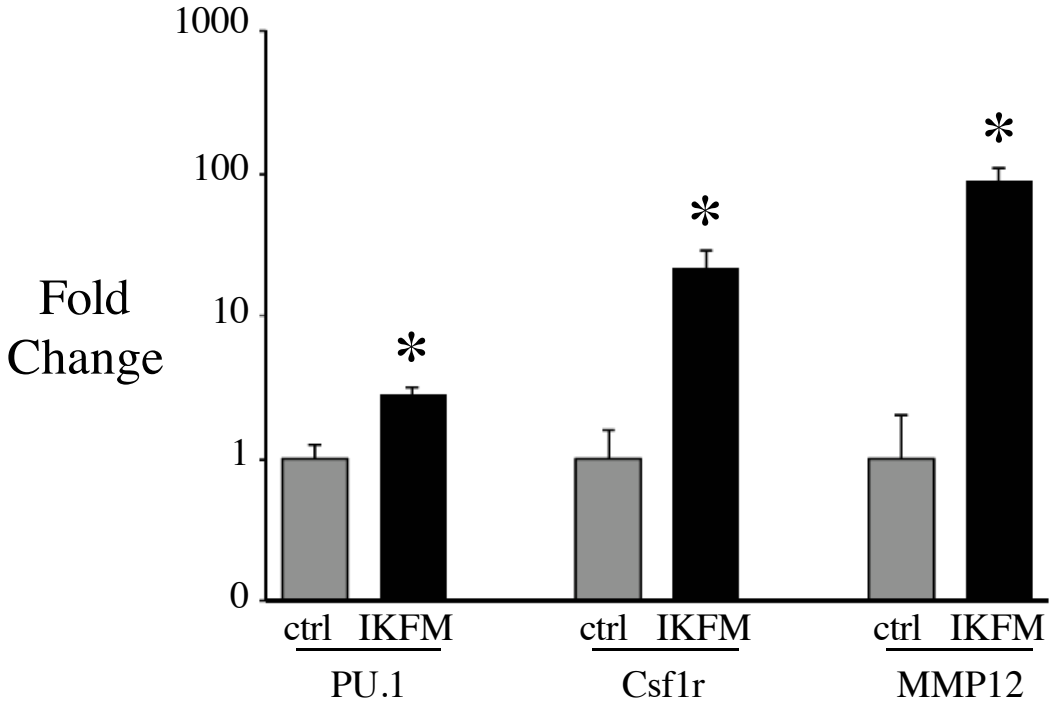

Figure 5.2. NF-κB increases expression of genes involved with macrophage maturation. Macrophages were isolated from E18 fetal lungs (dox E14-E18). Gene expression was measure by RT-PCR. NF-κB increased expression of PU.1, Csf1r, and MMP12 in fetal lung macrophages.

An important experiment to link macrophage maturation with inflammation is to analyze macrophage subpopulations in fetal lungs isolated from LysM-Cre:IKK$\beta^{f/f}$. Macrophages residing in LysM-Cre:IKK$\beta^{f/f}$ fetal lungs will have inhibited NF-κB activation. If NF-κB is required for macrophage maturation under basal conditions, we would expect to see a reduced proportion of the CD11b^{lo}F4/80^{hi} subpopulation. Further fetal lung macrophage subpopulation analysis could be done on a global scale, where IKFM macrophages are separated by FACS and are analyzed by RNA-SEQ. RNA-SEQ would show differences in expression of maturation-associated transcription factors that are regulated by NF-κB.

Determine if fetal lung macrophage subpopulations have different roles in lung development and the inflammatory response.

In adult lung, alveolar macrophages, interstitial macrophages, and monocytes each have a unique signature of markers. Alveolar macrophages are recognized as CD68^{hi}CD11b^{-}F4/80^{+}, while interstitial macrophages are CD68^{lo}CD11b^{+}F4/80^{-} (Zaynagetdinov et al. 2013). Macrophages in different niches within the adult lung have different marker expression profiles and may have separate functional roles as well. Marker expression corresponds to subsets in fetal lung macrophages, which can be divided into CD11b^{hi}F4/80^{lo} and CD11b^{lo}F4/80^{hi}. It is unknown if separate subpopulations in the fetal lung have distinct micro-locations or functions (Figure 5.3).

Fetal lung macrophages are clustered around blood vessels, adjacent to elongating airway tips, or throughout the mesenchyme. Lineage tracing of the CD11b^{hi}F4/80^{lo} and CD11b^{lo}F4/80^{hi} subsets simultaneously would identify micro-locations in the fetal lung to which specific macrophage populations are restricted. Identifying the micro-location of fetal lung macrophages

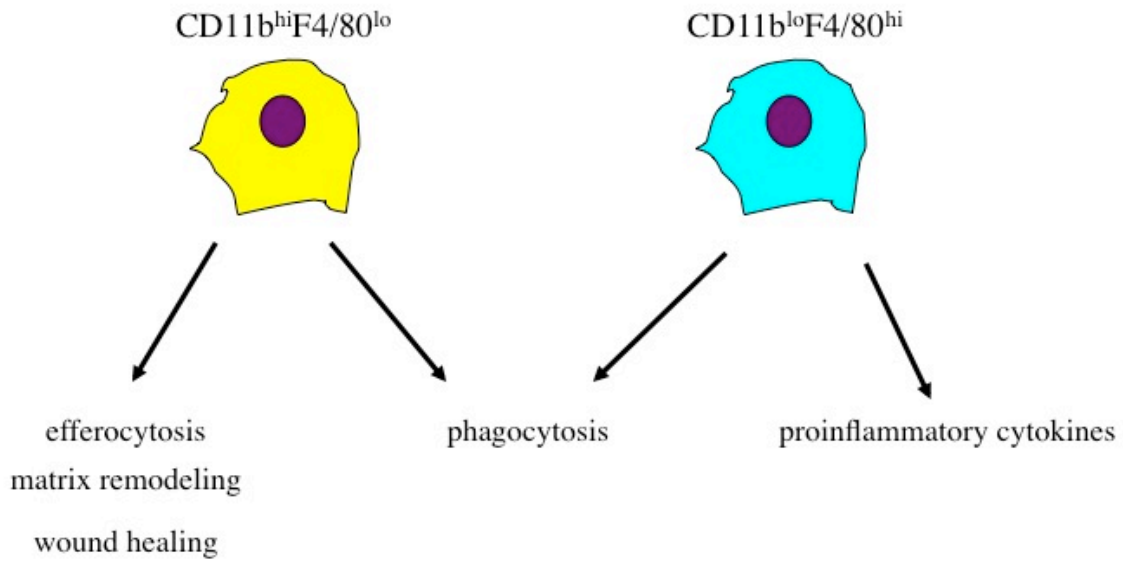

Figure 5.3. Fetal lung macrophages may have different roles that are niche specific. Future studies on macrophage function in the fetal lung should focus on the roles of the multiple macrophage subpopulations present. Macrophage subsets may have overlapping functions and unique, separate functions. Early macrophage maturation in response to inflammation may alter the function of lung macrophages, leading to disrupted lung development. Preliminary data suggests that $CD11b^{lo}F4/80^{hi}$ macrophages are responsible for the production of the proinflammatory cytokine IL-1β.

may lead to experiments determining unique functions of the subpopulations. Further, observation of both subpopulations in real time would provide new information determining if there are fluctuations of individual cells between subsets or if there is permanent subset specification during development. By isolating both $CD11b^{hi}F4/80^{lo}$ and $CD11b^{lo}F4/80^{hi}$, the phenotype of fetal lung macrophages may be further defined.

Previously, separation of fetal IKFM $CD11b^{hi}F4/80^{lo}$ and $CD11b^{lo}F4/80^{hi}$ macrophages by FACS showed gene expression differences between these subpopulations. $CD11b^{lo}F4/80^{hi}$ macrophages had increased expression of IL-1β compared to the $CD11b^{hi}F4/80^{lo}$ subpopulation. A higher level of IL-1β in these macrophages may indicate a primed state that will facilitate a faster inflammatory response in the event of infection. $CD11b^{lo}F4/80^{hi}$ macrophages also had increased cyclinD1 expression, which is a marker of mitosis. As the fetal IKFM $CD11b^{lo}F4/80^{hi}$ subset shares similar characteristics with mature macrophages, we speculate that this population may require enhanced proliferative ability in order to propagate the future airspace macrophages. Future research should focus on differences between the two macrophage subpopulations, including inflammasome activation and proinflammatory cytokine production.

Different subpopulations may each have separate, unique functions. Functions of fetal macrophages could include fighting infection, clearing debris and dying cells, and releasing growth factors that influence other cell types. Whether inflammation alters the role of both populations has yet to be answered. Isolating macrophage subpopulations from IKFM and NLRP3 lungs by FACS could identify differences between the macrophage subsets. We could use an IL-1β ELISA to show if either subpopulation releases significantly higher amounts of IL-1β protein. We suspect the $CD11b^{lo}F4/80^{hi}$ subpopulation may have increased inflammasome formation and IL1β release, as maturation of monocytes into macrophages leads to NF-κB

accumulation in the cell cytoplasm and a stronger response to LPS (Takashiba et al. 1999). We could use in vitro assays to measure the efficiency of phagocytosis and efferocytosis of the separated subpopulations. Analyzing gene expression of VEGF, MMPs, Wnt ligands, and TGF-β in separate macrophage subpopulations could more clearly define the signaling relationships between the many cells that are present in the fetal lung. Tissue macrophages have the ability to guide angiogenesis with VEGF production, construct or degrade extracellular matrix, and provide growth factors for stem cells (Mantovani et al 2012). Macrophage-released Wnt7b also contributes to epithelial cell repair in injured kidneys (Lin et al. 2010). Inflammation could have a large role in regulating growth factor expression and release by fetal lung macrophages.

References

Becker, Susanne, M. K. Warren, S. Haskill (1987) Colony-stimulating factor-induced monocyte survival and differentiation into macrophages in serum-free cultures. *J. Immunol*. **11**: 3703-3709.

DeKoter, Rodney P. and H. Singh (2000) Regulation of B lymphocyte and macrophage development by graded expression of PU.1. *Science* **288**: 1439-1441.

DeKoter, Rodney P., J. C. Walsh, H. Singh (1998) PU.1 regulates both cytokine-dependent proliferation and differentiation of granulocyte/macrophage progenitors. *EMBO J*. **17**: 4456-4468.

Feinberg, Mark W., A. K. Wara, Z. Cao, M. A. Lebedeva, F. Rosenbauer, H. Iwasaki, H. Hirai, J. P. Katz, R. L. Haspel, S. Gray, K. Akashi, J. Segre, K. H. Kaestner, D. G. Tenen, M. K. Jain (2007) The Kruppel-like factor KLF4 is a critical regulator of monocyte differentiation. *EMBO J*. **26**: 4138-4148.

Lin, Shuei-Liong, B. Li, S. Rao, E. Yeo, T. E. Hudson, B. T. Nowlin, H. Pei, L. Chen, J. J. Zheng, T. J. Carroll, J. W. Pollard, A. P. McMahon, R. A. Lang, J. S. Duffield (2010) Macrophage Wnt7b is critical for kidney repair and regeneration. *Proc. Natl. Acad. Sci. U. S. A*. **107**: 4194-4199.

Mantovani, Alberto, S. K. Biswas, M. R. Galdiero, A. Sica, M. Locati (2012) Macrophage plasticity and polarization in tissue repair and remodeling. *J. Pathol*. **229**: 176-185.

Ross, Ian L., X. Yue, M. C. Ostrowski, D. A. Hume (1998) Interaction between PU.1 and Another Ets Family Transcription Factor Promotes Macrophage-specific Basal Transcription Initiation. *J. Biol. Chem*. **273**: 6662-6669.

Shi, Can, M. Sakuma, T. Mooroka, A. Liscoe, H. Gao, K. J. Croce, A. Sharma, D. Kaplan, D. R. Greaves, Y. Wang, D. I. Simon (2008) Down-regulation of the forkhead transcription factor *Foxp1* is required for monocyte differentiation and macrophage function. *Blood* **112**: 4699-4711.

Shibata, Yoko, P. Berclaz, Z. C. Chroneos, M. Yoshida, J. A. Whitsett, B. C. Trapnell (2001) GM-CSF Regulates Alveolar Macrophage Differentiation and Innate Immunity in the Lung through PU.1. *Immunity* **15**: 557-567.

Takashiba, Shogo, T. E. Van Dyke, S. Amar, Y. Murayama, A. W. Soskolne, L. Shapira (1999) Differentiation of Monocytes to Macrophages Primes Cells for Lipopolysaccharide Stimulation via Accumulation of Cytoplasmic Nuclear Factor κB. *Infect. Immun*. **67**: 5573-5578.

Weigelt, Kain, M. Lichtinger, M. Rehil, T. Langman (2009) Transcriptomic profiling identifies a PU.1 regulatory network in macrophages. *Biochem. Biophys. Res. Commun.* **380**: 308-312.

Zaynagetdinov, Rinat, T. P. Sherrill, P. L. Kendall, B. H. Segal, K. P. Weller, R. M. Tighe, T. S. Blackwell (2013) Identification of Myeloid Cell Subsets in Murine Lungs Using Flow Cytometry. *Am. J. Respir. Cell Mol. Biol.* **49**: 180-189.

Zhang, Dong-Er, C. J. Hetherington, H. Chen, D. G. Tenen (1994) The Macrophage Transcription Factor PU.1 Directs Tissue-Specific Expression of the Macrophage Colony-Stimulating Factor Receptor. *Mol. Cell. Biol.* **14**: 373-381.